

**Identification of Potential Water Harvesting sites
in Ethiopia using Topographic Wetness Index
and Drought Indicators**

By:

Ethiopia Bisrat

Addis Ababa University

Addis Ababa, Ethiopia

November, 2017



Addis Ababa University

Addis Ababa Institute of Technology

School of Graduate Studies

School of Civil and Environmental Engineering

**Identification of Potential Water Harvesting sites in
Ethiopia using Topographic Wetness Index and Drought
Indicators**

By: Ethiopia Bisrat

A thesis submitted to the School of Graduate Studies of Addis Ababa University in Partial fulfillment of the Degree of Master of Science in Water Supply and Environmental Engineering.

Advisor: Dr. Belete Berhanu

November, 2017



Abstract

Drought damages are more prominent in areas where there is a direct threat to livelihood. This research attempts to address water scarcity that is exacerbated by reoccurring drought by providing a mechanism in which small scale water resource can be identified to relieve the stress from the existing water resources. The study develops a method for identifying potential water harvesting locations in Ethiopia that can be accessed to address drought induced water scarcity. The potential locations are selected in such a way that they satisfy both environmental sustainability and low land flow stagnation requirements. These locations are identified using remotely sensed landsat imagery and GIS and include consideration of a combination of soil characteristics, topography, vegetation and weather. Drought analysis and source identification were interlinked by first investigating the spatial and temporal characteristics of metrological drought in Ethiopia using a linear scaled bias corrected CFSR dataset. The Standardized Precipitation Index, programmed in R, was selected to represent prominent drought periods that resulted in a supportive premise that the seasonality of rainfall is pronounced rather than the lack of it. On basis of this finding, a method for a syndicate use of topography, land use and vegetation was performed and the performance was evaluated and mapped. The steady-state topographic wetness index (TWI) was used to represent the spatial distribution of water flow and water stagnating across the study area and the Normalized Difference Vegetation Index (NDVI) was used to detect surface water through multispectral analysis. Results showed that these two indices complimented each-other well and resulted in a joined spatial map of over 118,000 potential water harvesting sites, more or less uniformly distributed in the study area. Preliminary computations with regards to the volume of available water harvesting locations yielded over 4.5 BCM of potential sites by targeting small areas.

KEY WORDS: *Ethiopia, Metrological drought, Normalized Difference Vegetation Index, Water Harvesting, Remote sensing, Standardized Precipitation Index, Topographic Wetness Index*



Acknowledgements

I would like to express the deepest appreciation to my advisor, Dr. Belete Berhanu, who has the attitude and substance of a true researcher, for his exemplary guidance, technical and unending support throughout the entire course of this research.

I would like to thank my mother, Selamawit Haile for her wise counsel and continuous support. This thesis would not have been possible without your guidance and persistent help.

Dr. Yared Bayissa, Zelalem Tesfaye, Agazi Gebremedhin, for their technical support and for overall review of this thesis. Your input has gone a long way; thank you. Dr. Abdulkerim Seid, Ato Michael Abebe and Dr. Woubalem Fekade for the additional guidance and change of perspective that made this work what it is today. I am also grateful to Meklit Berihun for providing me with necessary data from across the continent. Besrat Eshetu, Bethelhem Wondimneh and Mahlet Melaku for the final review and added input; thank you all.



Table of Contents

Abstract.....	i
Acknowledgements	iv
List of Acronyms	ix
1. Introduction	1
1.1. Background	1
1.2. Statement of the Problem	4
1.3. Objectives	5
1.4. Organization of the thesis	6
2. Literature review.....	7
2.1. Drought characterization	10
2.1.1. Metrological Drought.....	10
2.1.2. Choice of Drought Index	11
2.1.3. The Standardized Precipitation Index	11
2.1.3.1. Computational procedure	12
2.1.3.2. SPI Advantages over other indices	13
2.1.3.3. Choice of dataset.....	14
2.1.3.4. Correcting Bias	15
2.1.3.5. Time scales in SPI.....	16
2.2. The Normalized Difference Vegetation Index	20
2.3. Identifying moisture characteristic areas - TWI	22
3. Data acquisition and processing	26
3.1. Description of study area	27
3.2. Dataset	29
3.2.1. Satellite data	29
3.2.2. Weather station data	31
3.3. Data Processing and Analysis	31
3.4. Spatio-Temporal assessment of Metrological drought	35
3.4.1. Spatial drought assessment.....	36
3.4.2. Yearly analysis	37
3.4.3. Spatio-temporal analysis to assess the spatial variability of drought frequency	38
3.4.4. Seasonal analysis.....	39
3.4.5. Monthly analysis.....	40



3.5.	Temporal Drought Assessment	41
3.6.	Water harvesting points identification.....	42
3.6.1.	Terrain Analysis - TWI.....	42
3.6.2.	Land-use Analysis	46
3.6.3.	Water Harvesting Categories.....	50
4.	Results and Discussion.....	52
4.1.	Performance evaluation of precipitation Dataset	52
4.2.	Spatio-temporal evaluation of metrological drought.....	55
4.2.1.	Spatial drought evaluation.....	55
4.2.1.1.	Evaluation of drought severity	58
4.2.2.	Temporal drought assessment	62
4.2.2.1.	Drought Frequency	63
4.2.3.	Seasonal drought evaluation	66
4.2.4.	Monthly drought evaluation	67
1.1.1.	Summary of Ethiopia’s prominent drought periods, 1979-2016	79
4.3.	Terrain Analysis	81
4.4.	Land use analysis	86
4.5.	Water Harvesting Categories	90
5.	Conclusions and Recommendations	100
5.1.	Conclusion.....	100
5.2.	Recommendations.....	101
6.	References	104
7.	Appendices	110



List of Tables

Table 1: Application of the SPI in different time scales	17
Table 2: SPI classification (McKee 1993)	18
Table 3: The NDVI classification (https://landcover.usgs.gov/landcoverdata.php) 21	
Table 4: EM-DAT The Emergency Events Database – Universite Catholique de Louvain (UCL) – CRED, D. Guha-Sapir – www.emdat.be , Brussels, Belgium - Summarized drought condition in Ethiopia	37
Table 5: Wider NDVI classification range	48
Table 6: Finer NDVI classification	49
Table 7: Country wide comparison of mean monthly rainfall for selected representative grid points.....	52
Table 8: Statistical measures of mean monthly raw and corrected CFSR and observed datasets	54
Table 9: Sample SPI-12 Values for the study period at representative grid points	55
Table 10: Percentage shares of dry and wet events for study area for pre-identified years	58
Table 11: Percentage shares of Drought anomalies by drought category	59
Table 12: Monthly SPI values and drought magnitude for drought year 1980	70
Table 13: Monthly SPI values and drought magnitude for drought year 1984	72
Table 14: Monthly SPI values and drought magnitude – Year 1995	74
Table 15: Monthly SPI values and drought magnitude – Year 2002	75
Table 16: Monthly SPI values and drought magnitude – Year 2009	76
Table 17: Monthly SPI values and drought magnitude – Year 2015	78
Table 18: Average precipitation amount - 1979-2016.....	79
Table 19: TWI Category and Adopted range	85
Table 20: Summarized NDVI results and corresponding study area coverage.....	87
Table 21: Desirable NDVI Category of the study area with areal coverage.....	88
Table 22: Ethiopia’s water volume analysis - Natural Lakes and Artificial Reservoirs	94
Table 23: Number and volume of identified locations	97



List of Figures

Figure 1: Percolation ponds harvesting water from the hillside to recharge groundwater (K. Woldearegay).....	9
Figure 2: Methodological flow chart	26
Figure 3: The location map of the study area.....	27
Figure 4: Spatial comparison of mean Observed and Corrected Rainfall.....	52
Figure 5: Statical evaluation of corrected rainfall data	53
Figure 6: The spatial patterns of the annual SPI (SPI-12) for the periods of 1980-2016. The red rectangular boxes in the figure shows the historic drought events in the country	57
Figure 7: The percentage areal extents of the annual drought for the selected historic drought years	60
Figure 8: Precipitation deviation from normal for selected drought years in Ethiopia	61
Figure 9: Time series plots of 12-month SPI for representative grids with trend analysis	64
Figure 10: The frequency of occurrence of mild, moderate, severe, and extreme droughts ...	65
Figure 11: Spatial patterns of 3-month SPI (SPI-3) for identified drought years in the country	66
Figure 12: Spatial patterns of monthly SPI for drought year - 1984.....	68
Figure 13: Spatial patterns of monthly SPI for drought year - 2010.....	69
Figure 14: Spatial pattern of 1-month SPI with grid based temporal distribution for drought year 1980.....	71
Figure 15: Spatial pattern of 1-month SPI with grid based temporal distribution for drought year 1984.....	73
Figure 16: Spatial pattern of 1-month SPI with grid based temporal distribution for drought year 1995.....	74
Figure 17: Spatial pattern of 1-month SPI with grid based temporal distribution for drought year 2002.....	76
Figure 18: Spatial pattern of 1-month SPI with grid based temporal distribution for drought Year 2009	77
Figure 19: Spatial pattern of 1-month SPI with grid based temporal distribution for drought year 2015.....	78
Figure 20: Spatial map of moisture contributing area of the country.....	82
Figure 21: Slope distribution of the country.....	82
Figure 22: Spatial map of TWI of the country	84
Figure 23: Reclassified TWI of the country.....	85
Figure 24: Desirable TWI category over threshold.....	86
Figure 25: Spatial distribution of NDVI of the country	87
Figure 26: Spatial distribution of desirable NDVI for RWH for the country	89
Figure 27: Preliminary identified water harvesting zones in the country	91
Figure 28: Water Harvesting Categories.....	92
Figure 29: Primary source locations	93
Figure 30: RWH map of the country	95
Figure 31: Drought year 1984 illustration with secondary rainwater harvesting sites	98



List of Acronyms

CFSR	-	Climate Forecast System Reanalysis
DEM	-	Digital Elevation Model
FAO	-	Food and Agricultural Organization
GIS	-	Geographic Information System
ET	-	Evapotranspiration
Ha	-	Hectare
ICOLD	-	International Commission on Large Dams
ITCZ	-	Inter Tropical Convergence Zone
NCEP	-	National Centers for Environmental Prediction
NDVI	-	Normalized Difference Vegetation Index
NIR	-	Near Infra Red
NMA	-	National Metrological Agency
NSE	-	Nush-Sutcliffe Efficiency
OLI	-	Operational Land Imager
PBIAS	-	Percentage Bias
PDSI	-	Palmer's Drought Severity Index
R	-	R programming
RMSE	-	Root Mean Square Error
RS	-	Remote Sensing
RWH	-	Rain Water Harvesting
SST	-	Sea Surface Temperature
SPI	-	Standardized Precipitation Index
TIRIS	-	Thermal Infrared Sensor
TM	-	Thematic Mapper
TRMM	-	Tropical Rainfall Measuring Mission
TWI	-	Topographic Wetness Index
USGS	-	United States Geological Survey
VBA	-	Visual Basic Application

1. Introduction

1.1. Background

Water scarcity is a factor affecting a vast majority of people, and is highly pronounced in dry or moderately dry areas resulting in economic, social and environmental problems. It occurs where there are insufficient water resources available to satisfy short/long -term average requirements. Population growth, more intensive agriculture, energy and manufacturing needs and tourism all contribute to increasing water use. Consecutively, the cause of scarcity itself can be chucked up to insufficiency of available water in catchments for supply, lacking basic water resource management with the available water, or wastage of such resources in general due a multitude of factors. As a consequence, in the most part of the world, lack of provision of safe supplies, and inadequate distribution systems are immense.

Water storage is like an insurance mechanism that tackles these consequences. Because of the intermittent nature of runoff events, storage is an integral part of the water harvesting system. It serves as a buffer against variability of rainfall in distinct regimes and increases resilience against dry spells. Storage opens the possibilities for new economic activities where water is a production factor. Reliable access to irrigation water from storage opens a great potential for crop diversification. In addition, more reliable water supply is improved from storage (Payen et al., 2012). Countries in sub-Saharan Africa store only about 4% of their annual renewable flow, compared with 70%-90% in many developed countries. (UNESCO, 2009) Water storage is essential to ensure reliable sources of water for irrigation, water supply and hydropower and to provide a buffer for flood management.

An unswerving cause for water scarcity is often associated with the shortfall of precipitation that eventually leads to the occurrence of drought. Drought can be characterized by using drought indexing that integrates hydro-climatic input variables. Drought indices simplify the complex inter-relationships between many climate parameters and address detailed drought issues such as frequency, intensity

and duration of drought, thereby tackling the social and economic value that is associated with this effect.

Drought is a natural hazard characterized by a significant decrease in water availability during a prolonged period of time over a large area. (Bayissa et al., 2015). The main types of physical droughts are metrological, hydrological, and agricultural droughts. These drought types occur in the particular order listed. Precipitation deficiency instigates metrological drought, which subsequently impacts soil moisture content (Zagar et al., 2011) thereby resulting in hydrological and agricultural droughts. Associated indicators then comprehensively characterize drought. Some indicators such as precipitation, potential evapotranspiration, and soil- and vegetation-cover have had wider applications and influence more than others. (Zagar et al., 2011)

The associated drought damages are more pronounced or prominent in areas where there is a direct threat to livelihoods (Palchaudhuri & Biswas, 2013). As such, Ethiopia is continuously being battered by extremes of weather, by cycles of drought and floods, with drought being one of the least documented naturally occurring anomalies (Sintayehu, 2007). The vastness of this issue has a direct effect towards regaining a nationwide balance between supply and demand of water resources considering climate change as an external resource.

Rain water harvesting has been used for several thousand years as a way of taking advantage of seasonal precipitation that would otherwise be lost as runoff (Kinkade-Levario et al., 2007). Rain water harvesting can be a valuable technique to supplement the other sources by reducing dependence on rivers and groundwater sources. However, selection of appropriate sites and determination of water harvesting on a large scale is difficult. (Pereira and Gowing, 2005).

Field surveys are the most common method for selecting suitable sites and Rain Water Harvesting (RWH) techniques for small areas. The selection of appropriate

sites for different RWH technologies in larger areas is a great challenge (Prinz et al. 1998). GIS and remote sensing in hydrology and water resources have relieved some of the stress from the large time and effort that has been invested in realizing spatial and temporal patterns and characteristics of individual hydrologic processes by providing access to spatial and temporal information on watershed, regional, continental and global scales (Bakir and Xingnan, 2008).

With the advent of these tools that may be used for providing an efficient water exploration means, one can suggest the best sites for extraction, storage and distribution of water to the users.

A connection between dry spells induced by drought anomalies and the need for storage system that is driven by biophysical criteria, such as rainfall, slope, soil type, drainage network, and land use, is obvious because of the country's continued dependence on effective water resource management. The correlation of spatial information technology and specified indices can analyze vulnerability of regions and help with the collection, storage, analysis, and visualization of key information and thereby help with the development of effective water resource programs and practices.

The need to address water scarcity that is exacerbated by reoccurring drought is high, now more than ever. Provision of a mechanism by which small scale water resource can be identified to relieve the stress from the existing water resources is thus essential.

1.2. Statement of the Problem

Balancing water-scarcity and population (human demand) is the major challenge in many arid and semi-arid regions of the world (Mays, 2009). Many urban areas of the world have been experiencing water shortages, which are expected to explode this century unless serious measures are taken to reduce the scale of this problem (Mortada, 2005). While these problems are not new, having been in existence for quite some time in a country with a recurring drought, never have they reached such wide spread and serious proportions. This begs the question, what is being done wrong and why isn't there an easy fix?

Ethiopia is endowed with water than many drought-prone countries (Mayes, 2009). The problem of water shortage emanates from the seasonality of rainfall and the lack of infrastructure for storage to capture excess runoff during flood seasons. Contemplating this situation, amongst drought management strategies, there needs to be a way for assessing potential water sources that possess the ability to be a solution if properly addressed.

The mean annual precipitation falling on the country amounts to 936 billion cubic meter (FAO-AQUASTAT database 2014). However owing to very few stored water resources, the current capacity only goes up to almost 32 billion cubic meters by volume (FAO-AQUASTAT database 2014). The country has only exploited 10% of its precipitation heritage: There is a rechargeable source, what is needed is a delivery system; thus water needs to be captured and stored. In such cases, rainwater harvested by local communities based on historical practices is the best option for mitigating drought.

The effect of drought is a context-dependent matter. Drought is especially a problem in areas where droughts are frequent and intense and where water resources are under massive use. In 2015 and 2016, Ethiopia was enormously affected by El Nino triggered droughts (Bachewe et al., 2016). The failure of two consecutive rainy seasons which normally feed 80-85% of Ethiopia between the months June and

September of 2015 has affected the livelihoods of many, and increased malnutrition across the country. As a consequence, it has resulted in the worst drought that has ever hit the country. This is a clear implication that proper drought preparedness means is not practiced in the country and a critical need for supplemental water supply now exists in many areas.

The country needs a source identification means that addresses or bases drought issues. A way by which water scarcity that is aggravated by recurring drought can be addressed; and a way by which small scale water resource can be identified, and put to use thereby relieving the stress from the existing water resources needs to be developed.

Previous attempts to develop water harvesting and sustainable land management have failed due to issues pertaining to unclear impact assessments, the policy environment and the history of governance. The existence of and potential for wider adoption of water harvesting practices has been largely reflected with agricultural water management being viewed as with irrigation (Abebe et al., 2012). Thus, this high demand for coordination and management has made water harvesting in Ethiopia a problem as easier means have not been considered nor found and practiced.

1.3. Objectives

The general objective of this research is to develop an applied technique for identifying potential water harvesting sites using GIS-based methods and atmospheric reanalysis datasets to address drought induced water scarcity.

The study is expected to achieve the following specific objectives:

- assess the spatial and temporal variability of metrological drought at several time scales in Ethiopia.
- develop and evaluate a methodology using remotely sensed landsat imagery and physical terrain attributes to locate potential sites for surface water harvesting.
- develop a RWH site map for Ethiopia.

1.4. Organization of the thesis

The thesis has been divided into five chapters, each with its own significance:

Chapter I Introduction: this chapter mainly deals with the rationale, need and primer of involved matter in the work. It provides an introduction to water scarcity and drought and the significance of storage by reviewing water harvesting. The drive for the thesis which is what the thesis aims to solve is depicted in the problem statement, and the general as well as specific aims that the study wishes to address are covered.

Chapter II Literature Review: is dedicated to illustrate the relevant literatures, key concept reviews and works related to drought indexing, land-use analysis and secondary terrain attributes. All adopted classifications for the indices and important associated assumptions are mentioned.

Chapter III Data Acquisition and Processing: holds the lion share of the work regarding the means practiced to achieve the objectives. This section involves the range of gathered data inputted, manipulations for fine tuning the data and use in analyzing for drought characterization and source identification.

Chapter IV Results and Interpretation: presents the analysis along with the results and discussions. The report findings are presented in a systematic manner corresponding to each methodology.

Chapter V Conclusions and Recommendations: the conclusions based on the interpretation of the study and corresponding recommendations are given in this section.

2. Literature review

When considering the sustainable use of fresh water, the amount of renewable water available is of most concern. This is of most concern when climatic variabilities and anomalies come into the equation.

A few drought management strategies were proposed by Dziegielewski et al. (1996) in response to anticipated shortages of water. These are: demand reduction options, improvements in efficiency in water supply and distribution system, and emergency water supplies. But, the problem of water shortage emanates from the seasonality of rainfall and the lack of infrastructure for storage to capture excess runoff during flood seasons (Mays, 2009).

Ethiopia ranks 57th in the world in terms of the total amount of water resources. The mean annual precipitation falling on the country amounts to 936 billion cubic meter (FAO-AQUASTAT 2014). The annual internal renewable water resources, composed of river runoff and non-repeated groundwater is about 122 billion cubic meter (FAO-AQUASTAT 2014).

Internal Renewable Water Resources (IRWR) is the long-term average annual flow of rivers and recharge of aquifers generated from endogenous precipitation. Double counting of surface water and groundwater resources is avoided by deducting the overlap from the sum of the surface water and groundwater resources. (FAO-AQUASTAT 2014). However owing to very few available resources, the current capacity only goes up 31.24 billion cubic meters by volume. Moreover, these limited water resources are unevenly distributed that most locations are not addressed.

The surface water resource potential is considerable, but little developed. Most of the rivers in Ethiopia are seasonal and about 70 per cent of the total runoff is obtained during the period June to August (Abebe et al., 2012)

Precipitation is the source of all renewable fresh water on earth. All water on the planet originates from precipitation. Part of it forms surface runoff and groundwater

flow and another part evaporates, returning to the sky. The first part comprises the water resources as commonly understood. However, water is a natural resource. In addition to the water resource development, rainwater utilization is another way to use water.

Zhu et al. (2015) describe in detail the adaptation of rainwater harvesting technology for where water resource to precipitation ratio is minimal. The approach was considered innovative and created a relief for agriculture and water supply.

Water harvesting is the process of concentrating rainfall as runoff from a catchment to be used in a target area (Narain, 2005). Rainwater harvesting technologies have become important options to supply drinking water, develop irrigated agriculture and improve the ecosystem in dry areas. Seventeen provinces in china have adopted rain-water utilization technique, building 5.6 million tanks with a total capacity of 1.8 billion cubic meters, supplying drinking water for approximately 15 million people and supplemental irrigation for 1.2 million ha of land (Zhu et al., 2015).

A study reviewed by (Abebe et al., 2012) on water harvesting practices was seen through ground water recharge by water harvesting, the case of Abreha Weatsbeha found 55Km north of Mekele in Tigray Region. The article presents an image of the location where interventions regarding soil water conservations were being done. Of these, stone check-dams, percolation ponds, deep trenches, stone/soil bunds, area closures (total protection from grazing), as well as afforestation in the higher reaches of the watershed were employed. As a result, percolation ponds harvesting water from the hillside for ground water recharge were developed. An image with the location is shown in Figure 1.



Figure 1: Percolation ponds harvesting water from the hillside to recharge groundwater (K. Woldearegay) Opportunities for building on tradition – time for action (Adane Abebe et al., 2012)

Awulachew et al. (2005) reviewed recent experiences and future opportunities for promoting small-scale irrigation and water harvesting in Ethiopia. They revealed mixed perceptions about the impacts of past initiatives.

The success of RWH systems depends heavily on the identification of suitable sites and their technical design (Al-Adamat et al., 2012). For relatively small areas (in the range of several hundred hectares) a ground truth carried out by a number of experienced people is the best technique to identify suitable areas for water harvesting. For medium range sizes of areas, the use of aeroplanes equipped with photographic equipment and for even larger areas, the application of remote sensing is considered to be the most relevant means of identification of areas suitable for certain techniques of water harvesting. For any of the above mentioned techniques, the application of a suitable GIS is indispensable. Of course, the application of even the best GIS will not guarantee the success of any water harvesting scheme, as a number of external factors such as water and land rights, macro-economic conditions, traditional rules and beliefs can hardly be incorporated into such a GIS. Nevertheless, these might strongly influence the development of the water harvesting scheme.

2.1. Drought characterization

Drought is a natural hazard characterized by a significant decrease in water availability during a prolonged period of time over a large area (Bayissa et al., 2015). It occurs in different parts of the world and may cause substantial impact on economic activities, human lives, and various elements of the environment (Dracup et al., 1980). Devising early warning systems, conducting drought risk analysis and contingency planning are only a few of the advantages of characterizing drought.

The main types of physical droughts based on the operational definition are metrological, agricultural and hydrological droughts in the order positioned respectively. Precipitation deficiency instigates metrological drought, which subsequently impacts soil moisture content (i.e., agricultural drought). Low recharge from the soil to water features such as streams and lakes causes a delayed hydrological drought (Zagar et al., 2011).

2.1.1. Metrological Drought

Drought can be considered as a strictly metrological phenomenon (Palmer, 1964). It can be evaluated as a metrological anomaly characterized by a prolonged and abnormal moisture deficiency. Indicators associated with metrological drought are used in assessing drought conditions that are dependent on the duration and magnitude of the abnormal moisture deficiency.

Drought indices are quantitative measures that characterize drought levels by assimilating data from one or several variables (indicators) such as precipitation and evapotranspiration into a single numerical value.

Complied by Zagar et al. (2011), using an index for drought characterization serves the following purposes, operationally:

- drought detection and real-time monitoring,
- declaring the beginning or end of a drought period,
- allowing drought managers to declare drought levels and instigate drought responses measures,
- drought evaluation representing the concept of drought in a region,

- correlating with quantitative drought impacts over variable scales of geography and time; and
- facilitating the communication of drought conditions among various interested entities.

2.1.2. Choice of Drought Index

Zagar et al. (2011) discussed six major drought indices that are frequently used in forecasting, monitoring, and planning operations. Of these, comparisons suggest that the SPI is widely adopted for research and operational modes for characterizing metrological drought. The SPI was chosen as “the one to use” by participants in the Inter-Regional Workshop on indices and early warning systems for drought in December 2009. The workshop was held to help determine the best metrological index and to recommend it for use by all national metrological services.

2.1.3. The Standardized Precipitation Index

The Standardized Precipitation Index (SPI) was developed by McKee et al., (1993) to give a better representation of abnormal wetness and dryness in comparison the Palmer indices. The SPI is probability based and was designed to be a spatially invariant indicator of drought that recognizes the importance of time scales in the analysis of water availability and water use. It is essentially a standardizing transform of the probability of the observed precipitation. Its fundamental strength is that it can be computed for a precipitation total observed over any duration desired by a user.

Short-term durations on the order of months (or even weeks) may be important to agricultural interests while very long term durations spanning years may be important to water supply management interests (Guttman et al., 1999). This application was seen in a study by Hayes et al. in the 1995-96 drought in the south western United States. A 5 month SPI map clearly showed dryness whereas PDSI maps did not accurately represent the true severity. SPI again provided a one month lead in recognizing drought which gave more time for policy and decision makers when devising drought mitigation and response actions.

2.1.3.1. Computational procedure

Several discussions (Thom 1996, Bayissa et al., 2016) found that the gamma distribution fit climatological precipitation series well. The gamma distribution is defined by its frequency and probability density function:

$$g(x) = \frac{1}{\beta^\alpha \Gamma(\alpha)} \int_0^x x^{\alpha-1} \exp^{-x/\beta} \quad (1)$$

Where $\alpha > 0$ is the shape parameter, $\beta > 0$ is a scale parameter and $x > 0$ is the amount of precipitation. $\Gamma(\alpha)$ defines the gamma functions.

The alpha and beta parameters of the gamma probability density function are estimated for each station, for each time scale of interest and for each month of the year. The maximum likelihood solutions are used to optimally estimate these parameters:

$$\hat{\alpha} = \frac{1}{4A} \left(1 + \sqrt{1 + \frac{4A}{3}} \right)$$

$$\hat{\beta} = \frac{\bar{x}}{\hat{\alpha}} \quad (2)$$

Where

$$A = \ln(\bar{x}) - \frac{\sum \ln(x)}{n} \text{ And } n = \text{number of precipitation observations}$$

The resulting parameters are then used to find the cumulative probability of an observed precipitation event for the given month and time scale for the station in question; the cumulative probability is given by:

$$G(x) = \int_0^x g(x) dx = \frac{1}{\hat{\beta}^{\hat{\alpha}} \Gamma(\hat{\alpha})} \int_0^x x^{\hat{\alpha}-1} e^{-x/\hat{\beta}} dx \quad (3)$$

$H(x)$ is the cumulative probability including probability of zero precipitation:

$$H(x) = q + (1 + q)G(x) \quad (4)$$

And q is the probability of zero precipitation where the gamma distribution becomes undefined, for $X = 0$ and $q = p(x = 0)$ (probability of zero precipitation is simply the number of observations of zero precipitation divided by the total number of observations).

An equiprobability transformation from fitted gamma distribution to the standard normal distribution is mentioned by Mckee (1993). But since it would be cumbersome to produce these types of figures for all stations at all times scales and for each month of the year, the Z or SPI value is more easily obtained computationally using an approximation provided by Abramowitz and Stegun (1965) that converts cumulative probability to the standard normal random variable Z:

$$Z = SPI = -\left(t - \frac{c_0 + c_1 t + c_2 t^2}{1 + d_1 t + d_2 t^2 + d_3 t^3}\right) \text{ For } 0 < H(x) \leq 0.5$$

$$Z = SPI = +\left(t - \frac{c_0 + c_1 t + c_2 t^2}{1 + d_1 t + d_2 t^2 + d_3 t^3}\right) \text{ For } 0.5 < H(x) \leq 1 \quad (5)$$

Where:

$$t = \sqrt{\ln\left(\frac{1}{(H(x))^2}\right)} \text{ For } 0 < H(x) \leq 0.5$$

$$t = \sqrt{\ln\left(\frac{1}{(1-H(x))^2}\right)} \text{ For } 0.5 < H(x) \leq 1 \quad (6)$$

$c_0 = 2.515517$, $c_1 = 0.802853$, $c_2 = 0.010328$, $d_1 = 1.432788$, $d_2 = 0.189269$, $d_3 = 0.001308$.

Conceptually, the SPI represents a z-score, or the number of standard deviations above or below that and event is from the mean. However, this is not exactly true for short time scales since the original precipitation distribution is skewed.

Mathematical programs are usually used to compute SPI values for a larger times series data as well as for multiple time scales.

2.1.3.2. SPI Advantages over other indices

The SPI calculation for any location is based on the long-term precipitation record for a desired period. This long-term record is fitted to a probability distribution, which is then transformed into a normal distribution so that the mean SPI for the location and desired period is zero (Edwards and McKee, 1997). Positive SPI values indicate a greater than median precipitation and negative values indicate a less than

median precipitation. Because the SPI is normalized, wetter and drier climates can be represented in the same way; thus, wet periods can also be monitored using SPI.

After the analysis on two separate droughts characterized by SPI, (Hayes, 2000) concluded that SPI accomplishes the objectives of a drought index in its ability to identify the intensity, duration, and spatial extent of droughts as they occur, providing monitoring at a near real-time level and serves quite well as a tool for an early warning system.

This standardization allows SPI to determine the rarity of a current drought event, as well as the probability of the precipitation necessary to end the current drought (McKee et al., 1993). It also allows the SPI to be computed at any location and at any number of time scales, depending upon the impacts of interest to the user. This and its availability for computation using any of the many probability distribution models studied for the index by Guttman (1999) are what makes the index desirable. The fact that the index is tractable for machine data processing for identified probability distribution makes it more desirable as it clearly recognizes that many users of the SPI would want a black box software package for which the input is precipitation time series and the output is the SPI.

Standardization of the procedure for computing the SPI is necessary so that all users are able to calculate index values which are comparable both spatially and temporally. If the same observed precipitation time series leads to different SPIs that depend on the computational procedures, then comparisons will not be of like quantities, and the comparisons will be confusing or misleading.

2.1.3.3. Choice of dataset

The sole input for metrological drought analysis is precipitation. For a study domain as large as Ethiopia, acquiring a uniformly distributed, long term historical rainfall data can be achieved easily by taking advantage of advances in remote sensing technology; viz. satellite-based rainfall estimates. (Bhatti et al., 2016).

The Climate Forecast System Reanalysis, completed over the 31-year period of 1979 to 2009 in January 2010, as stated by Saha et al., (2010) is more comprehensive because it includes analyses of both the ocean and sea ice, and it has higher resolution in space and time. The accuracy increases over time, especially in the Southern Hemisphere, where the use of satellite radiance data becomes very important. Many known errors in the observational data and execution of previous reanalysis were corrected in the CFSR. Many of the input datasets have been improved by years of quality control and by exposure to successive reanalysis at various centers.

For inter-annual variability, the CFSR shows improved precipitation correlation with observations over the Indian Ocean, Maritime Continent, and western Pacific (Wang et al., 2010). All aspects of the CFSR is open to the public (available online at (<http://cfs.ncep.noaa.gov/cfsr>)). Saha et al., (2010) describes features and data assimilation, forecast models and so on and with the accuracy measured using the 5-day forecast scores and concluded that CFSR is considerably more accurate than the previous global reanalysis made at NCEP in the 1990s. The efficiency of the recently released climate forecast system re-analysis (CFSR) dataset in capturing the daily rainfall patterns of Ethiopia is good (Berhanu et al., 2016). due to the global-level correction performed at the time of release, it induces some local-level bias.

2.1.3.4. Correcting Bias

Accuracy of CFSR data has to be evaluated and compared with ground truth rainfall measurement before use. Fang et al., (2015) mentioned five bias correction methods used for precipitation. These include Linear Scaling (LS), Local Intensity Scaling (LOCI), Power Transformation (PT), Distribution Mapping for precipitation using gamma distribution (DM) and Quintile Mapping (QM). Of which Linear scaling bias correction aims to match the monthly mean of corrected values perfectly with that of the observed ones (Lenderink et al., 2007).

This method is a mean based method which considerably reduces the deviation in the mean of observed and simulated data. The observed precipitation is corrected by a factor which is the ratio of long term monthly mean of observed and raw simulated precipitations (Beineke and B.S. Panda., 2016) and is given by:

$$P_{cor(m,d)} = P_{raw(m,d)} \frac{\mu(P_{m,obs})}{\mu(P_{m,raw})} \quad (7)$$

Here $P_{cor(m,d)}$ and $P_{raw(m,d)}$, are the corrected and raw simulated precipitation for d^{th} day of m^{th} month respectively and $\mu()$, represents the mean operator.

To test the accuracy of the bias corrected data set, frequency-based indices and time series performances against observed precipitation data need to be conducted (Berhanu et al., 2016). The frequency-based indices include mean, median, standard deviation, 90th percentile, probability of wet days and intensity of wet days. The time series-based metrics include the Nash-Sutcliffe measure of efficiency (NSE), the root-mean-square error (RMSE) and the percent bias (PBIAS). NSE indicates how well the simulation matches the observation, and it ranges between $-\infty$ and 1.0, with NSE=1 indicating a perfect fit. Readers are referred to the details of the performance evaluations done and adopted to the prior research by Berhanu et al. (2016).

2.1.3.5. Time scales in SPI

The SPI was designed to quantify the precipitation deficit for multiple timescales. These timescales reflect the impact of drought on the availability of the different water resources. Soil moisture conditions respond to precipitation anomalies on a relatively short scale. Groundwater, stream flow and reservoir storage reflect the longer-term precipitation anomalies. For these reasons, McKee et al., (1993) originally calculated the SPI for 3-, 6-,12-, 24- and 48-month timescales.

Andreau et al. (2007) computed SPI results in both short term (1 month – 9 months) as well as long term (12 months – 36 months) presenting a distributed SPI index for the whole extension of a basin study. The paper was able to characterize extreme low rainfall events using a 12 month SPI and was also able to identify that the short term values (1, 3, 6 months) displayed drought persistency well.

Drought categorization is often related to contextual-use. The phenomenon reflected and the type of impacts associated to the specific duration give SPI another added advantage. Table 1 shows how the SPI reflects different type of impact or application. Apart from addressing metrological anomalies, SPI can be deployed for longer time scales to reflect agricultural and hydrological droughts/impacts (Zagar et al., 2011).

Table 1: Application of the SPI in different time scales

SPI duration	Phenomena reflected	Application
1 month SPI	Short-term conditions	Short-term soil moisture and crop stress (especially during the growing season)
3 month SPI	Short- and medium-term moisture conditions	A seasonal estimation of precipitation
6 month SPI	Medium-term trends in precipitation	Potential for effectively showing the precipitation over distinct seasons.
9 month SPI	Precipitation patterns over a medium time scale	If SPI ₉ < -1.5 then it is a good indication that substantial impacts can occur in agriculture (and possibly other sectors)
12 month SPI	Long-term precipitation patterns	Possibly tied to stream flows, reservoir levels, and also groundwater levels

Nearly all metrological drought analysis that used SPI have comprehended a similar threshold definition. SPI values higher (lower) than 2.00 (-2.00) can be considered to represent extreme wet (dry) events (Guttman, 1999). Mckee et al. (1993) used the most applied classification system shown in Table 2 to define drought intensities resulting from SPI. The classification was also used to define the three dimensions by which it is fundamentally characterized: severity, duration and spatial distribution. Additional characteristics include: frequency, magnitude (cumulated deficit), predictability, rate of onset and timing (Zagar et al., 2011).

A drought event occurs any time the SPI is continuously negative and reaches an intensity of -1.0 or less. The event ends when the SPI becomes positive. Each drought event, therefore, has a duration defined by its beginning and end, and an intensity for each month that the event continues. Because of drought's dynamic nature, a region can experience wet and dry spells simultaneously when considering various timescales. The positive sum of the SPI (in other words the accumulated deficit of water below a threshold) for all the months within a drought event can be termed the drought's "magnitude" (McKee et al., 1993). This is given by

$$DM = - \left(\sum_{j=1}^x SPI_{ij} \right) \quad (8)$$

for any timescale.

Frequency is described by Zagar et al. (2011) as the average time between drought events that have a severity that is equal to or greater than a threshold. Yared et al. (2015) described frequency of drought occurrence by developing a trend in the graph of SPI values for the period under study. Strong trends of increasing frequency were easily identified as events with high return periods.

Wu et al. (2006) constructed a frequency distribution plot showing dry and wet categories resulting from 1, 4, 8, and 12 week SPI values for different periods showing the uneven behavior of frequency with event category for varying time scales at varying months.

Table 2: SPI classification (McKee 1993)

SPI	Classification	Probability
2.00 >	Extremely wet	2.3
1.50 to 1.99	Very wet	4.4
1.00 to 1.49	Moderately wet	9.2
0 to 0.99	Mildly wet	34.1
0 to -0.99	Mild drought	34.1
-1 to -1.49	Moderate drought	9.2
-1.50 to -1.99	Severe drought	4.4
-2.00 <	Extreme drought	2.3

Apart from signifying the basics involved in drought characterization, major abnormalities can also be checked according to the classification in Table 2. On the basis of an analysis of stations across Colorado, McKee et al. (1993) determined that the SPI is in mild drought 24% of the time, in moderate drought 9.2% of the time, in severe drought 4.4% of the time, and in extreme drought 2.3% of the time. These percentages are expected from a normal distribution of the SPI (Wu et al., 2006).

A study conducted in Greece resulted in an effective information and early warning system based on SPI to produce an overall adaptation plan. The study also showed that it depicted the drought conditions all over Greece with results showing when the drought began, when it peaked and when it dissipated. As a means of checking the accuracy of these results, water supply areas where the impact of the drought were intense were used to compare with the results from the SPI which is quite commendable. A shortcoming of this study is that all topologically different zones weren't all considered due to fragmented metrological information which would have contributed to the SPI approach. But in this study, a bias corrected CFSR data covering the entire region (high and low lands considered) on grid level is available to avoid this shortcoming.

Another flaw in SPI is that it lacks the ability to identify regions with greater tendency to droughts, equally represents both wet and dry, requires knowledge of the local climatology (Zagar et al., 2011) which shows that the best quality of SPI is in its ability to identify temporal characteristics rather than the spatial ones.

Another drawback is shown in a study by Hu and Willson (2000), highlighting that potential evapotranspiration is a valuable additional indicator since the index is loosely connected to ground conditions. The concept of contextual-use is key in tricking the index to work in ones favor.

Monitoring of changes using remote sensing technology is widely used in different applications, such as land use/cover change, disaster monitoring, forest and vegetation change, urban sprawl, and hydrology. Surface water is one of the

irreplaceable strategic resources for human survival and social development. Reliable information about the spatial distribution of open surface water is critically important in various scientific disciplines, such as the assessment of present and future water resources, climate models, agriculture suitability, river dynamics, wetland inventory, watershed analysis, surface water survey and management, flood mapping, and environment monitoring (Rokni et al., 2014).

2.2. The Normalized Difference Vegetation Index

NDVI, commonly depicted as a satellite based remote sensing for drought monitoring began in the 1980s. It is a simple mathematical transformation of two commonly available spectral bands (visible red and near infrared). This index is most commonly used because it has a very strong relationship with several biophysical parameters of vegetation (Wardlow et al., 2012).

The Normalized Difference Vegetation Index (NDVI) was agreed that it was the most efficient and simple metric to identify vegetated areas and their condition (Tucker, 1979). Normalization has many advantages, including minimizing directional reflectance and off-nadir viewing effects; reducing sun-angle, shadow, and topographic variation effects; and minimizing aerosol and water-vapor effects (Holben, 1986). This normalization enabled large-scale vegetation monitoring allowing comparison of different regions through time.

Theoretically, NDVI values can range between -1.0 and $+1.0$. However, the typical range of NDVI measured from vegetation and other earth surface materials is between about -0.1 (NIR less than RED) for non-vegetated surfaces and as high as 0.9 for dense green vegetation canopies (Tucker, 1979).

Over the past years, the NDVI has been widely used in many terrestrial applications. A study conducted by (Gadiso, 2007) on drought assessment for the Nile basin using meteosat second generation for the upper Blue Nile region denotes the clear limitation of using remote sensing for drought monitoring. For this reason, this research attempts to use NDVI as a tool for its strength in terrestrial applications: land cover classification.

In the process of evaluation, a water body is commonly regarded as an individual land object to be distinguished from others (Wei Ji, 2007). According to the characteristics of spectral reflectance of water body and vegetation, the near-infrared band is the most useful in distinguishing the land-and-water boundary and ground vegetation (Zhen and Chen 1995). Wavelengths that range from 0.62 to 67 μm and 0.84 to 0.87 μm , respectively, match bands 3 and 4 of the landsat Thematic Mapper (TM) images. These two bands were used to identify vegetation and water body. The most common NDVI classification given by USGS, 1998 category under Albedo values for different cover types followed the following ranges.

Table 3: The NDVI classification (<https://landcover.usgs.gov/landcoverdata.php>)

Cover Type	NDVI - low range value
Dense green leaf vegetation	0.5 - 1.0
Medium green leaf vegetation	0.14 - 0.5
Light green leaf vegetation	0.09 - 0.14
Bare soil	0.025 - 0.09
Clouds	0.002 - 0.025
Snow and Ice	-0.046 - -0.002
Water	-0.257 - -0.046
Deep water	-0.257 - -1

Thenkabail (2016) provided under the section 'Automated Methods of wetland Delineation and Mapping' where it was confirmed that values in the range -0.25 to 0.10 was regarded the appropriate threshold values that best delineated wetlands. This classification happens to generalize the scale denoted in Table 3.

Rokni et al. (2014) compared different feature extraction techniques for surface water extraction from landsat data. These included the Normalized Difference Water Index (NDWI), Normalized Difference Moisture Index (NDMI), Modified Normalized Difference Water Index (MNDWI), Water Ratio Index (WRI), Normalized Difference Vegetation Index (NDVI), and Automated Water Extraction Index (AWEI). After

analysis, the results showed that the NDMI was incapable of extracting the water surface of the Lake under analysis, while the NDWI and NDVI provided the highest accuracy results. The NDVI was developed mainly for separating green vegetation from other surfaces. However, it did perform well for surface water detection. Hence, this research favored the use of this index keeping the environmental gain in mind.

2.3. Identifying moisture characteristic areas – TWI

In digital terrain analysis, there exist two major types of attributes: Primary and Secondary attributes. The primary attributes include slope, aspect, plan and profiles, flow path length and upslope contributing area. The secondary attributes on the other hand are computed from two or more primary attributes and are important because they offer an opportunity to describe pattern as a function of process. (Wilson and Gallant, 2000)

These attributes contribute towards redistributing water in the landscape and affect soil characteristics, distribution and abundance of soil water, susceptibility of landscapes to erosion by water, distribution and abundance of flora and fauna.

These compound attributes may be derived empirically, or by simplifying equations describing the underlying physics of the processes. Topographic indices provide a knowledge-based approach to soil specific management and analysis and can be imbedded within the data analysis subsystems of a GIS. Because many GIS are based on a pixel or raster structure (i.e., grid cell), grid based methods of terrain analysis can provide the primary geographic data for GIS applications (Moore et al., 1993).

One of the topographic indices that incorporates these primary attributes which is extensively used to describe effects of topography on the location and size of saturated sources areas of runoff generation is known as Topographic Wetness Index and is given by

$$TWI = \ln \left(\frac{A_s}{\tan \beta} \right) \quad (9)$$

Where A_s is the specific catchment area (m^2m^{-1}) and β is the slope angle (degrees).

Some terrain indices account for factors other than topography that may influence soil moisture patterns, notably soil characteristics (Beven, 1986) or available energy from solar radiation (Moore et al., 1991). However, a more complex index does not necessarily ensure better predictions of soil moisture status.

Wilson and Gallant (2000) defined the attributes involved in this computation and their significance. The slope is a measure of gradient and is significant in defining overland and subsurface flow velocity and runoff rate, precipitation, vegetation, geomorphology, soil water content and land capability class. It is a means by which gravity induces flow of water by measure of change in elevation in the direction of steepest descent.

The upslope contributing area, often referred to as drainage/catchment area, is the area draining to catchment outlet and is significant in obtaining the runoff volume. The upslope contributing area was found to be the most important single factor explaining the spatial pattern of saturated areas in a study (Guntner, 2004).

When calculating these areas from gridded DEMs, the contour length is approximately the size of a single grid cell, and in the simplest case, the contributing area is determined by the number of cells contributing flow to that single cell.

Contributing areas are computed using different approaches as stated by Wilson and Gallant (2000). Among these, a short review on the single flow direction (D8) method and multiple flow direction method (FD8) is shown below.

The single flow direction algorithm is frequently used for determining contributing areas, primarily because of its simplicity. The D8 algorithm developed by O'Callaghan and Mark (1984) allows flow from a cell to only one of eight nearest neighbors based on the primary flow direction. Because flow can accumulate into a cell from several upslope cells but only flow out into a single cell.

A study conducted in Cottonwood Creek (Wilson and Gallant, 2000) showed a successful use of the D8 method for computing the upslope contributing area. It was shown that the valley bottoms were clearly defined as a line of high contributing area cells, and the ridges were identified as areas of low contribution. A flaw mentioned in various works regarding the single flow algorithm and also mentioned in this study is that this method tends to produce flow in parallel lines due to the fact that convergence of valleys is insufficient to force lines together. This significantly distorts the spatial pattern of the contributing area and results in values that are relatively unrealistic.

The multiple flow algorithm on the other hand allows flow to be distributed to multiple nearest-neighbor nodes in upland areas above defined channels and uses the D8 algorithm below points of presumed channel initiation. The FD8 algorithm gives a more realistic distribution of the contributing area in upslope areas, while also eliminating D8's parallel flow paths. (Wilson and Gallant 2000)

TWI, as a combination of the two, defines areas of saturated soil typically found in geomorphologically convergent segments. The estimation of both upslope contributing area and specific catchment area are dependent on the estimation of flow direction(s) from a given node. As such, the index depends on the method by which the parameters are computed.

The TWI equation incorporates the following seven key assumptions and limitations. (Beven and Kirkby 1979, Moore and Hutchinson, 1991)

1. The approach assumes that the steady-state downslope subsurface discharge is the product of average recharge and specific catchment area.
2. It assumes that the local hydraulic gradient can be approximated by local slope.
3. It assumes that the saturated hydraulic conductivity of the soil is an exponential function of depth.
4. It assumes steady-state conditions.

5. It assumes spatially uniform soil properties (in particular, soil transmissivity). As justified by Wood et al. (1990): the topographic component of the index dominates over the soil transmissivity at sub catchment scale. The spatial distribution of topographic attributes may capture the spatial variability of soil properties at the mesoscale because pedogenesis of the soil catena often occurs in response to the way water moves through the landscape in areas with uniform parent material.

This assumption is one of the most important assumptions that most have debated on and even attempted to find a work-around for, but, a general limitation of the type of deterministic index approach is the difficulty of quantitatively including categorical attributes such as geological features (like fractures or strata boundaries). Lack of the capacity to easily obtain and signify these factors allows for the assumption of a uniform soil property.

6. This approach implies that the locations in a catchment with the same value of the topographic wetness index will also have the same relationship between the local depth to the water table and the mean depth.
7. This approach also implies that those points with the same value of the topographic wetness index will respond in a similar way to the same inputs.

Index values may vary depending on the algorithm used for the calculations and by the manner in which topographic information is explored. For instance, the upstream contributing area can vary depending on whether or not topographic sinks were filled in the model. Wilson and Gallant (2000) in mapping Cottonwood Creek showed that a steady-state topographic wetness index depicts values over 8.5 to be areas of high contribution and areas below 5.5 to be low saturation areas. Commonly computed values fall within the range of 3-33, where smaller values indicate low saturation and high values indicate high water saturation levels.

This research combines the best features of land use analysis described above through remote sensing and features of topographic attributes that define saturated soil to be an indicator of potential water harvesting points.

3. Data acquisition and processing

The chart in figure 2 provides a preliminary outlook towards how the entire research is done. The summarized methodology defines the input required, the methodology behind each input and the corresponding output. Where the objects in the middle show the input, the objects on the left show the process required to bring about the objectives and the items on the right give the output at different levels of the work. The main objective of this research, i.e. developing a RWH map of Ethiopia that addresses drought was achieved by combining the best features of remotely sensed landsat analysis and secondary topographic attributes which were initially supported by drought indicators.

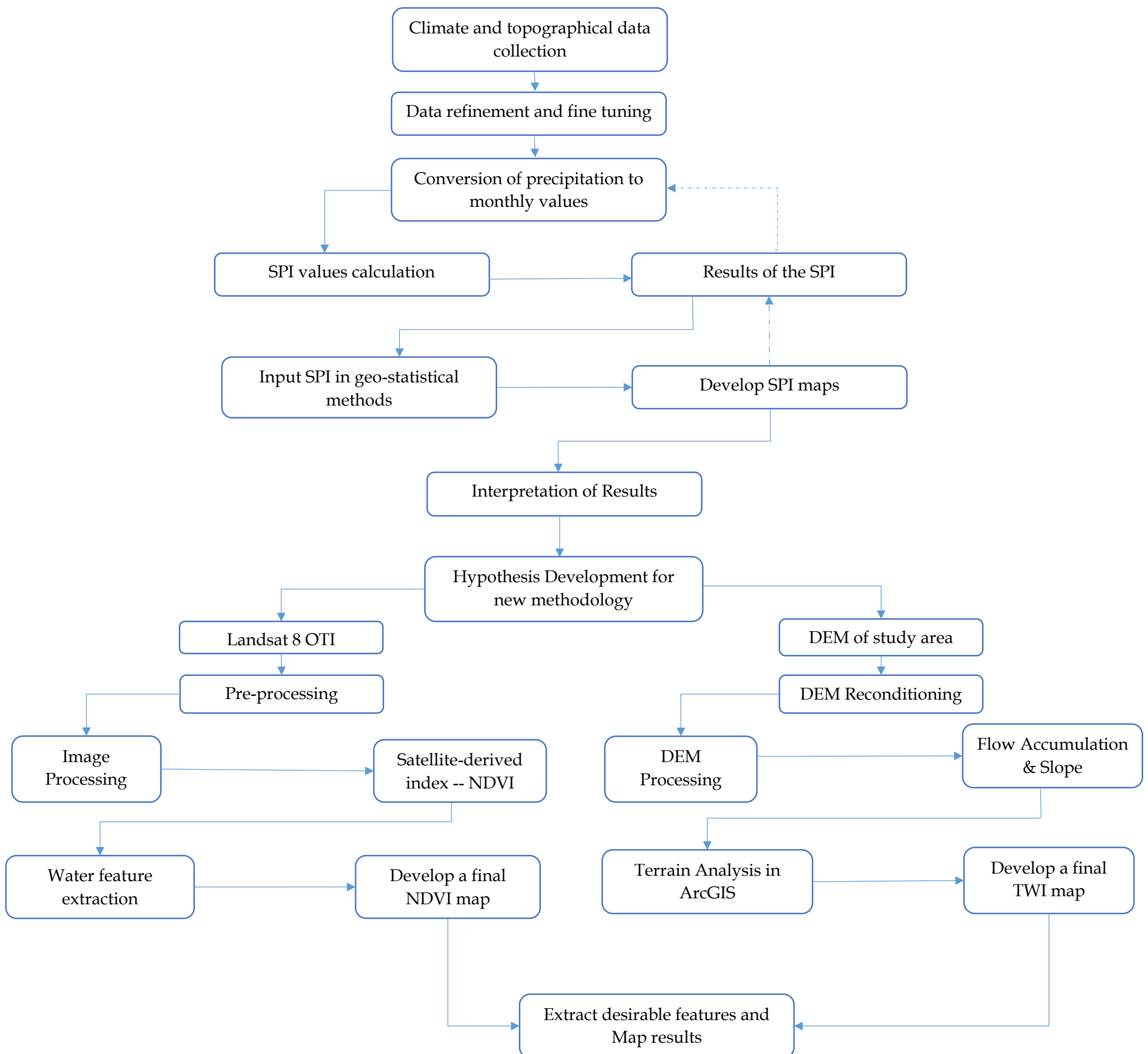


Figure 2: Methodological flow chart

3.1. Description of study area

Ethiopia is located in the northeastern corner of Africa between latitudes 3° and 15° North and longitudes 33° and 48° East. The country, which is the second most populous and the 9th largest in Africa, has an area of about 1.13 million km² of which 1.12 million km² is land area and the remaining 7,444 km² is water area (rivers, lakes, ponds etc.) (Berhanu et al., 2013).

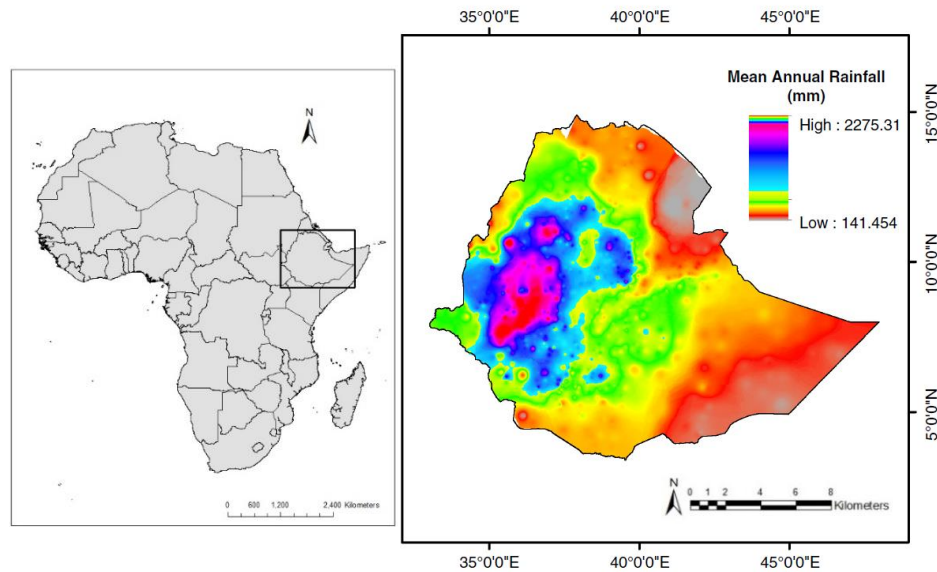


Figure 3: The location map of the study area

The sources of moisture that accounts for almost all rains in the country are the Indian and Atlantic Oceans. Southeasterly winds during the months February to May carry moisture from the Indian Ocean into the most parts of the country, while southwesterly as well as southeasterly winds bring moisture during June to September, the main rainy season (Degefu, 1988) As a general rule, rainfall should decrease as one moves from south to the north but this situation is modified by the topography of the country.

Although Ethiopia's complex relief defies easy classification, five topographic features are discernible. These are the Western Highlands, the Western Lowlands, the Eastern Highlands, the Eastern Lowlands, and the Rift Valley. The Western Highlands are the most extensive and rugged topographic component of Ethiopia. While the highlands are the main sources of water, the lowlands have expanses of flat lands through which the accumulated flows travel from the highlands to the

lower riparian countries (Bayissa et al., 2017). The transition between lowlands and highlands is commonly very sharp, resulting in a variety of climates, from very arid to very humid typical of equatorial mountains, with further differentiation at local scale. Moreover, precipitation varies with latitude, decreasing from south to north (Fazinni et al., 2015) with droughts occurring more frequently in all parts of the country for over 15 years (Viste et al., 2012).

Drought was recorded as long as 250 BC, but the rate of reoccurrence and the destructive aftermath of droughts affecting different regions of the country are totally unprecedented (Milkiyas, 2011). For some parts of the country, “Kiremt” is the main rainy season in which about 85-95% of the food crop of the country is produced (Degefu, 1987). The “Kiremt” rain, which begins around the end of May, overtaking the “Belg” rain, in the southwestern part of the country, gradually moves in the northern and northeasterly direction until by mid-July it approaches the northern tip of the country. The “Kiremt” rain ceases in the north around the end of August, with the retreat of the Inter Tropical Convergence Zone (ITCZ), which gradually moves southward until by early October, most of the country comes under the influence of the northeasterly trade winds.

Such a complex metrological framework is reflected by the distribution of annual precipitation. In the Danakil depression, it is constantly less than 250 mm but can be as low as 50 mm. By contrast, on the highlands, 2,000 mm can be locally exceeded. Similar values of annual precipitation, however, are recorded also in the southwestern lowlands, likely due to a larger contribution of the spring rains (Fazinni et al., 2015, Viste et al., 2012). Mean annual potential evapotranspiration varies between 1700 and 2600 mm in arid and semi-arid areas and 1600 and 2100 mm in dry sub-humid areas (Adane Abebe et al., 2013).

Three sets of data of the entire domain are required for analysis of the separate indices used for this study; precipitation, land use and topographical data. The following section presents the specific datasets and associated fine tuning mechanism employed for each.

3.2. Dataset

3.2.1. Satellite data

Daily gridded bias corrected CFSR precipitation dataset with 38Km spatial resolution starting from 1 January 1979 to 31 December 2010 that was corrected for bias was made available from a previous study (Berhanu et al., 2016) from which the raw data was obtained from <http://rda.ucar.edu/pub/cfsr.html>. From the available Remote Sensing (RS) rainfall products, the CFSR dataset was selected for this study for a few reasons.

The CFSR differed from the earlier reanalysis in that the first guess fields were from a 6-h coupled forecast, and not from an integration of an atmosphere-only model forced by the SST (Wanget al., 2010). And on a study conducted on Lake Tana River basin, CFSR satellite rainfall estimate for both point-to-grid and areal comparisons had better captured the rainfall pattern than that of TRMM satellite rainfall accounts (Worqlul et al., 2014).

Daily gridded raw precipitation data set with 22Km spatial resolution starting from January 1, 2011 to December 31, 2016 was directly accessed from the Global Precipitation and Climate Center (GPCC) under the framework of the Variability Analyses of Surface Climate Observations project. The data set was accessed via Netcdf format which has a complex multidimensional nature constituting of time bands, precipitation data as well as location in terms of longitude and latitude. This was manipulated in R to compile to 2232 grid point files as time series excel files using the following syntax.

```

# Script to convert netcdf to csv
# install.packages("ncdf4")
# load the library
library(ncdf4)
library(xlsx)
#Set your working directory here where you saved the netcdf files
setwd("C:/Users/etiopia/Desktop/files_needed/")
# for multiple files
file = list.files("C:/Users/etiopia/Desktop/files_needed/",full.names=TRUE,pattern=".nc")
print(file)
# loop through the files in file

v<-c(1:3790)
for (i in v){
filename = file[i]
data <- nc_open(filename)
print(data)

# getting the variables and data
lon <- data.frame(ncvar_get(data,"lon"))
lat <- data.frame(ncvar_get(data,"lat"))
time <- data.frame(ncvar_get(data,"time"))
pcp <- ncvar_get(data,"PRATE_L1_Avg_1")
# transposing lat and converting it to data frame
lat = t(data.frame(rbind(0,lat)))
# loop through the time intervals
for (t in 1:4)
{
pcp_flux = data.frame(pcp[,t])
pcp_flux= cbind(lon,pcp_flux)

colnames(lat)<- colnames(pcp_flux)
pcp_flux= rbind(lat,pcp_flux)

# writing the file
write.table(pcp_flux, paste(filename,t,"pcp.csv",sep = ""), sep=",", col.names=F, row.names=F)
}
}

```

A reconditioned digital elevation model of Ethiopia at 30-m for topographic classification as well as for use as a co-variable in interpolating rainfall was obtained from hydro-sheds USGS which can be accessed via (<https://hydrosheds.cr.usgs.gov>).

Landsat imagery to be used for land use analysis for each month for specific years was downloaded from earthexplorer (<https://earthexplorer.usgs.gov>) and obtained via The Bulk Download Application (BDA): a tool for downloading large quantities of satellite imagery and geospatial data. According to accuracy and availability, all bands corresponding to the years was downloaded. Land sat imagery for all months in the year 2002 was obtained in the form Landsat 4/5 TM C1 - Level 1 and that of

2015, in the form of landsat 8 OLI/TIRS C1 Level-1 with varying number of images covering the available spatial range.

3.2.2. Weather station data

Observed precipitation data was acquired from the NMA of Ethiopia for the period of 1979-2010. This dataset is the long term mean monthly rainfall from 221 rain gauge stations irregularly distributed throughout the country. Additional monthly rainfall data for performance evaluation was also obtained for the years 2011-2015 that was used for comparison at specific locations corresponding to the distinct rainfall regimes of the country.

3.3. Data Processing and Analysis

This research, as one objective, takes up the operational definition of drought which objectively defines criteria for drought start, end and severity for all preceding analysis. Thus, the research goes about the data processing in consecutive stages where one is input to the other. The first stage of the data manipulation is conducted with regards to input required for drought analysis. This involves making the satellite data usable for drought analysis.

Even though the CFSR rainfall data was selected, it cannot be used directly as it is bound to have some bias. For this reason, the accuracy has to be evaluated and compared with ground truth rainfall measurement before using it for further analysis in this study.

In order to maintain uniformity, a prior devised methodology used in bias correcting CFSR dataset called Linear scaling bias correction method was selected for this research. The linear Scaling (LS) bias correction technique, which is often preferred for magnitude bias correction, was previously selected to adjust the 32 year (1979–2010) daily dataset (Berhanu et al., 2016). This method also aims to match the monthly mean of corrected values perfectly with that of the observed ones (Lenderink et al., 2007).

The Linear scaling bias correction operates with monthly correction values based on the difference between observed and raw data. The change factor for precipitation is a multiplier that is computed from the ratio of the monthly mean of the observed to the raw dataset (Berhanu et al., 2016)

$$P_{d, cor} = P_{d, raw} \left(\frac{\mu(P_{m, obs})}{\mu(P_{m, raw})} \right) \quad (10)$$

Where $P_{d, cor}$ is the corrected daily precipitation and $P_{d, raw}$ is the daily raw precipitation data from CFSR. In this case, $(P_{m, obs})$ is the long-term mean monthly rainfall of observed data, and $(P_{m, raw})$ is the long-term mean value of the monthly raw CFSR rainfall data.

For observed data, information on precipitation is available and was collected from ground based metrological gauging stations. Since ground-based rainfall observation station networks are unevenly and sparsely distributed, for area coverage, estimates were spatially interpolated using the co-kriging approach with elevation as a covariant to arrive at representation of spatially distributed rainfall fields. Co-kriging was selected because it offers a good representation of the spatial coverage of precipitation over the domain.

For each month, elevation was used as a covariant to obtain a uniformly distributed mean monthly rainfall data corresponding to the available grid points.

Mean monthly rainfall values from the observed dataset ranged from a minimum of zero to a maximum 385.78mm and the corresponding gridded raw rainfall amount ranged from zero to 83mm rainfall per month.

All manipulations to compute the Linear Scaling factor for all 2232 grid points spatially covering Ethiopia as well as for correcting the raw precipitation corresponding to the grids was programmed using Visual Basic Application in Microsoft excel following the provided procedure. A number of VBA codes have been written to reach the results and a sample is shown.

```

Private Sub command()

Dim sheet As Worksheet
Dim wb As Workbook
Dim wb2 As Workbook
Dim jname As String
Dim i As Integer

Set sheet = Workbooks("Separated_o.xlsm").Worksheets("parameters")

For i = 1 To 949

'destination file name
jname = sheet.Cells(i, 1).Value
'activate sheet
'Find the current path for this file to use in opening workbooks in the same directory
    Dim rootPath As String
    rootPath = ThisWorkbook.Path
    On Error Resume Next

'open the destination workbook
Set wb2 = Workbooks.Open(rootPath & "\wbks\" & jname & ".xlsx")

Workbooks("Separated_o.xlsm").Sheets(i).Activate
'get file from list on the sheet

    Dim fname As String
    Dim j As Integer
    For j = 2 To 5
        'Workbooks("Separated_o.xlsm").Sheets(i).Activate
        fname = Sheets(i).Cells(j, 5).Value

'file name is located on the 3rd column
'process the data arrangement
        Set wb = Workbooks.Open(rootPath & "\finished\" & fname & ".xlsx")

'activate the sheet

Sheets("Sheet3").Select
Sheets("Sheet3").Copy Before:=Workbooks(jname & ".xlsx").Sheets(1)
wb.Save
wb.Close

Workbooks("Separated_o.xlsm").Sheets(i).Activate
Next j
wb2.Save
wb2.Close

Next i
End Sub

```

After the correction, in order to maintain compatibility and to finalize the time series data, a theissen polygon was constructed to match the previous 949 grid points with 38Km resolution with the current 2232 grid points with 22Km resolution. Simple averaging techniques were used for this conversion and a complete and continuous

38 years daily bias corrected CFSR precipitation dataset for 949 grid points with 38Km resolution was obtained.

A performance evaluation was carried out to prepare the precipitation data for drought characterization. Two sets of evaluations were carried out in this section. The first evaluation is simple but a necessary one that was conducted to check the accuracy of the program written to manipulate multiple data for multiple grid points. This evaluation, as mentioned in the literature section, focused on both frequency and time-series matrices. The comparison targeted the interpolated, mean monthly observed rainfall on one side, and the bias corrected daily data, converted to averaged monthly values on the other. If the results from the evaluation are acceptable, then the program coded for the purpose of bias correcting the data is accurate enough, which means monthly grid based comparisons can be conducted.

The second comparison (i.e. Grid-based comparison) was done by preselecting 12 representative grid points from the 12 rainfall regimes that appportion the study area. Following this, computation of the corresponding frequency and time series matrices, namely the mean, median, standard deviation, 90th percentile, NSE, RMSE and PBIAS was done.

Data correction for Landsat imagery and DEM was not necessary as both are delivered with the necessary corrections, i.e. radiometric and geometric corrections and reconditioning respectively.

3.4. Spatio-Temporal assessment of Metrological drought

Long-term record (1979-2016) daily CFSR precipitation dataset was accumulated to generate a monthly time series that was used to study the spatial and temporal extent of metrological drought in the country.

The Standardized Precipitation Index approach was used for the analysis. Guttman, (1997) recommended that the SPI be used as a primary drought index over Palmers index, another contender in use as a drought characterizing tool, because it is simple, spatially invariant in its interpretation, and probabilistic so that it can be used in risk and decision analysis. It can also be tailored to time periods of concern to the user. On the contrary, it was noted that the other most commonly used tool, the PDSI, is very complex, spatially variant, difficult to interpret, and has an inherent fixed time scale of about 9-12 months. This implies that the spatial and temporal comparisons of PDSI values may be misleading and erroneous. For these reasons, SPI was the most appropriate and suited tool to use.

It is apparent that there are indeed some limitations to using this index. Two key limitations i.e. consideration of evapotranspiration and lacking the ability to analyze multi-year drought conditions have been flagged in this study, which may have been necessary for drought analysis. This research did not quantify the Evapotranspiration when computing the drought index due to the fact that the main drought driving factor considered for water harvesting in this study is precipitation and for this level of analysis reliable ET estimates for the entire study period and study area are not available and/or are very hard to test and verify.

Multi-year drought analysis was also not considered as small scale drought driven water harvesting structures are intended for a relatively short period of time. Hence individual-year based analyses were considered to be sufficient for this study.

The SPI is computed in three stages making use of the index's versatility of variable time scale computation. Yearly, seasonal and monthly SPI for all 949 grid point

values were computed using R programming. A sample syntax making use of the SPI package in R is shown.

```
# install.packages("spi")
# install.packages("xlsx")
# load the library
library(spi)
library(xlsx)
setwd("C:\\Users\\etiopia\\Desktop\\New Folder")
v<-c(1:100)
for(i in v){
  filename = paste("sheet", format(i), ".txt", sep="")
  sheetname= paste("sheet", format(i), ".txt", sep="")
  data<-spi(3,filename,1979,2016)
  if(i==1)
  write.xlsx(data,"C:\\Users\\etiopia\\Documents\\ResultstoExcel\\Sheet(i).xlsx",sheetName=sheetname)
  else
  write.xlsx(data,"C:\\Users\\etiopia\\Documents\\ResultstoExcel\\Sheet(i).xlsx",sheetName=sheetname,
  append=TRUE)
  i=i+1
}
```

Defining SPI for each grid point representing the spatial extent of the domain is highly tedious, hence a less demanding computerized program in R programming was used for all SPI computations following the procedure mentioned in the literature section where input is a precipitation time series and for which the output is the SPI converted back to excel format. The method follows the standard procedure which mimics computing z-score where the latter uses normal distribution and the prior uses Gamma distribution. The SPI-based drought classes proposed by McKee et al. (1993), were adopted in this study, because of their wider applicability to different regions of climatology (Kumar et al. 2009).

3.4.1. Spatial drought assessment

The spatial patterns of metrological drought were studied over the country within the study period. Since drought is a regional phenomenon, the point-based SPI time series values of each metrological station were interpolated using the co-kriging technique to assess the spatial extent of drought in the study area.

Three SPI based analysis: yearly, seasonal and monthly analysis were done pertaining to the spatial drought assessment.

3.4.2. Yearly analysis

Monthly precipitation data were summed to twelve month values in order to use as input in R. Emphasizing the relative context of drought, the program compares the consecutive twelve month sums with that of the preceding and following twelve months. This yearly SPI, based on McKee's (1993) classification, was used to identify specific drought years from the long term record that will be used for further analysis. The identification was done on a spatial scale by converting the SPI values computed at each grid point to spatial products that show the percentage shares of the drought categories over the country.

The performance of this Index was evaluated on how well it characterized the known historic drought years (i.e. 1980, 1984, 1995, 2002, 2009, and 2015) by cross referencing from previous studies and EM-DAT, the international disaster database which is compiled from different sources and can be accessed through (<http://www.emdat.be/database>) (Bayissa et al. 2015). For purposes of cross referencing, Table 4 has been summarized from the database.

Table 4: EM-DAT The Emergency Events Database – Universite Catholique de Louvain (UCL) – CRED, D. Guha-Sapir – www.emdat.be, Brussels, Belgium - Summarized drought condition in Ethiopia

Start date	End date	Location	Disaster type
/05/1983	//1984	Wollo, Gondar, Goe, Eritrea, Tigray, Shoa, Harerge, Sidamo	Drought
/06/1987	//1987	Ogaden, Eritrea, Tigray, Wello, Shewa, Gama, Gofa, Sidamo, Gondar, Bale	Drought
/10/1989	//1994	Northern Ethiopia, Eritrea, Tigray, Wollo, Gondar, Harerge	Drought
/02/1997	//1997	Borena, Bale (Oromiya state) South Ome zone, Somali state	Drought
/09/1999	/12/2000	North Wollo, South Wollo, Oromia, Wag Himra districts (Amhara province), Southern district (Tigray province), Beneshangul Gumu, Gambela, Oromia, SNNPR, Somali provinces	Drought
//2003	//2004	Tigray, Oromia, Amhara, Somali, Afar provinces	Drought
/11/2005	//2006	Afder, Liben districts (Somali province), Gode zones (Shabelle district, Somali province), Borena district (Oromiya province)	Drought
/05/2008	/10/2009	Oromia, Somali, Amhara, Afar, Tigray, SNNPR provinces	Drought

/01/2009	/08/2010	Somali, Oromia, Afar, Tigray, Amhara, SNNP, Gambela provinces	Drought
/01/2011	/01/2012	Somali, Oromia, Afar, Tigray, Amhara provinces	Drought
//2012	//2012	Dire Dawa, Gambela, Hareri, Oromia, SNNPR, Somali, Addis Ababa provinces (Southern Ethiopia)	Drought
/09/2015	/04/2017	Somali, Afar, Oromia, Amhara, Nations du Sud provinces	Drought

The severity of the identified drought years were also analyzed according to the areal extent of the classification to choose those which were gravely affected based on McKee's probability criteria shown in table 2.

Even though SPI may be used to directly compare different locations, the practical implication of an SPI-defined drought which is the deviation from normal amount of precipitation, will vary from one place to another (Viste et al., 2012). In order to address this, and at the same time to confirm the accuracy of the SPI results, a plot of precipitation deviation from the normal value for identified drought years was conducted and plotted for spatial analysis.

3.4.3. Spatio-temporal analysis to assess the spatial variability of drought frequency

In order to identify the areas most frequently struck by drought, the frequency of occurrence of drought was analyzed using a trend. A trend line for the tendency of the frequency of occurrence of drought in the region was constructed that is represented by the grid points. The outcome of this analysis is either one of two things. Positive or negative trend, indicating less and more drought recurrence, respectively. Before reaching a conclusion regarding this, the trend was checked for statistical significance using the Mann-Kendall method. The Standardize MK statistic, Z_{mk} was compared with the standardized normal distribution for a 95% significance level.

Computational procedure follows the calculation of the Test statistics, S , Variance $Var(S)$ and standardized MK statistic Z_{mk} , given by:

$$S = \sum_{i=1}^{n-1} \sum_{j=i+1}^n \text{sgn}(x_j - x_i) \quad (11)$$

$$\text{Var}(S) = \frac{n(n-1)(2n+5) - \sum_{p=1}^q t_p(t_p-1)(2t_p+5)}{18} \quad (12)$$

$$Zmk = \begin{cases} \frac{S-1}{\sqrt{\text{Var}(s)}} \dots S > 0 \\ 0 \dots S = 0 \\ \frac{S+1}{\sqrt{\text{Var}(s)}} \dots S < 0 \end{cases} \quad (13)$$

Where the x_j are the sequential data values

n is the length of the dataset

t_p is the number ties for the p^{th} value (number of data in the p^{th} group)

q is the number of tied values (number of groups with equal values/ties)

The frequency of occurrence of each drought category was also computed for each grid at each time-scale by taking the ratio of the number of occurrences of drought of a particular category and time-scale to the total number of data years (Bayissa et al., 2015, Edossa et al., 2009). This analysis was used to identify the areas that are most frequently struck by a specific type of drought. The classification was made according to Mckee's range of values for each drought category (Mild, Moderate, Severe and Extreme) and for all 949 grid points spatially covering the study area. Values were interpolated using the kriging technique and the results were mapped for ease of understanding.

3.4.4. Seasonal analysis

The failure of the main seasonal rainfall in the respective regimes most often causes devastation since most agricultural practices are fully dependent on the seasonal rainfall (Bayissa et al., 2017). Based upon the findings of the initial analysis, the seasonal analysis of the selected drought years was done according to the three gross rainfall shape regimes of Ethiopia with peaking rainfall times of March/April and July/August for rainfall regime covering north, north east, central and eastern

Ethiopia; peaking rainfall at July/August for areas north, north west and central Ethiopia and peak rainfall time of March/April and October/November for the remaining spatial portion.

Yearly analysis alone is not sufficient for characterizing the drought and hence the aim of this part of the analysis is to further assess the causes that led the year to be categorized under a major drought event.

The hypothesis on which locating a plausible working source is based upon is that there is enough amount of rainfall available every year but the “when” and “amount” has not been properly monitored for devising a system that would be able to harvest rain water. Whether or not lack of precipitation was the cause of the recorded drought for the selected drought years was assessed in the seasonal comparison.

In order to compute seasonal SPI, the monthly precipitation data for the distinct rainfall seasons were added to estimate the seasonal total precipitation for each grid point representing the domain. These seasonal sums were used to compute the SPI-3 value in R using the same algorithm used for the computation of SPI-12. Expected results from this part of the analysis are addressed according to the expected peaking periods as mentioned at the beginning.

3.4.5. Monthly analysis

The drought months for the selected years and for representative grids for each rainfall regime was conducted to view the accuracy of the monthly SPIs. As was done for the prior two analysis, the monthly precipitation values were used as direct input for the program in R to obtain an SPI-1. As an additional interpretation key, graphical analysis was done for selected representative grid points corresponding to the distinct rainfall regimes to comprehend the similarity of the drought patterns with that of the recorded precipitation. The anticipated result from this analysis is to observe a close relationship between the SPI and actual rainfall. This was achieved

by cross referencing the constructed SPI-1 maps for the representative locations with that of the observed rainfall for that particular location.

Drought events were also identified from the SPI-1 results where, by definition, it occurs anytime the SPI is continuously negative and reaches an intensity of -1 or less. Drought magnitudes for all stations were also computed by summing the corresponding negative one month SPIs. For this, the SPI-1 results were closely analyzed and tabulated. In doing so, due attention was given to the misperception created by the strong seasonality of precipitation. Meaning, dry climatology and drought in the sense of abnormally little precipitation may be confusing. For this reason, parallel to recording the drought event and computing the drought magnitude as well as duration, seasonality was addressed.

3.5. Temporal Drought Assessment

In the temporal drought analysis, duration of drought was assessed by making use of the monthly SPI results i.e. a third continuation of the analysis. Consecutively, the duration of the drought event was assessed using this same monthly SPI values.

Duration of drought: the beginning of drought closely follows the onset of an extended period of unusually dry weather. It follows, therefore that the end of metrological drought should coincide with the time when some rather major and fairly abrupt readjustment in the large scale circulation pattern begins to produce weather which is normal or wetter and continues so for a significant length of time (Palmer, 1965). This analysis is required subsequent to seasonal assessment for purposes of identifying the actual dry period for which this thesis aims at providing a source for.

At this point, the methodological framework meets the mid-stage where results from the analysis up-to now become necessary input for what comes next. If the initial hypothesis proves to be correct and that sufficient amount of rainfall is met for purposes of rainwater harvesting, then the continuation has value. Otherwise, another alternative would need to be sought. According to the results obtained from

the initial analysis, rainwater harvesting is an applicable option. Hence, remotely sensed input is assessed by this research.

3.6. Water harvesting points identification

Water harvesting and conservation at basin, area, field or micro level can play a significant role in bringing sustainability to the water sector and, consequently, increase water availability in drought years.

The following analysis is based on the theory that the location of variable source areas of runoff generation and the distribution of water are influenced by soil characteristics, topography, vegetation and weather. As such, Topographic Wetness Index was used to address the topographical aspect of the analysis and the Normalized Difference Vegetation index was used to analyze the soil and vegetation characteristics. Both, in combination were expected to address locations for water harvesting throughout the study area. Input datasets were integrated and analyzed using ArcGIS 10.2.2 as part of the process for locating suitable sites for surface water harvesting.

3.6.1. Terrain Analysis - TWI

Beven and Kirkby (1979) developed an algorithm for predicting pattern of soil water deficit from topography and soil hydraulic characteristics. As such, in this paper, the steady-state topographic wetness index was used to represent the spatial distribution of water flow and water stagnating across the study area.

Locating saturated areas is highly impractical due to data limitations and lack of understanding or proper surveying of the governing processes at scales from plots to catchments. These data involve devising a highly parameterized approach that models governing processes defining the spatial and temporal distribution of soil moisture (Gunter et al., 2004). The second best thing to use for locating saturated areas is the use of terrain indices.

Topographic Wetness Index, to analyze the saturation capacity/lowest point/water holding capacity of the land that is purely based on topography is a function of the upstream contributing area and slope. It is based on a widely available DEM and was calculated using spatial analyst tools in ArcGIS.

The TWI was manipulated in ArcGIS hydrology tool making use of functional inputs: flow accumulation and slope. These two attributes were computed separately in ArcGIS.

Flow accumulation was used as a method of identifying the upstream contributing area and estimating the overland flow. Before watershed delineation, the DEM was pre-processed to fill any sinks and allocate flow direction. Flow directions between cells were established using arcHydro, an extension in ArcGIS. The raster from this output was used to compute the flow accumulation.

From the different approaches for calculating the contributing area, D8 (deterministic-eight node) was used implicitly defined in ArcGIS flow accumulation tool. With the use of this method, it follows that flow can accumulate into a cell from several upslope cells but only flow out into a single cell. Even with the defects in this method, the D8 algorithm is still frequently used for determining contributing area, due to its simplicity and its adequacy to delineate specific catchment boundaries. As such, this method was applied to this research as well.

The popular formula for computing TWI is

$$TWI = \ln\left(\frac{\alpha}{\tan \beta}\right) \quad (14)$$

Where α is the upslope contributing area per unit contour length or Specific catchment area. This is a measure of the potential area that can deliver water via lateral flow pathways and thus influence the soil moisture status. It is assumed that the larger the contributing area, the larger the incoming accumulated flow volumes and β is the local slope gradient for reflecting the local drainage potential.

This particular equation assumes steady-state conditions and uniform soil properties (i.e transmissivity is constant throughout the catchment and equal to unity – this is due to the fact that spatially varying transmissivity is rarely available except for small experimental catchments). Normally only topographic attributes are used to characterize soil water distribution.

Due to sensitivity of TWI, significant changes than the actual case in the result of α may occur with varying upslope contributing area methods. To cater for this drawback, the computation for flow direction was repeated using the multiple flow algorithm to get a smoother result with less streaking effect and less flow partitioning.

TauDEM (Terrain Analysis Using Digital Elevation Models) was the tool which fitted the task best. This tool was developed at Utah State University (USU) for hydrologic digital elevation model analysis and watershed delineation and may be obtained from <http://hydrology.usu.edu/taudem/taudem5.0/>. This method assumes that flow from the current position could drain into more than one downslope neighboring pixel (Cheng-Zhi Qin et al., 2009).

The 30m DEM was initially projected and was manipulated in ArcGIS' spatial analyst tool and was filled under hydrology. Using this as input, the flow direction was computed and consequently the flow accumulation denoted by α .

Computation of β on the other hand was done by computing the slope with the surface tool in spatial analyst of ArcGIS from the same projected DEM which results in an output raster with slope in degrees. This was then converted to radians for manipulation in raster calculator in ArcGIS using this relationship:

$$SlopeRad = \frac{Slope \times \Pi}{180} \quad (15)$$

Slope is depicted here as an index of the hydraulic gradient and the rate at which water is shed from a location. From the mathematical form of the TWI, it can be seen that it's value increases with specific catchment area and decreases with slope.

Hence, the index is high in valley (high specific catchment area and low slope) where water concentrates, and low on steep hill slopes (high slope) where water is free to drain (Mackey, 2002).

The flow accumulation raster was used in place of α and the slope raster was used in place of β to modify the equation for use in raster calculator into the following:

$$TWI = \ln \left(\frac{(Flow_accumulation) \times Pixelsize^2}{\tan(Slope(rad))} \right) \quad (16)$$

Another modification to this equation was made to account for undefined values for flow accumulation as well as for slope. Border pixel values have zero flow accumulation when used in ArcGIS, hence undefined output raster results are avoided by adding a unit magnitude during TWI computation. In a similar manner, slopes that reach a value of zero will also result, again, in an undefined pixel. A correction recommended for this was to add a tan function of an almost flat land to avoid division by zero. Having this in mind, the adjusted TWI computation follows the following formula:

$$TWI = \ln \left(\frac{(Flow_accumulation + 1) \times Pixelsize^2}{\tan(Slope(rad))} \right) \quad (17)$$

For slope values approaching zero, the following formula was used:

$$TWI = \ln \left(\frac{(Flow_accumulation + 1) \times Pixelsize^2}{"0.00565" + \tan(Slope(rad))} \right) \quad (18)$$

Accordingly, the results were expected to be in the form of a raster as a combination of the upstream contributing area and slope, clearly signifying the soil water holding capacity. Once these results were obtained, re-categorization was required to group the values according to their representation.

Regarding ranges of TWI, a relative classification was selected for this study based on previous works. Most works involved depend on the resolution of the available DEM and in computing topographic attributes, classify TWI on unit ranges with values of over 10 being labeled as large values. The TWI results of over 10 have shown to have higher flows upon review with reference to known lakes and water bodies. These locations, as mentioned before, are with lower slopes and are found

usually downstream of the watershed. Owing to this, they have characteristics such as higher potential for higher soil moisture hence are areas of recharge with green land cover due to the presence of soil moisture.

Considering the factors that influence runoff generation and distribution as well as stagnation, it is safe to say that the Topographic Wetness Index covers a major portion. Nevertheless, consideration of vegetation in terms of land use can make the hypothesis on which locating water resources is based on more solid. Some parameters not considered in TWI will also get a chance to be influential.

Primarily, wetlands are topographical lowlands and hence the DEM data offer a significant opportunity to delineate lowlands from uplands as discussed previously for manipulation through terrain analysis using Topographic Wetness Index.

Considering the second input: remote sensing satellites at different spatial, spectral, and temporal resolutions provide an enormous amount of data that have become primary sources, being extensively used for detecting and extracting surface water and its changes in recent decades (Rokni et al., 2014). To make use of these methods is to keep up with the current norms and exploit these desirable features as additional input for locating water harvesting points.

3.6.2. Land-use Analysis

More than 40 multispectral remote sensing based indices have been developed and used to monitor water and vegetation properties. Among these, NDVI (Rouse et al., 1974) is the most widely used source of satellite data (Rulinda et al., 2010), which is commonly calculated by using image data from polar orbiting satellites that carry sensors that detect radiation in red and infrared wavelengths (Fensholt et al., 2006). The NDVI was developed mainly for separating green vegetation from other surfaces. However, it also performed well for surface water detection (Rokni et al., 2014).

GIS techniques were used to extract satellite data as well as for use in the mosaicking and analysis of the remotely sensed imagery. These near real-time products generated were obtained for NDVI computation and are available at 30m spatial resolution and were obtained via Geo-TIFF format. Depending on the type of landsat imagery, the bands required for NDVI computation were filtered and used.

For landsat 4/5 Thematic Mapper, bands 3 and 4 corresponding to Red and Near Infra-Red respectively, were filtered for the year 2002, and for landsat 8 OTI, bands 4 and 5, again, corresponding to Red and Near Infra-Red were filtered for the year 2015.

To prepare the input satellite images for further processing, and considering that necessary corrections were included in the data, the images of each year were mosaicked to generate new images covering the entire country.

Raster calculator in ArcGIS was used to transform the raw satellite data into NDVI values, to create a raster image that gives a measure of vegetation type, amount, and condition on land surfaces.

After completing the pre-processing of the satellite images, the NDVI values of the images were calculated in raster calculator using the following formula

$$NDVI = \left(\frac{NIR - R}{NIR + R} \right) \quad (19)$$

Where R (0.4-0.7 μm) and NIR (0.75-1.1 μm) are reflectance in red and near infrared bands of the satellite imageries, respectively.

For visual interpretation of water bodies, the near-infrared (NIR) band is usually preferred, because NIR is strongly absorbed by water and is strongly reflected by the terrestrial vegetation and dry soil (Sun et al., 2012). Thus, band 5 of Landsat data was selected in this study due to its higher ability to discriminate water and dry/land areas.

According to the initial drought analysis, the worst case drought scenario that surpassed the dry threshold in magnitude as well as extent was frequently seen in months January and February. Hence, the two months were selected for NDVI computation. Needless to say, all months were computed and checked against the SPI values to reach this conclusion. NDVI computation for landsat 8 imagery in ArcGIS' raster calculator follows:

$$NDVI = \left(\frac{Band5 - Band4}{Band5 + Band4} \right) \quad (20)$$

This was classified according to (USGS 1998) classification table.

Calculations of NDVI for a given pixel always result in a number that ranges from minus one (-1) to plus one (+1). Values greater than 0.5 indicate dense vegetation, whereas values lower than 0.1 indicate near zero vegetation such as barren area, rock, sand, or snow (Tucker, 1979). The classification was done according to the ranges shown in Table 3.

Table 5: Wider NDVI classification range

Cover Type	NDVI - range value
Dense green leaf vegetation	0.85 – 1.0
	0.7 – 0.85
	0.5 – 0.7
Medium green leaf vegetation	0.25 – 0.5
	0.09 – 0.25
Light green leaf vegetation	0.09 – 0.14
Bare soil	0.025 – 0.09
Clouds	0.002 – 0.025
Light water bodies	-0.046 – -0.002
Water bodies	-0.257 – -0.046
Deep water bodies	-0.257 – -1

Keeping this in mind, the NDVI was reclassified to eleven sub values to see how much area was covered by each, and to perfectly observe the contrasting difference. Following this, a land-water threshold was manually applied to classify the images into distinct classes shown in Table 5. From which “light green leaf vegetation”, “clouds” and the most obvious category, “water bodies” were selected as the most favorable options for the required water availability.

Light green vegetation was selected as favorable since density of forest is less and at the same time it would be an area with sufficient amount of soil water. Clouds in this paper were selected because these specific areas exhibited behaviors of a swampy area and were cross referenced to real time global images to confirm this. Alongside this confirmation, studies in wetland mapping have recommended the use of the range -0.25 to 0.1. These were regarded as areas that would be ideal for locating potential water sources next to actual identified lakes. Upon this deduction, the classification was further reduced to amplify the specific classes for this study and the results are depicted in the following chapter.

Table 6: Finer NDVI classification

Cover Type	NDVI - range value
Dense green leaf vegetation	0.5 - 1.0
Medium green leaf vegetation	0.14 - 0.5
Light green leaf vegetation	0.09 - 0.14
Bare soil	0.025 - 0.09
Swampy areas/wet lands	0.002 - 0.025
Water Bodies	-0.046 - -1

At this stage, separate, yet desirable features of both land use and terrain analysis have been completed. What follows next is joining the desirable features from the two separate analysis using an overlay mechanism that is fit to be manipulated in ArcGIS.

3.6.3. Water Harvesting Categories

The final step was to combine the various factors in order to identify the most suitable sites for water harvesting. Multiple overlay mechanisms were considered for locating those areas that fell under the same desirable category. TWI values of over 15 (for the sake of selecting a narrowed yet most desirable range) and NDVI values of “light green vegetation”, “swampy areas” and “water bodies”. Weighted overlay was the initial consideration but it resulted in lesser flexibility in the output raster. Hence, it was replaced with the normal overlay in raster calculator tool that was used to select values that corresponded to both features.

Results from this overlay were also reviewed to see the suitability of the method and appropriate alternatives for mapping were devised.

Recalling the aim of this study, locating potential water harvesting positions is the final objective with the intention of targeting small areas. To reiterate, smaller locations have the advantage of being operationally efficient. They are flexible, close to the point of use, and require relatively few parties for management. Because of these attributes, they can be responsive to demands and the supply to demand mismatch has been shown to be minimized (Keller et al., 2000). The great operational benefit of small storages is their rapid response time: i.e. they can respond rapidly to precipitation runoff, often refilling several times a year. For these reasons, several categories of rainfall harvesting targets that satisfied small reservoir requirements were identified and quantified.

Needless to say, all possible locations from the chosen overlay mechanism were identified using ArcGIS select features by location tool. It is from this, that manageable small-sized potential water harvesting locations were again filtered out. This target was identified using the select by attributes tool in ArcGIS to spatially locate them, obtaining the last and main objective of this study.

In order to make this study more descriptive, a last portion of computing volume of identified locations was carried out. This capacity determination was manipulated

through ArcGIS surface volume computation tool by extracting the area from the identified locations.

At this point, the most suitable sites for water harvesting have been identified in three categories; namely Primary, Secondary and Tertiary sources. From the identified zones, area ranges as well as number of locations were listed. As an illustration, an assessment of the capacity of small and manageable water harvesting zones was undertaken to determine the number and volume of water it would be able to hold.

Computation of reservoir volume is considered vital in order to give the output meaning. This was made possible by using ArcGIS surface volume computation tool on the identified locations. This paper will not pass without mentioning a key concept that may compromise volume computation in ArcGIS. This is, Lidar and Micro wave signals that are the source of any Digital Elevation Model available do not penetrate water. Hence capacity determination for locations with deep waters usually requires information from bathymetry. With this in mind, volumes for locations that correspond to Primary water harvesting sources (mentioned in results and discussion) were directly accessed from a capacity analysis report.

On the contrary, volume computation through the use of DEM will work on shallow locations but it is also unreliable, to some scale. Most DEMs have ± 2 meter vertical accuracy and unless the DEM is corrected with sonar data, the accuracy might be questionable. Considering this disclaimer and the practicality of water harvesting ponding structures, an average depth of 4m was taken for all small scale water harvesting locations to compute the volume in ArcGIS.

4. Results and Discussion

4.1. Performance evaluation of precipitation Dataset

Performance evaluation was conducted based on the method's ability to reproduce the observed precipitation. To check the accuracy of the obtained result, a grid based comparison of observed and corrected CFSR for all grid points in Ethiopia was plotted using the co-kriging technique to describe the spatial resolution of the precipitation.

Similar to (Berhanu et al., 2016), statistical measures for the comparison of observed and corrected rainfall was conducted for annual scale as well as for selected grids. Figure 4 shows the annual spatial comparison.

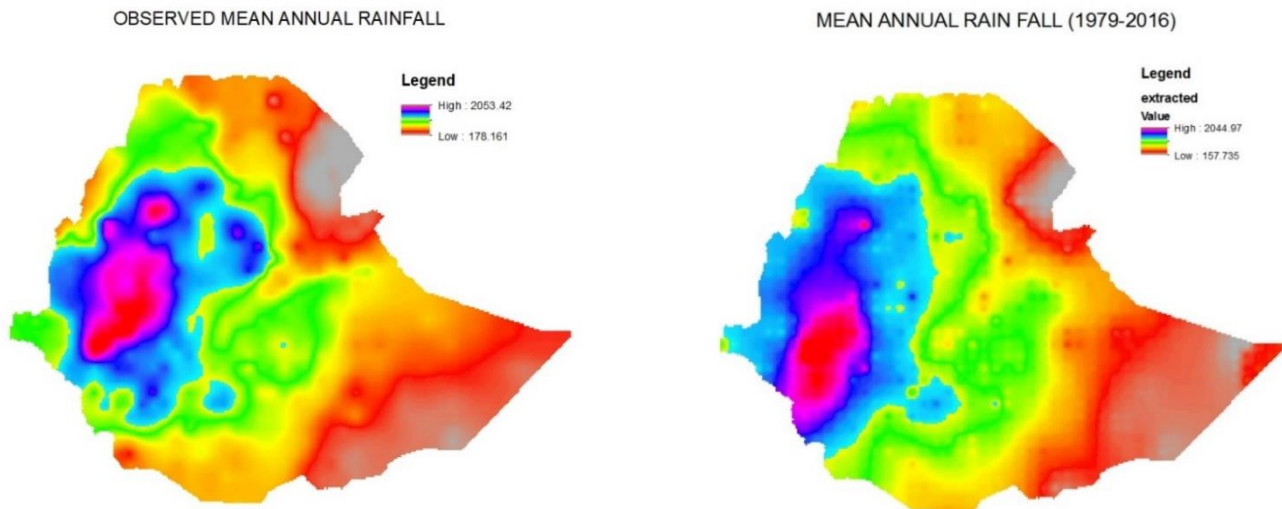


Figure 4: Spatial comparison of mean Observed and Corrected Rainfall

Frequency based comparison for selected representative grid points between the observed mean monthly rainfall used as input for bias correction and its bias corrected counterpart was also done as shown in Table 8.

Table 7: Country wide comparison of mean monthly rainfall for selected representative grid points

	Max	Min	mean	90 th Q.	10 th Q.	Median	SD	CV	RMSE	NSE	PBAIS
Obs. Mean Mon.	1510.3	157.0	846.2	1319.0	330.4	811.3	432.3	0.5			
CFSR Mon	1551.0	199.7	845.1	1336.8	297.9	822.3	446.8	0.5	15.73	1.00	0.13

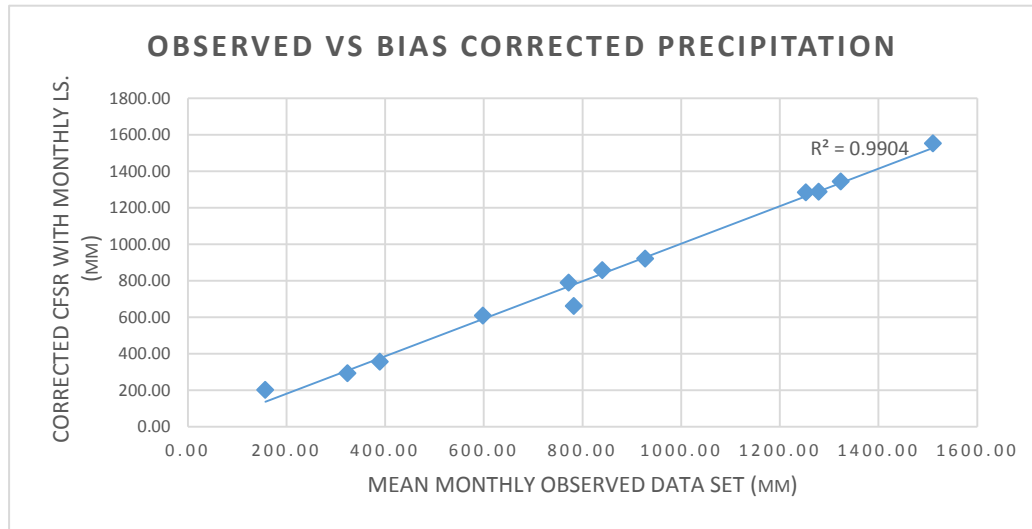


Figure 5: Statical evaluation of corrected rainfall data

Table 7 and Figure 5 show perfect correlation ($R^2 = 0.99$) of the long term observed and bias corrected mean monthly values guaranteeing the accuracy of the written programs, hence the use in conducting further analysis.

Monthly statistical comparison for selected representative grid points was conducted and shown using frequency and time series matrices in Table 8. The statical measures indicated in the table contain three comparisons: ground observed precipitation, raw CFSR precipitation and corrected precipitation data through monthly linear scaling.

The performance evaluation showed satisfactory results where most focus was given to the NSE value, which at almost all grid points was 0.99, indicating an almost perfect fit. Graphical representations of these comparisons showing how the raw data was corrected to mimic the observed data is shown under Appendix A.

Table 8: Statistical measures of mean monthly raw and corrected CFSR and observed datasets

Adama (obs.)	Max	Min	mean	90 th Q.	10 th Q.	Median	SD	CV	RMSE	NSE	PBAIS
Obs.	218.5	7.3	70.6	200.9	9.1	51.3	72.5	1.0			
CFSR raw	17.1	0.5	4.4	12.6	0.6	1.9	5.4	1.2	92.5	-0.72	93.7
CFSR Mon	215.8	8.9	71.4	202.7	9.9	54.6	71.8	1.0	8.50	0.99	-1.09
Assaita (obs.)	Max	Min	mean	90 th Q.	10 th Q.	Median	SD	CV	RMSE	NSE	PBAIS
Obs.	37.5	1.8	12.8	28.5	3.4	9.1	11.3	0.9			
CFSR raw	53.4	1.3	16.0	48.5	2.3	8.3	18.2	1.1	8.5	0.98	-24.9
CFSR Mon	52.8	3.5	16.6	40.8	4.7	10.0	15.9	1.0	4.52	1.00	-29.86
Bahir Dar (obs.)	Max	Min	mean	90 th Q.	10 th Q.	Median	SD	CV	RMSE	NSE	PBAIS
Obs.	424.8	1.9	116.3	350.2	2.7	52.5	147.4	1.3			
CFSR raw	222.9	0.1	45.8	189.0	0.5	8.7	80.1	1.7	18.2	0.52	60.6
CFSR Mon	394.6	3.0	111.9	334.4	3.3	56.2	137.5	1.2	1.88	0.99	3.80
Degahbure (obs.)	Max	Min	mean	90 th Q.	10 th Q.	Median	SD	CV	RMSE	NSE	PBAIS
Obs.	86.4	2.8	27.7	81.4	3.6	11.6	31.5	1.1			
CFSR raw	71.0	2.4	23.4	58.4	2.6	16.7	22.4	1.0	2.6	0.95	15.6
CFSR Mon	86.0	3.1	29.5	82.4	4.4	13.5	30.7	1.0	1.02	0.99	-6.71
DireDawa (obs.)	Max	Min	mean	90 th Q.	10 th Q.	Median	SD	CV	RMSE	NSE	PBAIS
Obs.	117.8	12.1	51.7	97.6	16.7	38.9	36.5	0.7			
CFSR raw	47.3	4.9	22.7	44.2	6.2	19.3	15.9	0.7	6.9	0.35	56.2
CFSR Mon	124.0	11.4	55.0	100.6	16.5	46.8	38.3	0.7	1.38	0.97	-6.36
Kebri Dehar (obs.)	Max	Min	mean	90 th Q.	10 th Q.	Median	SD	CV	RMSE	NSE	PBAIS
Obs.	87.0	0.3	22.8	68.3	0.5	6.9	30.2	1.3			
CFSR raw	53.2	0.7	17.9	50.9	1.2	6.4	20.1	1.1	2.6	0.95	21.5
CFSR Mon	85.7	1.1	23.2	69.1	1.9	6.9	29.9	1.3	0.88	0.99	-1.87
HagereSelam (obs.)	Max	Min	mean	90 th Q.	10 th Q.	Median	SD	CV	RMSE	NSE	PBAIS
Obs.	161.0	43.3	106.6	156.5	47.4	120.5	47.5	0.4			
CFSR raw	316.8	18.1	148.7	281.7	18.7	157.1	112.9	0.8	16.1	-2.00	-39.4
CFSR Mon	176.3	36.6	107.3	170.2	39.5	117.2	52.3	0.5	1.88	0.96	-0.62
Jimma (obs.)	Max	Min	mean	90 th Q.	10 th Q.	Median	SD	CV	RMSE	NSE	PBAIS
Obs.	212.6	35.4	126.6	209.9	38.3	122.1	72.3	0.6			
CFSR raw	305.3	37.2	167.4	301.9	41.0	171.3	108.3	0.6	10.2	0.53	-32.3
CFSR Mon	234.1	35.3	129.2	231.1	36.0	119.7	79.0	0.6	2.08	0.98	-2.10
Jinka (obs.)	Max	Min	mean	90 th Q.	10 th Q.	Median	SD	CV	RMSE	NSE	PBAIS
Obs.	177.0	46.5	105.7	161.5	53.4	102.2	41.5	0.4			
CFSR raw	386.3	35.9	158.3	360.5	41.5	116.8	119.0	0.8	17.2	-3.33	-49.8
CFSR Mon	178.4	47.2	106.9	161.0	52.3	105.2	41.1	0.4	1.88	0.95	-1.12
Mekele (obs.)	Max	Min	mean	90 th Q.	10 th Q.	Median	SD	CV	RMSE	NSE	PBAIS
Obs.	226.8	0.7	50.2	180.4	3.6	26.8	76.7	1.5			
CFSR raw	401.9	1.4	78.2	337.3	1.9	13.4	144.6	1.9	13.1	0.20	-55.6
CFSR Mon	209.6	3.4	50.6	174.2	4.0	29.0	70.9	1.4	1.30	0.99	-0.79

Negele (obs.)	Max	Min	mean	90 th Q.	10 th Q.	Median	SD	CV	RMSE	NSE	PBAIS
Obs.	212.0	5.0	58.2	138.7	5.4	24.1	68.5	1.2			
CFSR raw	416.2	16.3	150.3	401.2	20.4	91.1	151.5	1.0	22.8	-2.22	-158.1
CFSR Mon	209.2	12.3	65.6	148.4	15.9	34.7	66.6	1.0	1.55	0.99	-12.75
Sinana(obs.)	Max	Min	mean	90 th Q.	10 th Q.	Median	SD	CV	RMSE	NSE	PBAIS
Obs.	154.4	20.5	74.7	141.1	21.8	61.9	49.4	0.7			
CFSR raw	194.6	13.7	69.6	143.5	19.6	55.5	54.7	0.8	5.6	0.59	6.7
CFSR Mon	164.8	20.2	76.7	131.9	22.6	67.6	48.0	0.6	1.61	0.97	-2.68

The derivation of these monthly precipitation values is highly critical as the main and only input for drought analysis is monthly precipitation for all time scales.

4.2. Spatio-temporal evaluation of metrological drought

4.2.1. Spatial drought evaluation

After computation of the SPI, the resulting areal extent was expressed as a percentage of the country in drought conditions. The spatial analysis was done for the three time periods mentioned in the methods section and are presented in detail.

Table 9: Sample SPI-12 Values for the study period at representative grid points

SPI-12	Jinka	Jimma	Bahir Dar	Hageresalam	Mekelle	Adama	Negele	Sinana	Assaita	Dire Dawa	Deghabure	Keabri Dahar
1980	-1.59	-0.76	-0.21	-0.67	-0.67	0.07	-1.59	-1.59	-0.28	-1.38	-0.76	-0.59
1981	0.43	0.28	0.67	-0.14	0.67	2.20	1.91	1.38	0.97	0.86	0.43	1.59
1982	0.00	-1.09	-0.43	-0.14	-0.51	1.22	1.22	2.20	1.59	2.20	2.20	2.20
1983	1.91	2.20	0.67	0.76	2.20	1.22	-0.51	2.20	2.20	2.20	-0.36	-2.20
1984	-2.20	-2.20	0.36	-0.28	-2.20	-0.43	-1.59	-0.86	-2.20	-0.07	-1.38	-1.22
1985	-0.21	0.14	-0.43	-0.28	1.38	-1.91	-0.07	0.59	-1.09	2.20	2.20	-0.14
1986	0.28	0.67	0.67	0.76	2.20	1.09	0.36	2.20	0.59	2.20	1.38	-1.59
1987	0.00	-0.43	0.14	0.00	0.21	0.59	-0.51	-0.21	-1.09	1.59	2.20	0.28
1988	2.20	-0.97	0.36	0.76	2.20	1.09	0.36	2.20	2.20	2.20	1.38	0.14
1989	2.20	1.22	-0.36	1.91	-1.59	1.22	1.91	1.59	2.20	2.20	0.28	1.59
1990	1.91	1.91	-1.38	1.91	-1.09	-0.97	2.20	1.22	0.59	0.59	-0.07	0.00
1991	0.76	-0.28	-0.86	1.38	2.20	-0.14	-0.36	0.00	-0.97	2.20	0.86	-0.07
1992	0.07	1.09	-0.36	0.36	0.07	1.09	-0.51	-0.86	2.20	-0.59	-1.09	-0.36
1993	-0.36	1.59	0.00	0.76	-0.51	1.09	-0.51	1.38	1.22	0.14	-0.28	0.14
1994	1.91	-0.97	-0.14	0.76	2.20	1.09	0.43	0.51	1.22	0.21	0.67	2.20
1995	0.51	-0.28	-1.22	0.36	2.20	-0.97	0.14	-0.59	1.22	-0.67	-0.28	1.59
1996	1.91	2.20	0.43	0.76	2.20	2.20	-0.43	-0.28	1.22	1.59	-0.21	0.28
1997	2.20	1.59	0.00	2.20	1.91	1.09	2.20	2.20	0.86	2.20	2.20	2.20
1998	2.20	1.91	2.20	2.20	2.20	1.22	1.22	1.59	2.20	1.09	2.20	-0.14
1999	1.59	0.97	0.36	2.20	-0.28	-1.09	1.59	0.51	-2.20	-0.59	-1.22	-0.21
2000	1.38	1.38	0.36	2.20	-1.22	-1.59	-0.14	0.51	-0.21	-2.20	-0.59	0.21
2001	0.07	2.20	-0.43	0.76	-1.22	-0.14	0.28	-0.67	-0.43	-1.09	-1.38	-0.14
2002	0.51	0.43	-2.20	-0.07	-2.20	-2.20	1.22	-0.76	-2.20	-2.20	2.20	2.20
2003	0.59	-1.22	-0.59	-0.21	-1.22	1.09	0.36	-0.86	-0.36	-0.28	-1.22	2.20
2004	1.59	1.22	-2.20	-0.07	-2.20	-0.97	0.21	0.14	-2.20	-0.59	-0.59	1.91
2005	0.59	0.67	-0.43	0.07	-2.20	-0.97	0.43	0.59	-2.20	-0.28	2.20	2.20
2006	2.20	0.67	0.36	-0.14	-0.86	-1.91	1.91	1.59	0.86	-0.21	-0.28	2.20
2007	1.91	0.00	-0.43	-0.14	0.86	1.09	0.28	-0.28	-2.20	0.21	-0.14	0.67
2008	0.59	0.59	-2.20	-0.97	-2.20	-0.86	-0.14	-0.59	-2.20	-0.76	-1.22	1.59
2009	0.28	0.00	-2.20	-0.14	-2.20	0.51	0.28	-0.59	-2.20	-0.67	-2.20	-0.14
2010	2.20	2.20	-0.36	2.20	2.20	2.20	2.20	2.20	0.59	2.20	2.20	0.76
2011	0.76	0.67	-0.36	0.00	2.20	1.09	-0.14	-0.59	-1.59	-0.07	-0.43	0.67
2012	0.59	-0.28	-0.59	0.21	-0.07	1.09	-0.51	-0.07	-0.36	-0.21	0.43	2.20
2013	1.91	0.59	0.36	0.76	-0.97	1.09	2.20	2.20	0.86	2.20	2.20	2.20
2014	2.20	2.20	0.36	0.76	1.09	1.09	0.97	2.20	2.20	1.09	0.97	1.91
2015	0.51	-0.51	-1.22	-0.21	0.07	1.09	2.20	1.59	0.14	-0.59	2.20	-0.51
2016	2.20	0.97	-1.91	0.00	1.59	1.09	-0.51	1.59	2.20	-0.28	-2.20	2.20

Table 9 depicts the calculated numerical values of the 12 month SPI for twelve selected grids within distinct rainfall regimes in the domain for the study period.

Correspondingly, for temporal analysis, the output from this numerical computation in R resulted in a highly descriptive graphical representation of these selected grid points without breaking continuity and in a moving SPI fashion as shown in Appendix B.

The fact that the plot is of a 12 month cumulative result is seen in its smooth partitioning from one threshold value to the next. No sudden or major variation in SPI values is seen in the plot and is mostly desired for long term drought analysis and in this case, for identifying major drought periods. Parallel to temporal identification, the spatial mapping was particularly appealing due to the fact that it showed the drought phenomenon every year vividly.

Figure 6 shows the spatial extent of the drought during the years in the study period. The major drought years are also depicted for ease of identification and corresponding figures showing SPI-12 results for representative locations are also indicated. The maps are presented so as to show that 1 corresponds to extreme drought and 8 corresponds to extreme wet periods.

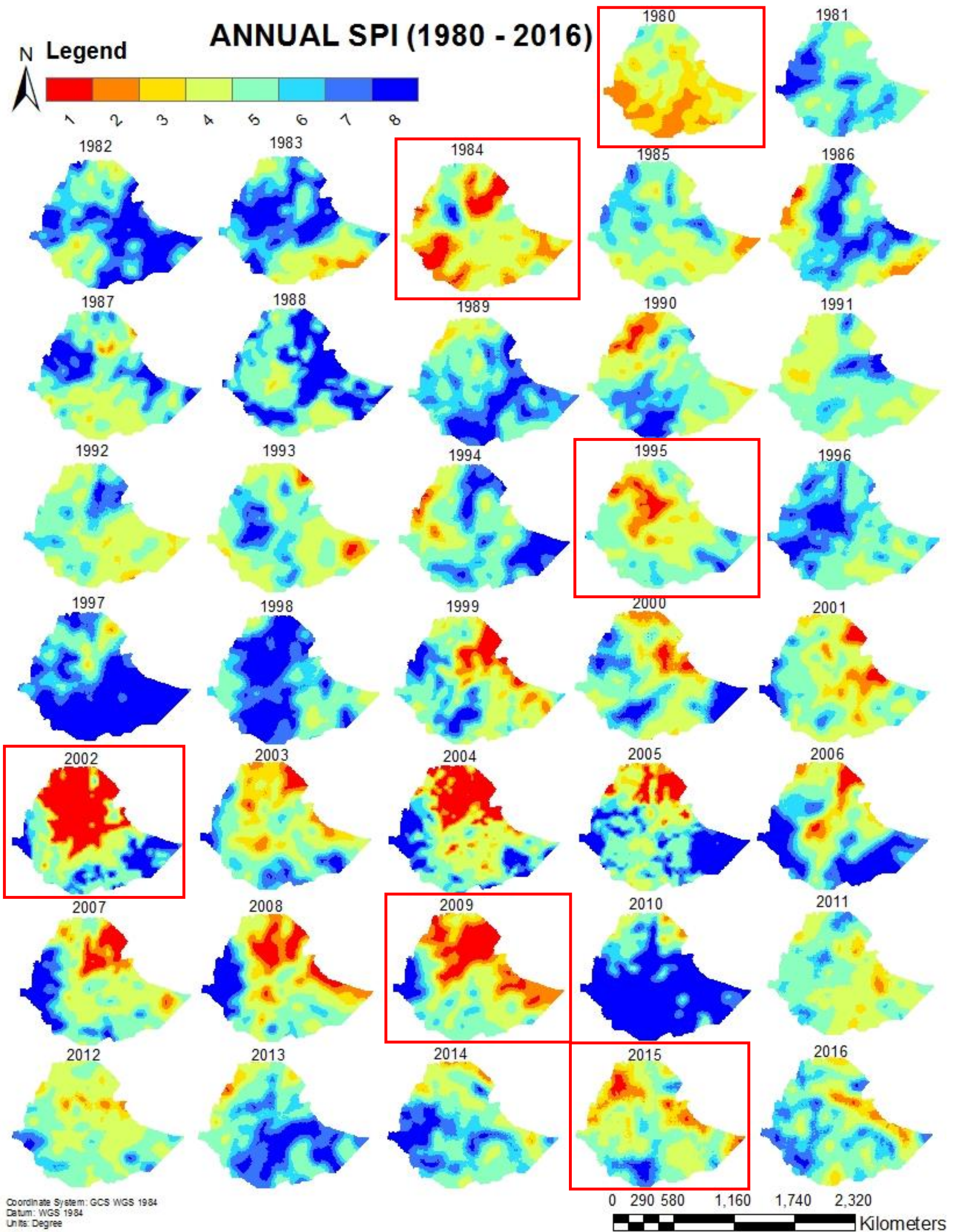


Figure 6: The spatial patterns of the annual SPI (SPI-12) for the periods of 1980-2016. The red rectangular boxes in the figure shows the historic drought events in the country

4.2.1.1. Evaluation of drought severity

The drought severity of the 12-month SPI was analyzed via multiple criteria which are stated here.

Criteria 1: The first interpretation of supposed drought years was to, on a general scale, look at the drought condition according to McKee’s (1993) classification. This stage of evaluation is purely based on visual analysis of the spatial drought map of the years in the study period. Table 10 summarizes the pre-selected ‘potential’ drought years and their percentage shares of study area. From this, years with percentages of drought of over 50 were identified as potential drought years. According to the table, years 1980, 1984, 1995, 2002, 2009 and 2015 have been identified as drought years.

Table 10: Percentage shares of dry and wet events for study area for pre-identified years

Year	1980	1984	1995	1999	2000	2002	2009	2011	2012	2015
Drought	91.11%	93.15%	53.26%	49.33%	44.31%	58.09%	66.49%	49.63%	51.00%	58.20%
Wet	8.89%	18.57%	46.43%	50.67%	55.69%	41.91%	33.51%	50.37%	49.00%	41.80%

Criteria 2: The follow-up interpretation was made based on comparison of the severity conditions. According to McKee’s (1993) classification, the probability of falling under Mild, Moderate, Severe and Extreme drought conditions are 34.1%, 9.2%, 4.4% and 2.3% respectively. Values surpassing these probabilities show an extreme event for the drought condition in question. Accordingly, 1984, 1995, 1999, 2002 and 2009 have large extreme value coverage compared to the mentioned classification. When compared to the other extremity, wetness, years 1984, 2002 and 2009 showed great difference.

Similarly, all except the year 2012 have resulted in large severe values. When compared to severe wetness, years 1980, 1984, 1995 and 2009 show large difference. Moderate drought conditions were also analyzed in years 1980, 1984, 2009 and 2015 showing moderate drought cases that have passed the indicated threshold. Upon self-comparison, large deviation was seen in the years 1980 and 1984.

Moving to the mild category, 1980, 1984, 2012 and 2015 have equaled and surpassed the threshold set.

Table 11: Percentage shares of Drought anomalies by drought category

Category	1980	1984	1995	1999	2000	2002	2009	2012	2015
Extreme Drought	0%	11.72%	3.05%	6.47%	1.78%	33.04%	16.34%	0%	1.82%
Severe Drought	18.82%	16.63%	8.99%	6.86%	6.67%	4.89%	17.73%	1.42%	8.56%
Moderate Drought	35.11%	18.65%	8.99%	7.94%	6.81%	3.57%	9.81%	5.37%	12.64%
Mild Drought	37.18%	46.15%	32.58%	28.06%	29.04%	16.60%	22.61%	44.21%	35.18%
Mildly Wet	8.47%	14.01%	36.78%	26.70%	25.68%	18.49%	22.75%	38.05%	27.76%
Moderately Wet	0.42%	2.29%	6.40%	10.44%	11.13%	7.10%	4.38%	6.88%	7.33%
Very Wet	0%	1.38%	2.87%	7.94%	9.78%	6.02%	2.01%	3.42%	4.90%
Extremely Wet	0%	0.89%	0.39%	5.60%	9.10%	10.29%	4.36%	0.65%	1.80%

Even though SPI measures wet events equally effectively as dry events, realistically, the effect a specified distribution has on the number, length and intensity of dry events is perhaps more important to users of the SPI (Guttman et al., 1999). Hence, Figure 7 shows only the severity of the drought condition summarized for selected drought years.

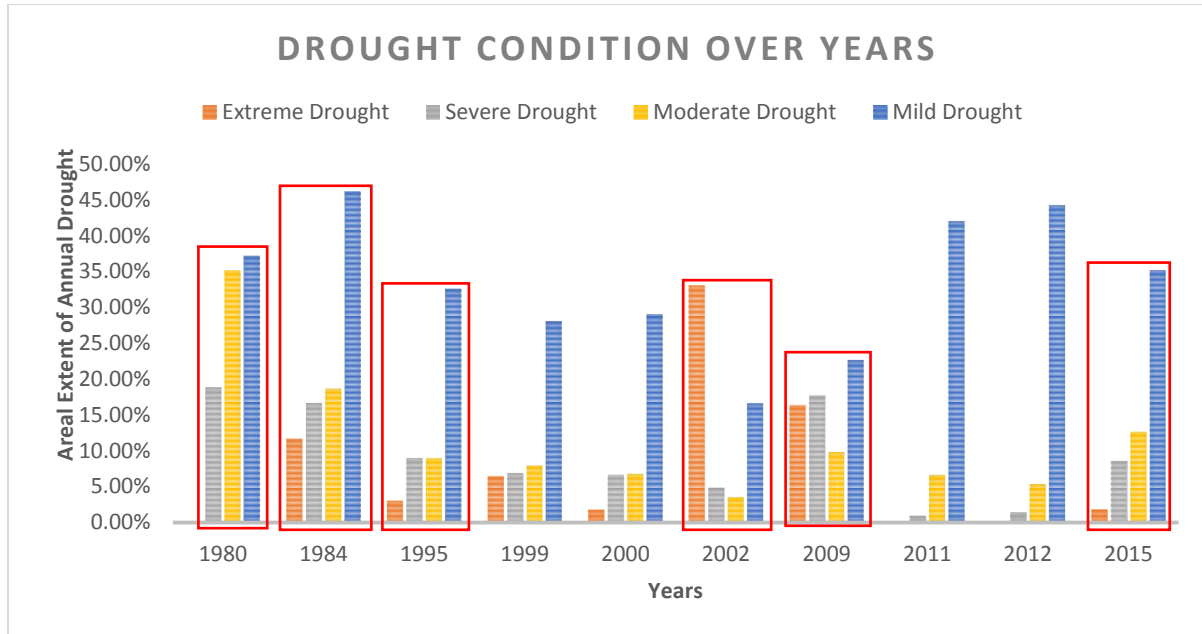
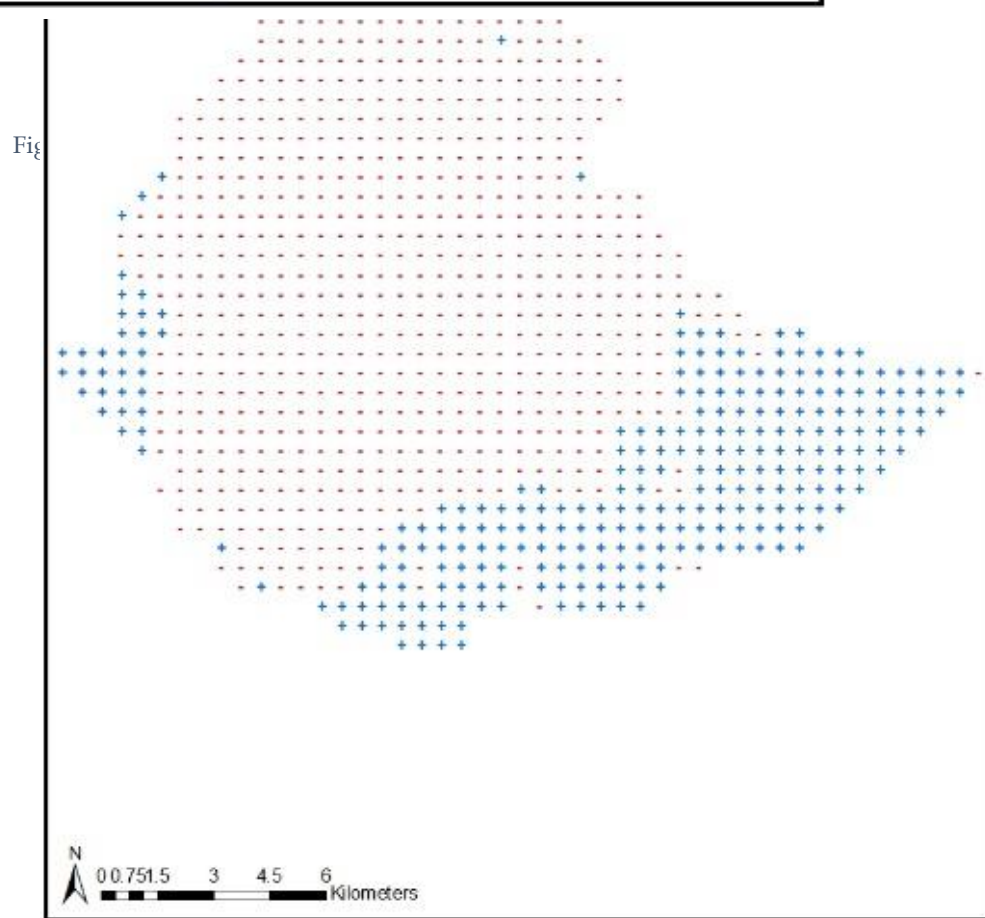
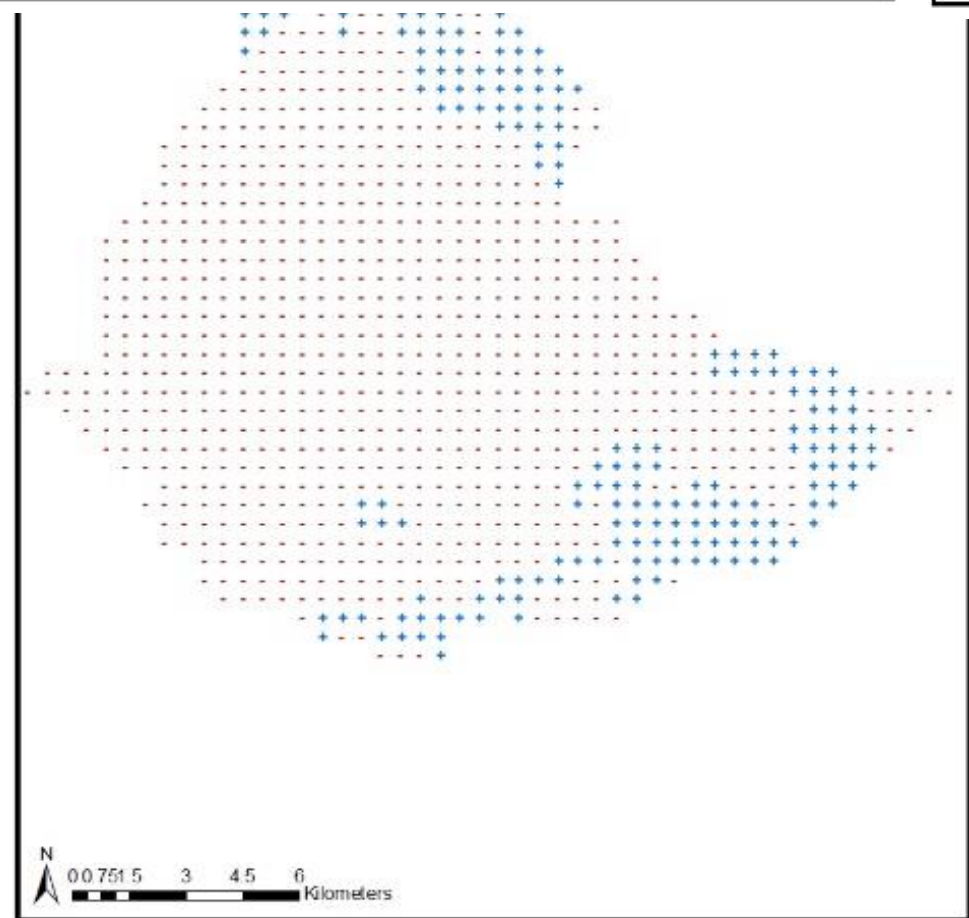
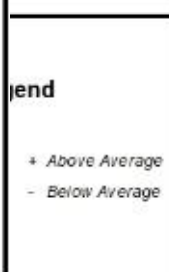
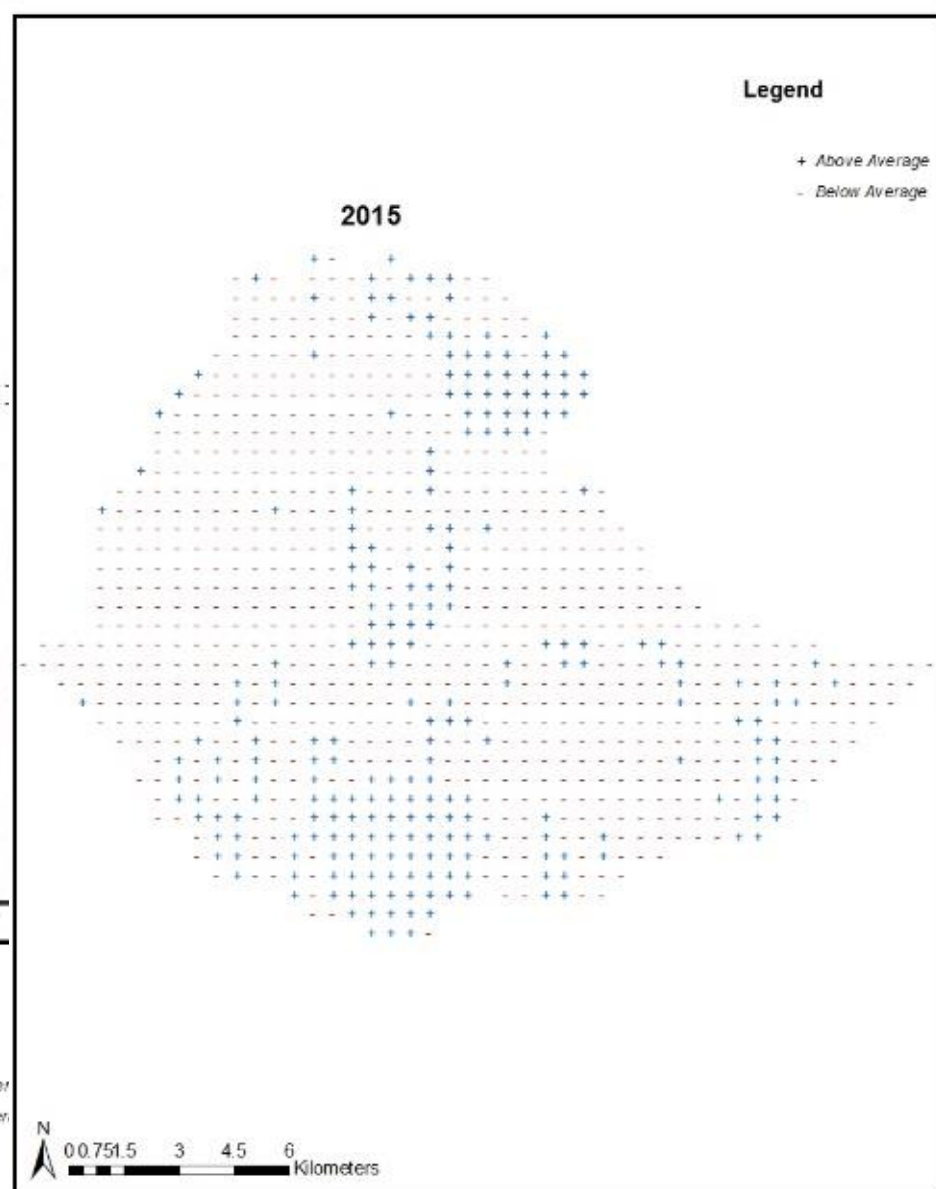
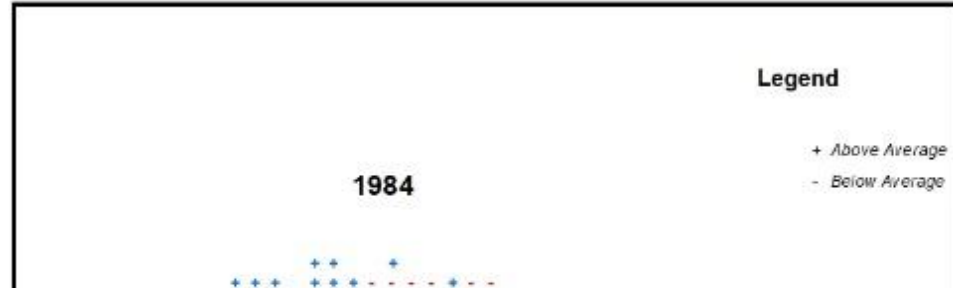
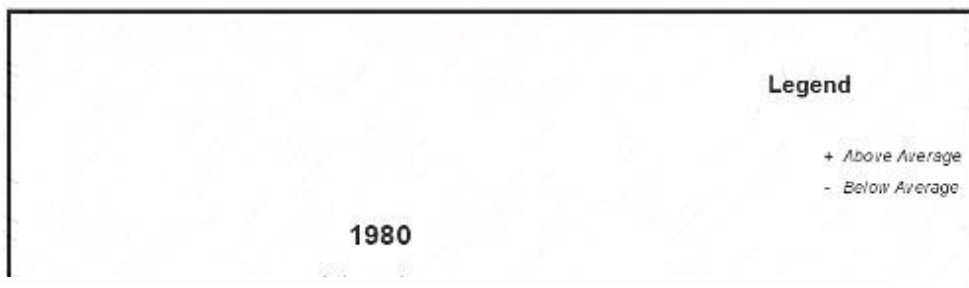


Figure 7: The percentage areal extents of the annual drought for the selected historic drought years

As a way of realizing the practical implication of an SPI-defined drought which is the deviation from normal amount of precipitation, a spatial plot of precipitation deviation from the normal value for identified drought years was conducted and plotted for spatial analysis in Figure 8.



All six subsections in Figure 8 show the comparison of yearly rainfall of uniformly distributed grids covering Ethiopia with the normal rainfall computed for the 38 study years at each grid. These results are plotted in blue with “+” sign denoting positive deviation, and in red with “-” sign denoting negative deviation. The deviation of actual precipitation from the expected normal precipitation gives a fairly direct measure of the departure of the moisture aspect of the weather from normal.

Upon these comparisons, the major historical drought events within the study period (1979-2016) as mentioned earlier were identified. These were cross referenced with EM-DAT (shown in Table 4) whilst considering that the reports consisted of prolonged droughts. This means that it addresses the long term drought conditions such socio-economic and hydrological droughts. Years 1980, 1984, 1995, 2002, 2009 and 2015 were selected as major drought years in Ethiopia. The consistency of the SPI indicated goes well with the identified historic drought periods and is in-line with previous studies (Viste et al., 2015, Bayissa et al., 2017). The index clearly indicated the drought and wet years in the country.

4.2.2. Temporal drought assessment

The results from the yearly analysis show that there is an occurrence of mild to extreme drought in all identified historic drought years. Severity levels are highly variable and all representative grids recorded a minimum SPI of -2.2 during the historic drought years except 1980 where the minimum recorded value was -1.914. (Shown in Table 9)

The years 1980 and 1984 for all regions have values that fall under mild to extreme drought conditions, whereas all regions in 2002 and 2009 with the exception central and south central parts of the study domain, experienced moderate to extreme drought conditions. Years 1995 and 2015 had mild drought magnitudes in half of the regions, whereas the remaining half was characterized by wet conditions.

4.2.2.1. Drought Frequency

A plot of SPI values against the study periods was drawn for frequency analysis. According to figure 9, regions central and southern parts of the domain exhibit less drought frequency as the years progress whereas the remaining regions have an increasing drought occurrence trend. The Man-Kendall trend test was checked for statistical significance for all representative grid points and the trend was only statistically significant at the 95% confidence level for grid points represented by the cities Kebri Dahar, BahirDar and Jinka.

To complement this evaluation, spatio-temporal procedures were also carried out. Shown in Figure 9, tabulated (in Appendix D) and graphically represented, are parameters: the test statistics S , the variance $Var(S)$, and the Standardized MK statistic Z_{mk} computed for the mann-kendall trend test for 95% confidence along with the trend-line drawn for each representative station.





Figure 9: Time series plots of 12-month SPI for representative grids with trend analysis

According to the spatio-temporal analysis for spatial variability of drought frequency, in Figure 10 (a) the annual frequency shows that the relative frequency of mild drought at a 12-month time step was high in the northwest and south-central parts of the study area. Relatively moderate drought conditions shown in Figure 10 (b) were also observed in the south-east, north-west and a small coverage in north-eastern location. The frequency of occurrence of extreme droughts (Figure 10(d)) further shows that the north eastern and north central parts of the study area are struck more frequently by extreme droughts at an annual scale.

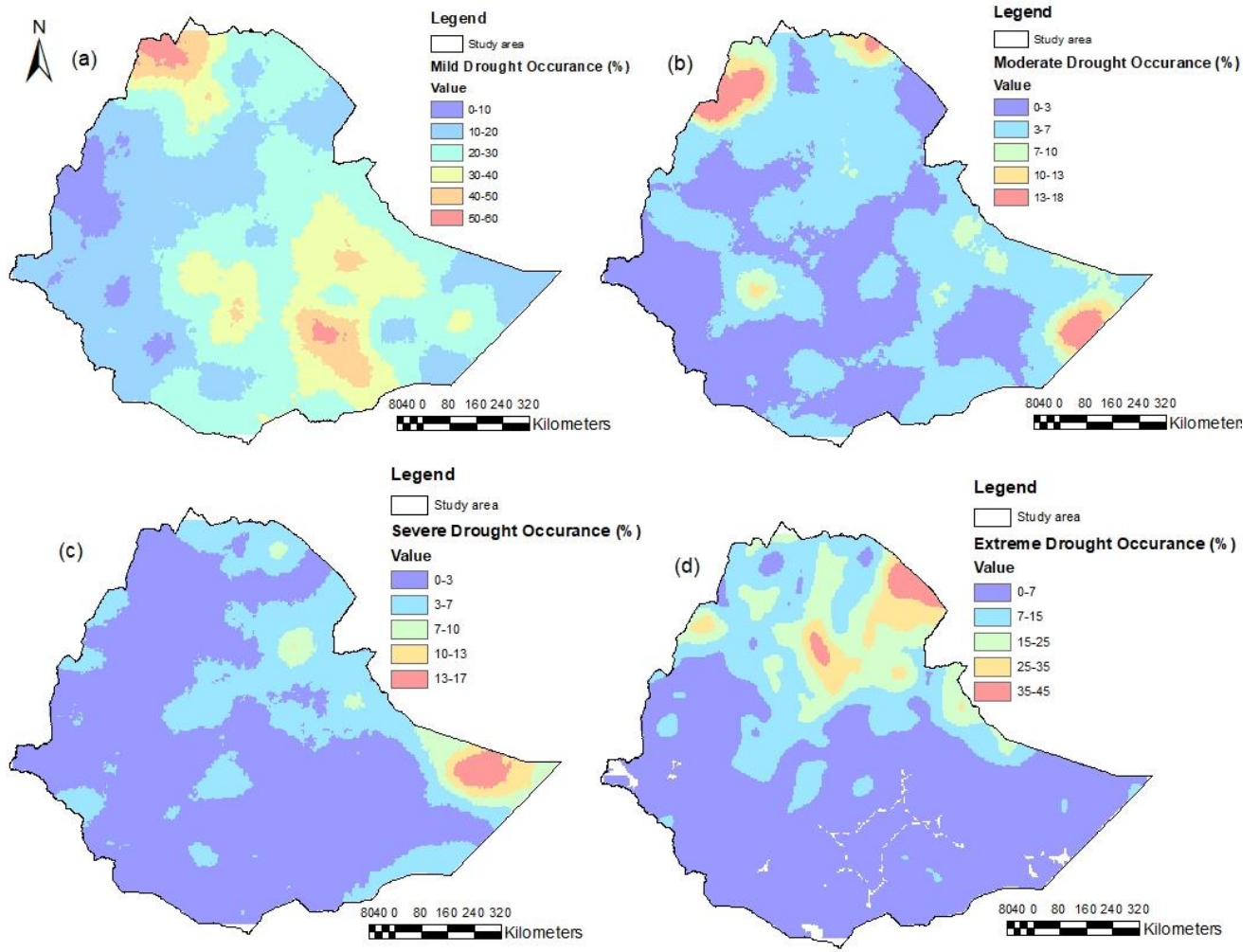


Figure 10: The frequency of occurrence of mild, moderate, severe, and extreme droughts

4.2.3. Seasonal drought evaluation

The 3-month numerical SPI results were computed in R for all 949 grid points covering the study area and are spatially mapped in Figure 11. Ranges depicted are again based on McKee's classification criteria, where a value of 1 symbolizes extreme drought and that of 8 symbolizes extreme wet conditions.

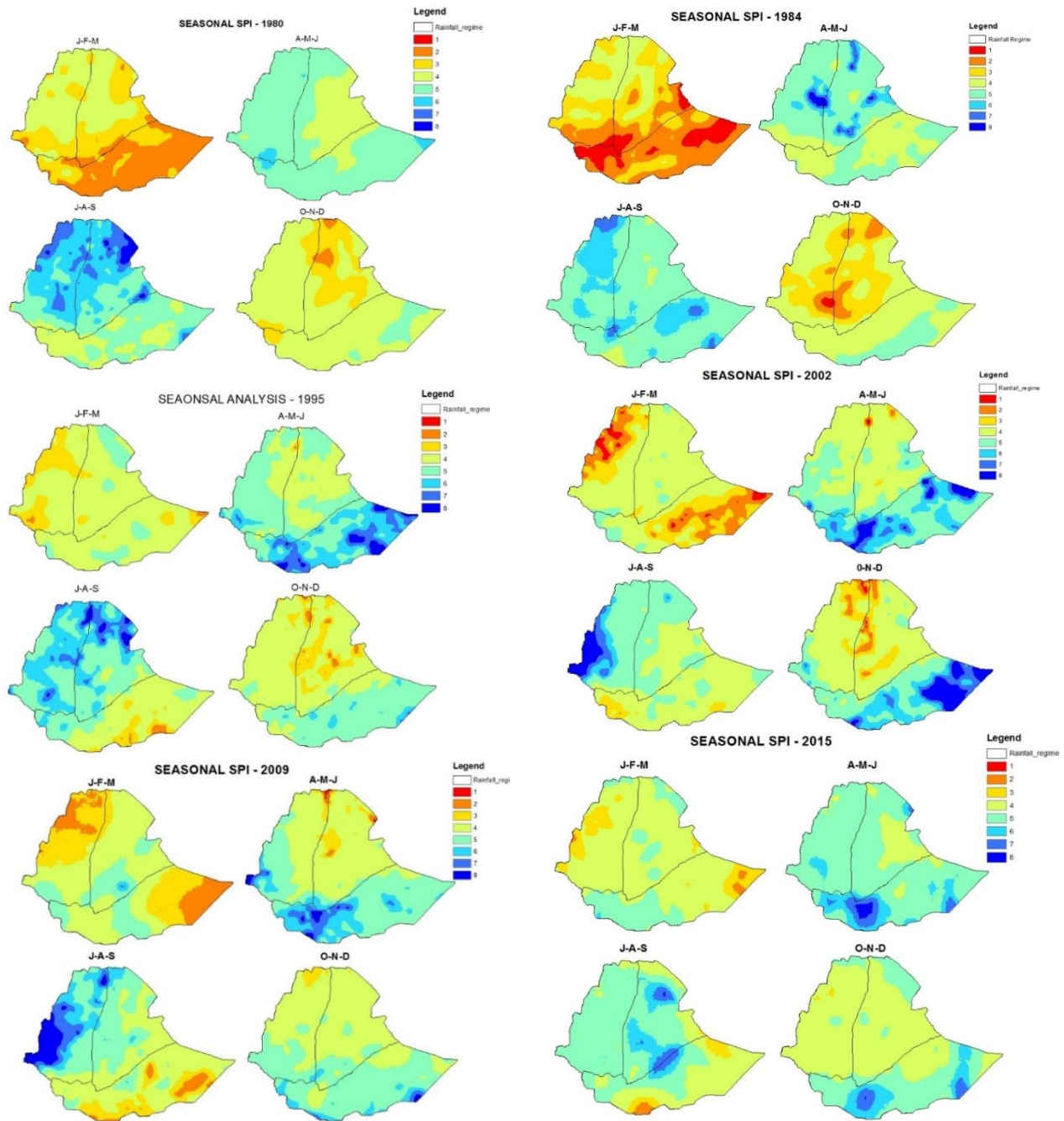


Figure 11: Spatial patterns of 3-month SPI (SPI-3) for identified drought years in the country

Indicated in the methods, this was used as a means to analyze the seasonality of drought in the study area, to assess the availability of precipitation and assess the condition over the three major rainfall regimes.

This analysis only revealed patterns in all selected drought years that correlate with the distinct rainfall regimes A, B and C. One keen observation seen in this analysis basing the yearly SPI maps is that reducing the time scale allows one to see into the specific months for signs of year round drought events. This was observed more specifically during the years 2000-2009 which showed continuous drought characteristics on a yearly scale. The necessity of the 3-month SPI surfaces here, i.e. when reviewed on a seasonal scale, showed that there was sufficient amount of rainfall available and that the source to be found needs to sustain the area for not more than one season. To further support this conclusion, the monthly analysis results are depicted next.

4.2.4. Monthly drought evaluation

Based on the indicated methodology, the monthly SPI results were interpolated and mapped. The classification, based on Mckee's (1993) classification criteria shown in Table 2 was used for this analysis as well with 1 indicating extreme drought and 8 indicating extreme wet characteristic. It was seen that similar situations were common in practically all the identified drought years and one key discovery was made. Shown in Figure 12 , is a sample display map for year 1984. The remaining maps are under the appendix section.

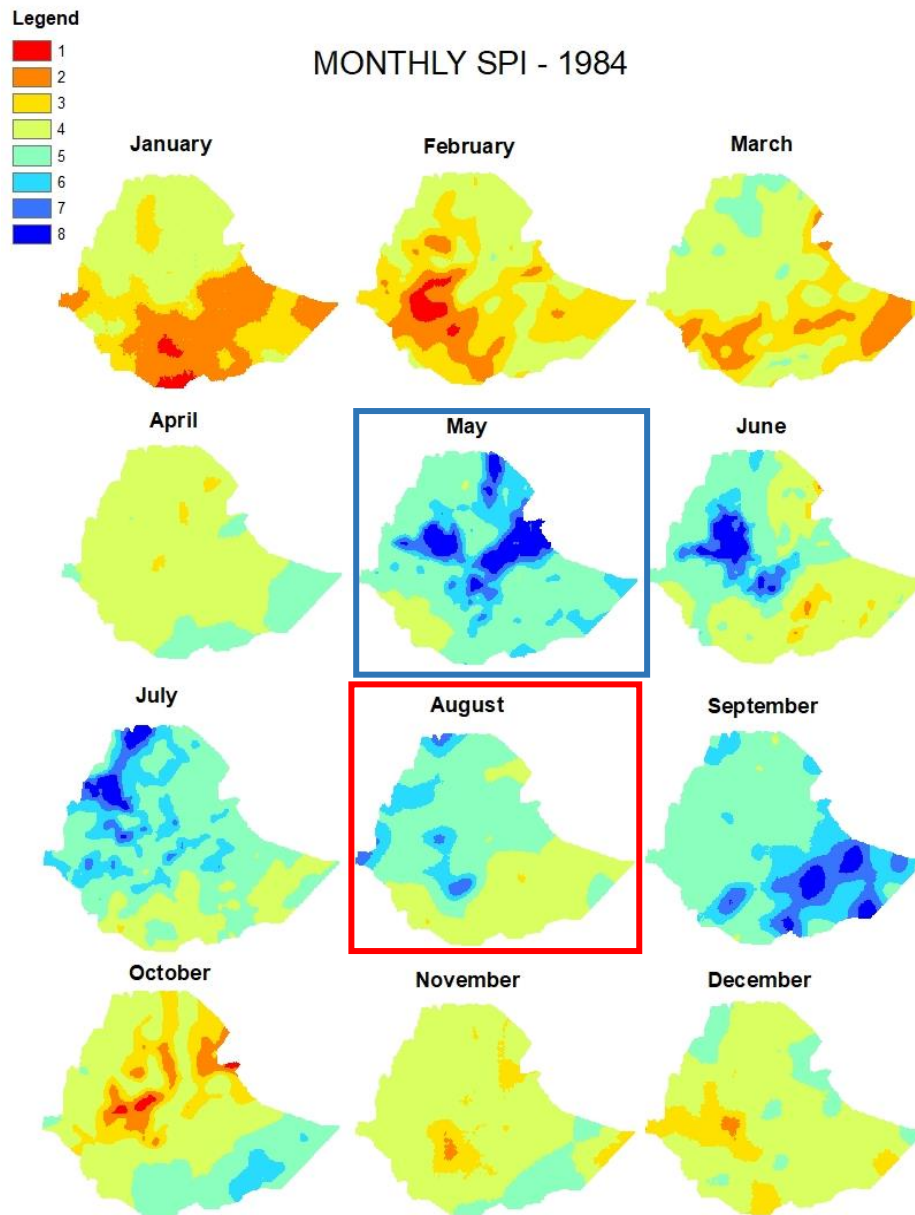


Figure 12: Spatial patterns of monthly SPI for drought year - 1984

Coupled with Figure 11, seasonal SPI of the year 1984, it is seen in this analysis that the expected rain during the “Kiremt” season (i.e. July and mainly August) was inconsistent as compared to what is anticipated. On the contrary, much of the rainfall induced SPI is of high wetness severity and extremity and is indicated in months May (inscribed in blue) and partially in June. Considering 85-95% of crop production takes place in the “Kiremt” season (Degefu, 1987) and that 70% of the total runoff is expected

in that same season, the means of capturing this rain could potentially be by the use of water harvesting.

It is obvious that previous forecasting have not been reliable enough to indicate specific drought affected months as a preparedness means and the seasonality has randomness as seen in Figure 12. Expected peaking periods in the expected rainfall regimes appear to either lead or lag. If it were, however, possible to harvest this water in months June and May, it will be able to fill the gap seen in lacking months (August).

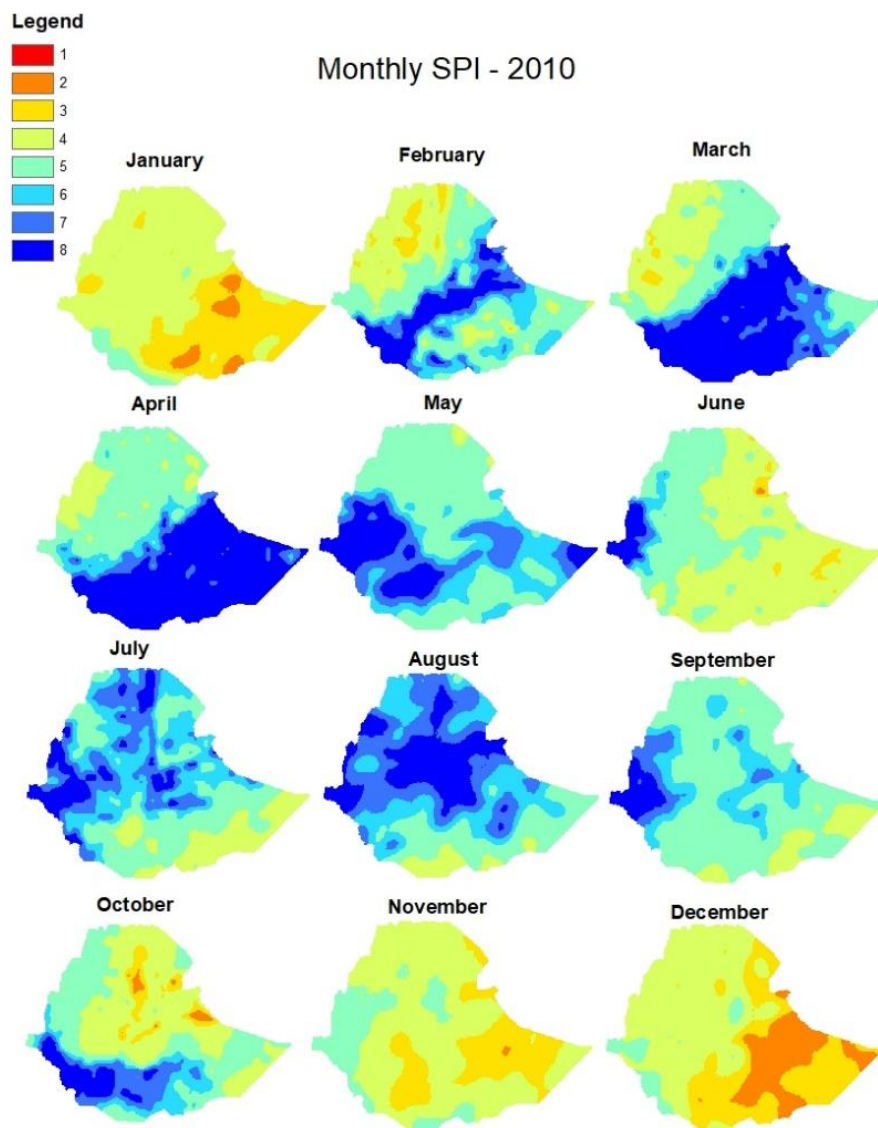


Figure 13: Spatial patterns of monthly SPI for drought year - 2010

A typical representation of expected rainfall denoted by the SPI-1 value is shown in Figure 13 for the sake of comparison. As can be seen, compared to May, August is considered the wettest month, where under normal expected circumstances, water would be available in that season. The high deviation in this characteristic leads us to lean towards rainwater harvesting when situations like those observed in 1984 and the other drought years transpire.

The following analysis reviews each drought year and corresponding 1-month SPIs. From the results of monthly SPI values, the drought magnitudes for drought year - 1980 of the representative grids is shown in Table 12. Year 1980, for fifteen representative grid point values, resulted in noticeable maximum drought magnitudes of 4.81 and 4.37 with a corresponding drought duration of four months in months January to April. Whereas the summer season in all locations did not show any abnormality to be dubbed a drought event.

Table 12: Monthly SPI values and drought magnitude for drought year 1980

January	February	March	April	May	June	July	August	Sept	Oct	Nov	Dec	Drought Magnitude	Rainfall Regimes
-1.59	-1.22	-0.76	-0.21	1.09	0.51	0.43	0.86	0.36	-0.36	-0.86	-1.91	3.79, 3.13	R5-B3
-0.59	-0.97	-0.21	0.28	0.21	0.59	0.97	0.76	0.36	0.07	-0.97	-0.97		R4-B4
-1.38	-1.59	-0.97	-0.86	1.59	0.21	-0.28	-0.76	-0.43	0.07	-1.09	-1.91	4.81, 3.00	R4-C2
-1.38	0.36	-0.21	0.28	-0.14	0.97	1.91	1.59	0.43	0.07	-0.51	-0.97	1.38	R3-B5
-0.28	0.14	-0.14	0.00	0.07	1.09	1.91	1.59	0.43	-0.07	-0.28	-0.28		R2-B6
0.14	0.14	0.14	1.38	0.14	0.36	1.59	2.20	0.28	0.14	0.14	0.14		R3-A5
-1.22	-1.59	-0.97	-0.59	1.09	0.97	-0.14	0.00	1.59	1.38	-1.38	-1.91	4.37, 3.30	R4-A3
0.21	-0.51	0.43	-0.51	-0.51	1.09	1.91	1.59	-0.51	-0.51	-0.51	-0.51		R3-A4
-1.09	-1.09	-0.97	-0.76	1.38	-0.14	0.14	0.59	0.43	-0.21	-1.09	-1.09	3.90, 2.38	R3-C4
-0.86	-0.86	-0.86	-0.86	-0.51	1.22	0.86	0.21	0.67	0.36	-0.86	-0.86		R3-A3
0.00	0.67	0.28	-0.07	-0.07	1.09	0.97	2.20	-0.07	-0.07	-0.07	-0.07		R2-A6
-0.86	-0.21	-0.97	-0.14	0.14	0.43	1.59	1.38	1.09	-0.28	-1.91	-1.22	3.42	R2-C5
0.07	-0.51	-0.07	-0.51	-0.51	0.86	1.91	0.67	-0.14	-0.51	-0.51	-0.51		R1-A5
-1.59	-0.51	-1.22	-0.76	1.22	-0.21	0.14	0.28	1.38	-0.36	-1.38	-1.59	4.09, 3.33	R2-A5
-1.38	-0.97	-1.59	-0.36	1.59	-0.86	-0.59	-0.51	0.67	1.22	0.97	-1.59	4.30	R1-C6

From the conditions on the ground, it may be difficult to distinguish between a dry climatology and drought in the sense of abnormally little precipitation. The strong seasonality of precipitation adds to the misconception. A dry summer season has more severe effects in the north than in the south, where not much rain can be expected to fall at that time of the year (Viste et al., 2015). Accordingly, Figure 14 better clarifies the effect of expected precipitation with reference to the corresponding locations.

To understand the patterns in the figures, the reader is advised to refer to the analysis conducted by (Berhanu et al., 2016) for assimilating the regional rainfall classifications used in this research.

R4-C2 and R3-C4 experienced a two month drought event in months November and December which is a result of rainfall deficiency in the preceding months. Similarly in locations R2-A5 and R1-C6, where peaking rainfall was expected to be on months March and April, a drought with a magnitude of 4.09 and 4.3 respectively occurred in a drought event that that lasted for four months.

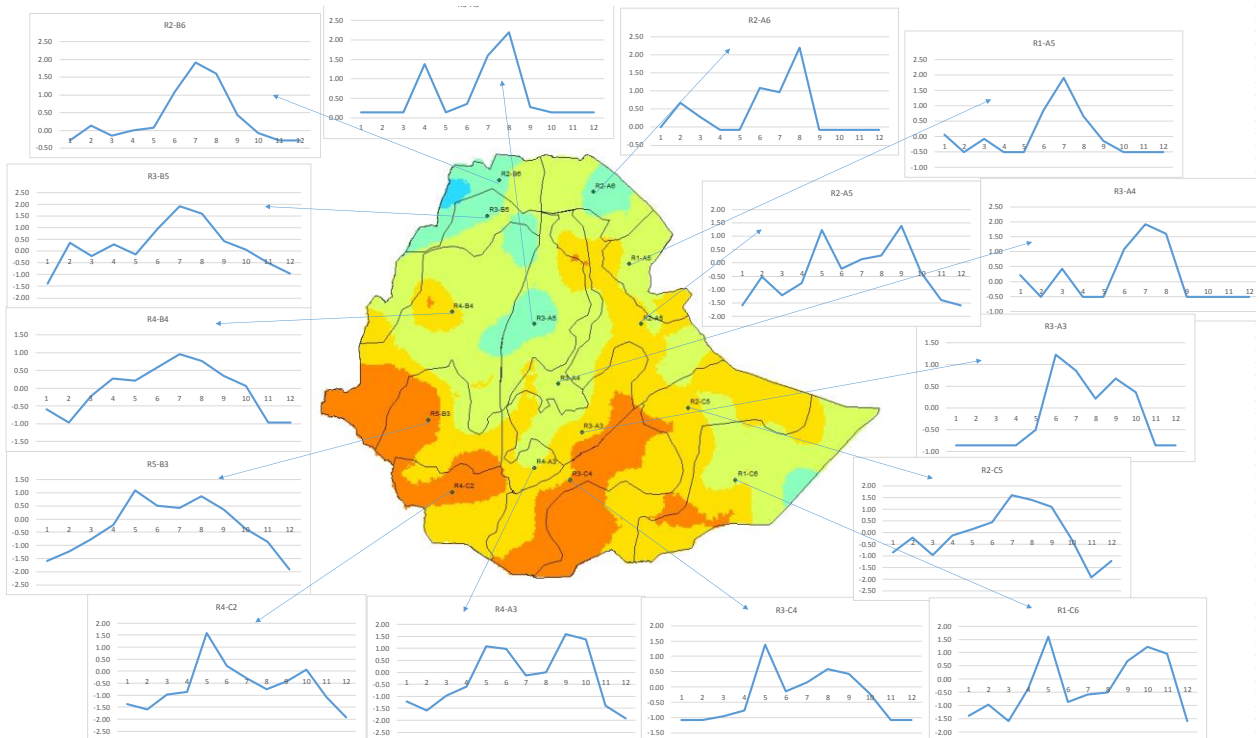


Figure 14: Spatial pattern of 1-month SPI with grid based temporal distribution for drought year 1980

The background maps used for representing cases in the distinct rainfall regimes was taken from the 12-month SPI analysis shown in Figure 6.

Year 1984 was characterized for recording the largest drought event that lasted from January to August at station R4-C2 that summed to 7.66 in magnitude, which normally expects a peaking rainfall in months March/April. A similar situation was seen in R4-A3 and R1-A5, where months March/April and July/August were expected to result in the peak rainfall.

Table 13: Monthly SPI values and drought magnitude for drought year 1984

Jan	Feb	Mar	Apr	May	June	July	Aug	Sep	Oct	Nov	Dec	Drought magnitude	Rainfall Regimes
-1.22	-1.91	-0.86	-0.51	0.43	0.21	1.22	0.28	0.21	-1.09	-0.51	-1.09	4.51, 2.68	R5-B3
-0.28	-0.97	0.14	0.00	2.20	1.91	1.59	0.59	0.51	-0.97	-0.28	-0.97		R4-B4
-1.91	-1.59	-1.59	-0.67	-0.43	-0.43	-0.43	-0.59	0.86	-0.43	-0.43	-0.43	7.66	R4-C2
-0.43	-1.09	0.07	0.07	2.20	2.20	2.20	0.59	0.86	-1.09	-0.67	-1.09	1.52	R3-B5
-1.38	-1.38	0.28	-0.43	0.43	0.86	1.38	0.97	0.86	-0.51	-0.43	-0.07	2.91, 1.01	R2-B6
0.14	0.14	0.14	0.14	0.86	0.76	0.86	0.76	0.28	0.14	0.14	0.76		R3-A5
-1.91	-1.91	-1.38	-0.59	1.59	-0.07	-0.14	1.91	1.38	-0.28	-1.09	-1.09	5.80, 2.45	R4-A3
0.21	0.21	-0.51	-0.51	1.59	0.97	0.59	0.51	1.22	-0.51	-0.51	0.43	1.02	R3-A4
-1.09	-1.09	-0.86	-0.36	1.91	0.28	0.07	-0.28	1.38	0.43	-0.76	0.21	3.39	R3-C4
-0.86	-0.86	-0.86	-0.86	1.91	1.91	-0.21	0.00	0.97	-0.36	-0.51	-0.59		R3-A3
0.00	-0.07	-0.07	-0.07	2.20	-0.07	0.86	0.76	0.36	-0.07	-0.07	-0.07		R2-A6
-0.51	-0.59	-1.22	-0.28	1.38	-0.28	0.43	0.07	0.67	-1.91	-0.59	0.51	2.60, 2.50	R1-A5
-0.07	-0.43	-0.51	0.28	2.20	-0.51	1.22	0.59	1.91	-0.51	-0.51	-0.51		R2-A5
-1.59	-0.76	-0.97	-0.97	0.97	-0.51	0.86	0.07	1.59	-0.51	-0.51	-0.97	4.29	R2-C5
-1.38	-1.22	-1.38	0.14	0.97	-0.67	-0.36	-0.51	1.22	1.22	0.36	-0.59	3.99	R1-C6

Table 13 shows the values of the 1-month SPI computed in R and arranged to conceptually cover the entire study area through representative grid points. According to the definition of drought magnitude, SPI values that are below zero and that have reached a value of -1 qualify as a drought event. Accordingly, drought magnitudes are depicted in the column following the monthly SPI values. The drought magnitude was computed by summing the negative SPI values in an identified drought event.

For ease of interpretation, the one-year time series comprising of the monthly SPI values are plotted according to the respective rainfall regimes. The SPI patterns are in line with the expected rainfall patterns for the respective regimes in terms of modality and peaking season. The map shows a mono-modal graph for the north-west, central-west and western parts of the study domain and a bi-modal pattern with differing peaking months for the remaining regimes.

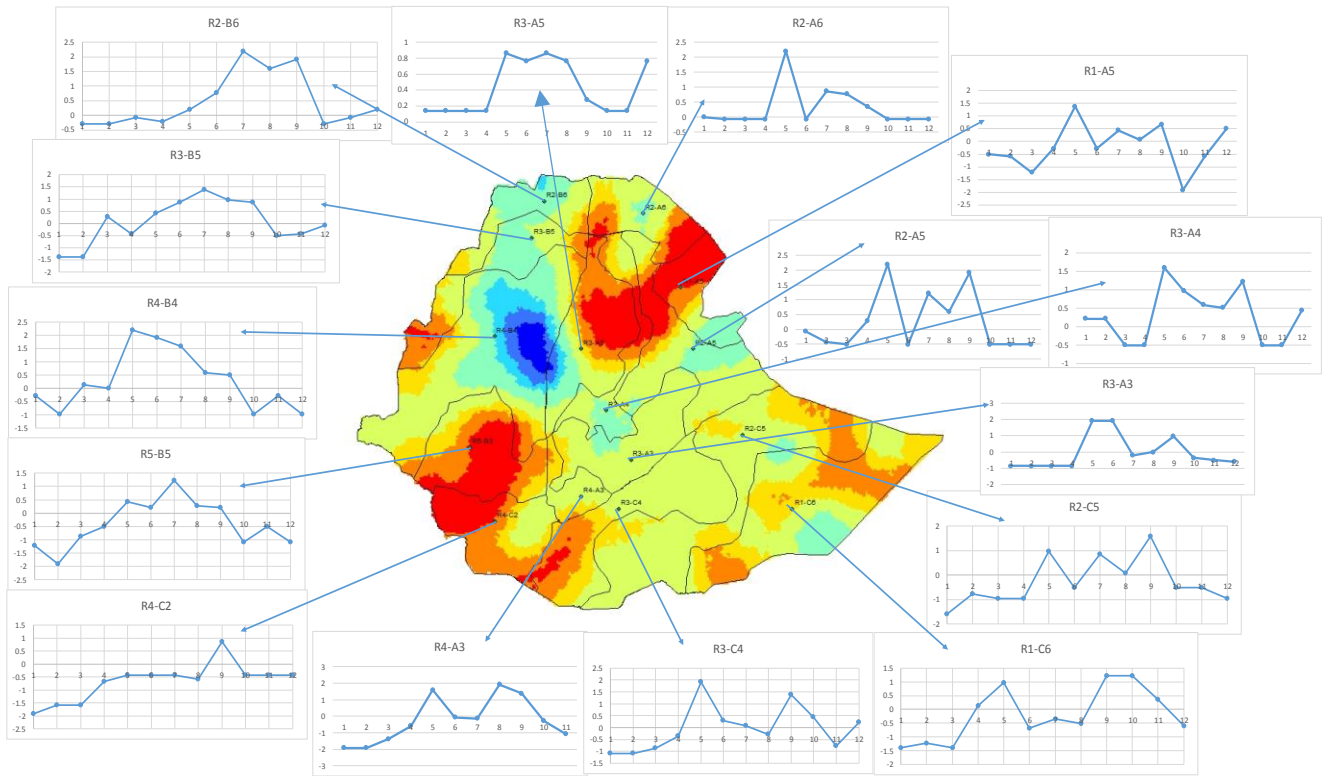


Figure 15: Spatial pattern of 1-month SPI with grid based temporal distribution for drought year 1984

With a similar tabularization technique, year 1995 was also represented by the representative rainfall regimes and the drought magnitudes were computed accordingly. Table 14 summarizes the 1-month SPI for drought year 1995. The largest drought magnitude observed in this analysis is 3.143 at one station but did not qualify as an anomalous event owing to what was previously mentioned regarding the distinction between a dry climatology and drought and what qualifies as a dry period with respect to the seasonality of rainfall in the study area.

Table 14: Monthly SPI values and drought magnitude – Year 1995

January	February	March	April	May	June	July	August	Sept	Oct	Nov	Dec	Drought Magnitude	Rainfall Regimes
-1.38	-1.09	-0.67	0.28	0.43	0.43	1.59	1.59	1.22	0.14	-0.43	-0.51	3.143	R5-B3
-0.97	-0.97	0.51	0.00	0.36	0.28	0.97	2.20	0.59	0.28	0.28	-0.76		R4-B4
-0.67	0.00	-0.28	0.97	0.76	-0.43	0.36	-0.43	0.67	1.22	0.36	-0.51		R4-C2
-1.22	0.00	0.28	-0.21	0.36	0.07	1.38	0.97	0.59	-0.21	-0.43	-0.43	1.221	R3-B5
-0.28	-0.07	0.00	-0.28	0.97	-0.07	1.59	0.36	0.97	0.00	0.07	0.14		R2-B6
0.14	0.14	0.28	0.14	0.14	0.28	0.86	1.09	0.59	0.14	0.14	0.14		R3-A5
-1.91	-0.14	-0.28	0.97	-0.14	-0.14	-0.07	0.43	1.59	0.51	-0.43	-0.51	2.336	R4-A3
-0.14	0.36	-0.28	0.21	1.38	-0.51	1.38	0.67	0.36	0.36	-0.51	-0.51		R3-A4
-1.09	-0.51	-0.51	1.38	0.67	-0.36	0.43	0.07	1.09	1.09	-0.07	-0.59	2.102	R3-C4
-0.86	-0.67	0.21	-0.21	-0.59	-0.86	0.36	-0.21	1.59	0.51	-0.86	0.51		R3-A3
-0.07	0.67	1.22	0.76	-0.07	1.38	1.59	0.36	0.21	-0.07	-0.07	-0.07		R2-A6
-0.76	0.67	1.09	-0.51	0.21	-0.21	1.91	1.09	0.14	0.59	-0.14	0.00		R2-C5
-0.51	-0.21	1.22	-0.51	0.00	-0.28	1.91	0.14	-0.43	-0.51	-0.51	0.59		R1-A5
-1.59	-0.51	0.21	1.59	0.97	-0.36	-0.21	0.07	0.07	0.97	-0.97	-0.97	2.102	R2-A5
-1.59	-1.38	1.22	2.20	1.22	-0.51	-0.67	-0.36	0.07	1.91	0.07	-0.67	2.970	R1-C6

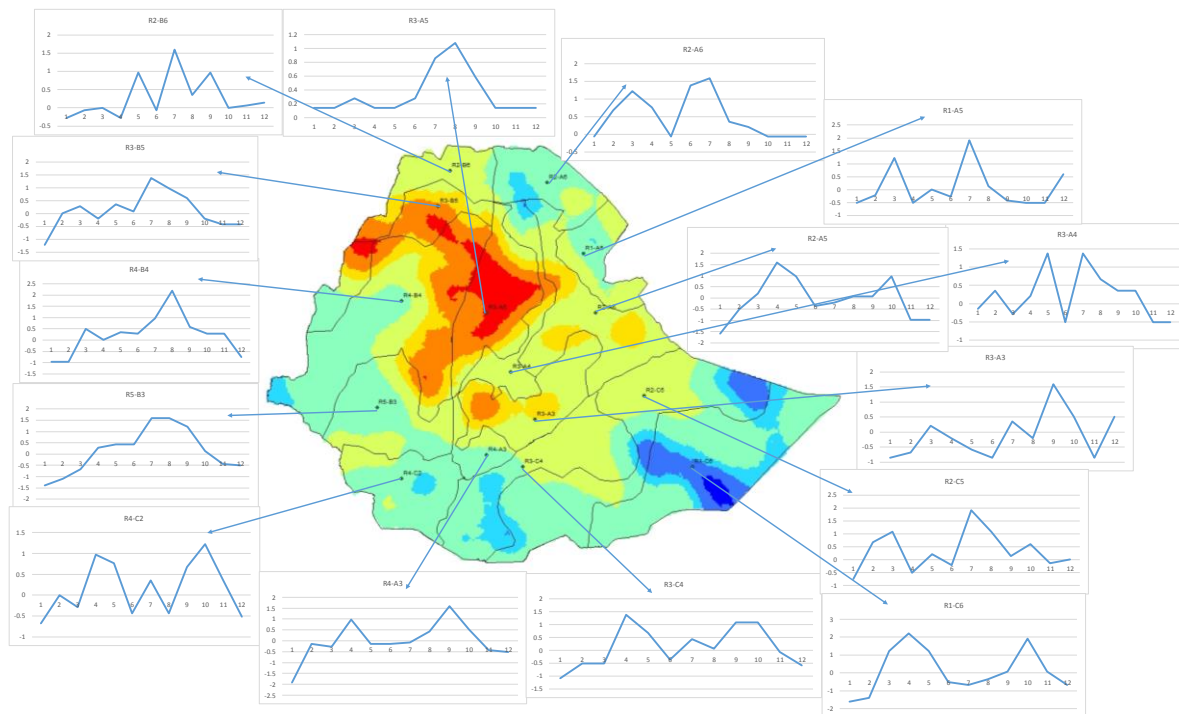


Figure 16: Spatial pattern of 1-month SPI with grid based temporal distribution for drought year 1995

The largest recorded drought magnitude in year 2002 was 3.83 which showed anomalies in months May and June, which is a result of rainfall deficiency during the preceding months. Representative grid R3-C4 also showed an anomalous event in the month November where a peaking rainfall period was expected to occur.

Table 15: Monthly SPI values and drought magnitude - Year 2002

January	February	March	April	May	June	July	August	Sept	Oct	Nov	Dec	Drought magnitude	Rainfall Regimes
-0.51	-1.59	-0.51	-0.51	-0.43	1.91	0.28	1.91	0.43	0.21	-0.86	-0.43	3.55	R5-B3
-0.43	-0.97	-0.43	0.00	0.28	0.97	0.76	0.97	0.28	0.28	-0.51	0.00		R4-B4
-0.28	-0.67	0.86	0.36	1.91	0.21	-0.67	-0.51	-0.43	0.67	0.00	1.22		R4-C2
-0.59	-1.09	-0.14	0.28	-0.14	0.51	0.59	0.59	0.07	-0.67	-1.09	0.07	1.76	R3-B5
-1.38	-1.38	0.14	-0.67	-0.28	0.28	0.59	0.97	0.07	-0.43	-0.67	-0.43	2.77	R2-B6
0.14	0.14	0.14	0.86	0.14	0.21	0.51	0.59	0.14	0.14	0.14	0.14		R3-A5
-0.67	-1.91	-0.43	-0.14	1.59	0.51	-0.14	1.91	-0.36	0.51	-0.86	-0.43	3.16	R4-A3
-0.14	-0.51	1.09	0.00	-0.51	-0.51	-0.51	-0.14	0.07	-0.51	-0.51	0.51		R3-A4
-0.36	-1.09	-0.86	0.43	1.91	0.07	-0.14	0.67	0.21	1.91	-1.09	0.67	2.30	R3-C4
0.86	-0.86	0.97	1.91	-0.59	-0.76	-0.76	0.00	-0.14	-0.21	-0.86	0.21	2.29	R3-A3
0.36	-0.07	0.28	0.00	-0.07	-0.07	0.21	0.67	1.91	-0.07	-0.07	0.36		R2-A6
-0.43	-1.59	-0.97	1.59	0.14	0.07	-0.59	0.14	0.36	1.59	-0.97	-0.97	2.99	R2-C5
0.67	-0.59	0.36	0.67	-1.91	-1.91	0.36	0.67	0.67	-1.91	-1.22	1.09	3.83	R1-A5
0.28	-0.36	0.28	1.91	-0.51	-0.51	-0.51	0.28	0.28	-0.51	-0.51	0.28		R2-A5
-1.38	-1.09	-0.59	1.91	0.67	-0.59	-0.76	-0.67	0.67	2.20	1.22	0.07	3.06	R1-C6

Majority of the spatially mapped result of the year 2002, similar to the previous ones, show a common pattern that mimics the rainfall pattern well, especially in the southern part of the study domain where bi-modal patterns are common.

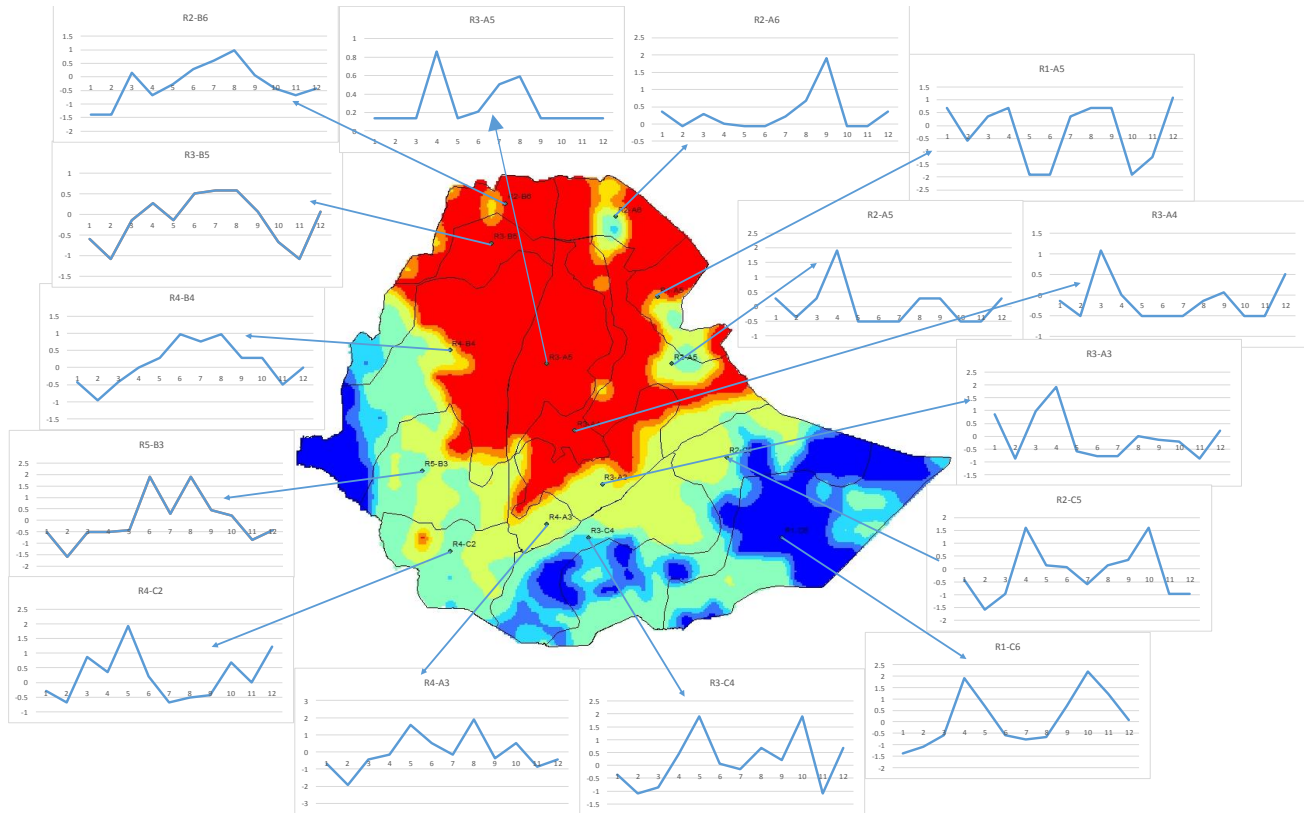


Figure 17: Spatial pattern of 1-month SPI with grid based temporal distribution for drought year 2002

More than half the representative grids have shown anomalous events in the year 2009 with relatively smaller drought magnitudes as compared to the other years. The results are summarized in table 16 with a graphical representation following it.

Table 16: Monthly SPI values and drought magnitude – Year 2009

January	February	March	April	May	June	July	August	Sept	Oct	Nov	Dec	Drought Magnitude	Rainfall Regimes
-0.51	-0.07	0.14	-0.07	0.07	0.21	0.14	1.22	0.43	0.67	-0.86	0.36	0.58	R5-B3
-0.97	-0.67	-0.43	0.14	0.28	0.28	2.20	0.97	0.28	0.43	-0.86	0.00	2.07	R4-B4
-0.21	-1.09	0.43	1.38	1.22	-0.43	-0.97	-0.43	-0.36	0.67	-0.43	1.59	1.30,2.18	R4-C2
-1.38	0.00	-0.14	-0.21	-0.28	0.36	1.38	0.97	0.28	0.07	-0.59	0.00	1.38	R3-B5
-0.28	-0.28	-0.28	-0.28	-0.28	-0.07	1.91	0.97	0.21	-0.21	-0.28	-0.28	0.56	R2-B6
0.14	0.14	0.14	0.14	0.14	0.14	0.97	0.76	0.59	0.14	0.14	0.14	0.28	R3-A5
-0.86	-1.38	-0.28	0.21	1.59	-0.43	-0.43	-0.36	-0.28	0.43	-0.97	0.21	2.53	R4-A3
0.21	-0.51	1.38	0.36	-0.14	-0.36	1.91	-0.14	-0.07	0.97	-0.51	-0.07	0.51	R3-A4
-0.43	-0.36	1.38	1.91	1.38	-0.07	0.21	0.43	0.67	0.97	-0.76	0.07	0.79	R3-C4
-0.14	-0.86	2.20	0.86	-0.76	-0.86	0.00	-0.43	0.07	1.22	-0.43	0.67	1.00	R3-A3

January	February	March	April	May	June	July	August	Sept	Oct	Nov	Dec	Drought Magnitude	Rainfall Regimes
0.00	0.00	0.36	0.00	0.28	-0.07	0.36	1.22	-0.07	0.00	0.00	-0.07	0.00	R2-A6
-1.22	-1.22	-0.43	0.59	0.36	-0.86	0.00	-0.59	0.28	0.97	-0.59	-1.22	2.87	R2-C5
0.14	-0.21	0.36	0.43	0.14	-0.76	0.28	0.67	-0.21	0.59	-0.14	-0.28	0.07,0.42	R1-A5
0.36	-0.51	1.91	-0.43	-0.51	0.00	0.59	0.00	-0.51	0.00	0.21	-0.07	0.15	R2-A5
-1.09	-0.67	-0.76	1.38	0.86	-1.09	-0.67	-1.09	-0.59	1.59	0.21	-1.09	2.52	R1-C6

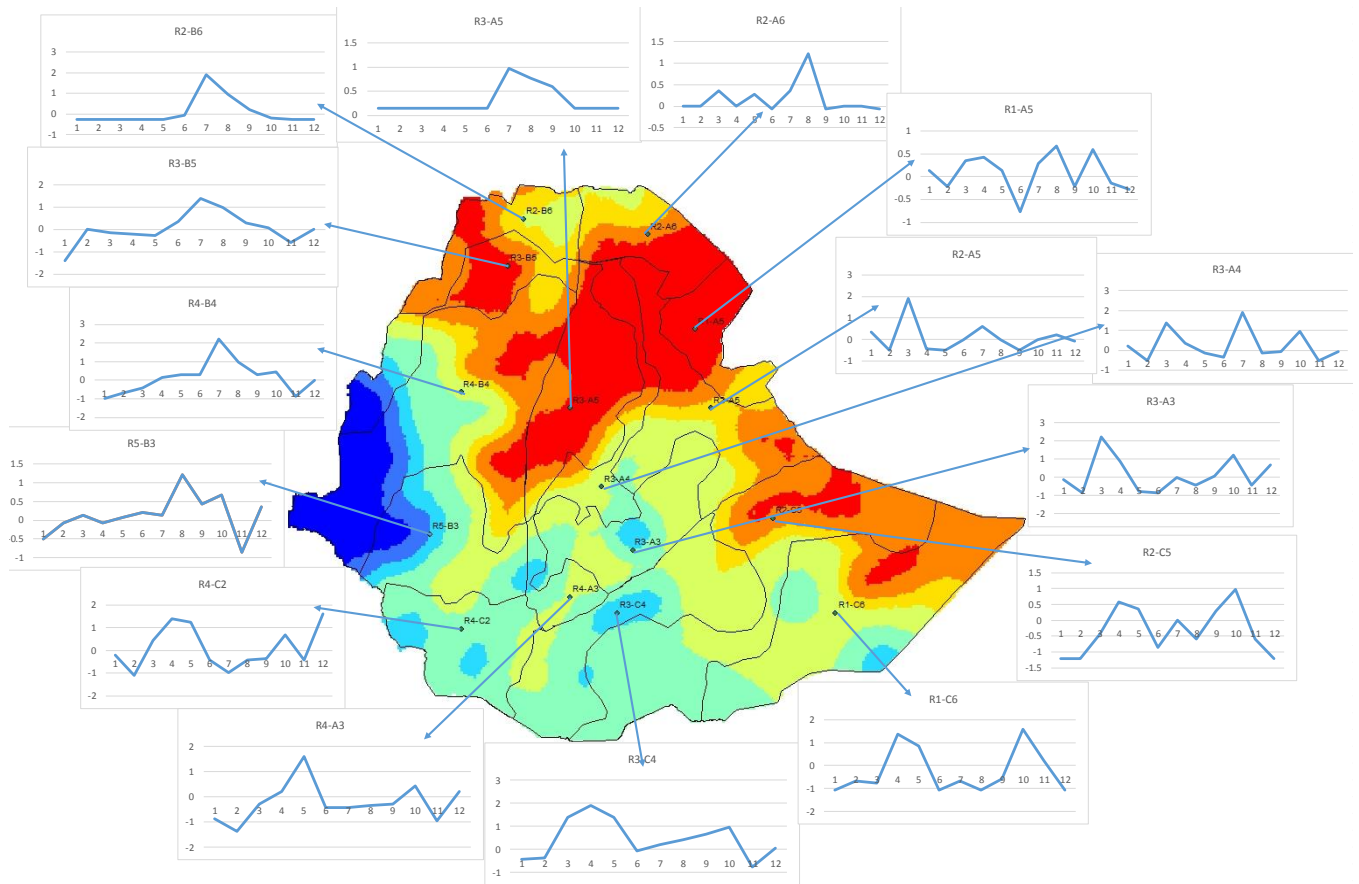


Figure 18: Spatial pattern of 1-month SPI with grid based temporal distribution for drought Year 2009

Year 2015 was characterized by the seasonality effect. Expected peaking times west and north-west of the domain had led by a month thereby resulting in relatively low SPI results during the peaking season. The largest drought magnitude was observed in the southern region with 5.74. Similar to previous deductions, this too was expected for the period July – September, as the regime expects a dual peak during months March/April and October/November. The results are summarized and tabulated in Table 17.

Table 17: Monthly SPI values and drought magnitude – Year 2015

January	February	March	April	May	June	July	August	Sept	Oct	Nov	Dec	Drought magnitude	Rainfall Regimes
-1.09	-1.22	-0.28	-2.20	0.43	2.20	-0.97	0.28	0.43	-1.59	-0.97	-0.51	4.79, 3.07	R5-B3
-0.86	-0.97	0.14	-0.28	0.51	2.20	0.43	0.51	0.28	0.28	0.28	0.00		R4-B4
-0.36	-1.09	1.91	-2.20	1.22	2.20	-2.20	-1.59	-1.59	-0.36	0.59	0.28	1.44, 5.74	R4-C2
-1.38	-1.09	0.00	0.00	0.36	0.67	0.36	0.86	0.00	0.36	-0.14	-0.51	2.47	R3-B5
-0.28	-0.28	0.21	0.14	0.21	0.97	1.09	1.38	0.00	0.28	0.00	-0.07		R2-B6
0.14	0.14	0.86	0.86	0.86	0.86	1.38	1.22	0.59	0.76	0.59	0.59		R3-A5
-1.59	-0.97	1.38	-0.43	0.59	0.67	-0.14	-0.28	-0.43	-0.14	-0.36	-0.36	2.56	R4-A3
-0.51	-0.14	1.22	0.97	0.97	0.76	1.38	1.91	0.07	0.67	0.21	0.21		R3-A4
-0.97	-0.43	1.91	1.91	1.59	0.14	1.91	2.20	-0.43	1.09	0.36	0.14		R3-C4
-0.21	0.51	0.97	0.59	0.97	0.86	1.91	0.97	0.86	0.67	0.21	0.21		R3-A3
0.00	0.59	1.22	1.38	1.22	0.36	0.28	0.28	0.59	1.38	1.22	1.22		R2-A6
-0.97	-0.43	0.36	1.09	0.36	0.36	0.36	0.36	0.86	-0.43	-0.43	0.14		R2-C5
-1.09	0.00	0.67	0.67	0.67	0.67	1.22	1.59	0.67	0.14	0.59	0.67	1.09	R1-A5
0.59	0.14	0.86	0.36	0.28	0.14	0.97	1.22	0.76	0.28	0.51	0.36		R2-A5
-1.09	-1.22	0.28	0.07	1.38	-0.21	-1.22	-0.97	0.14	0.86	0.67	0.07	2.31	R1-C6

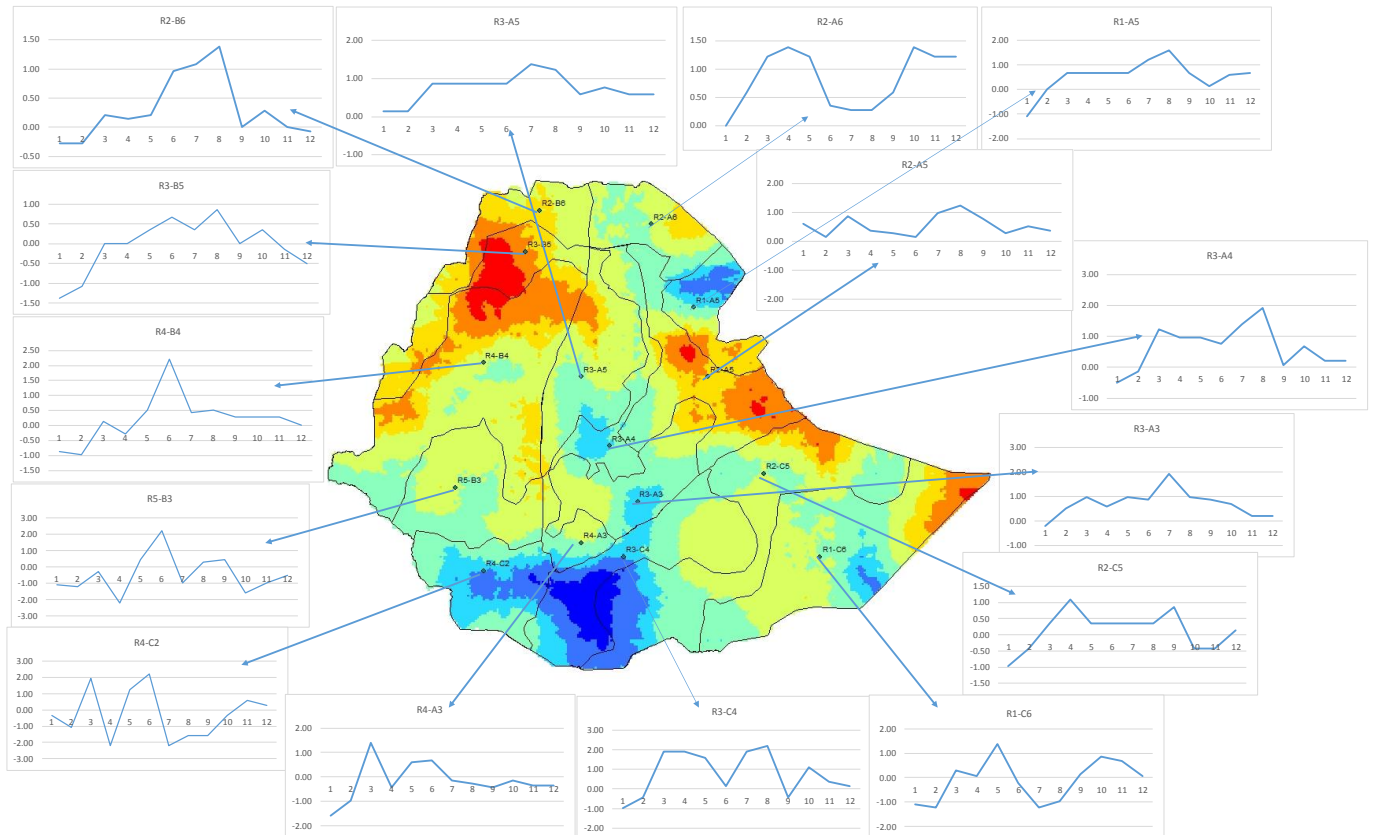


Figure 19: Spatial pattern of 1-month SPI with grid based temporal distribution for drought year 2015

The monthly analysis clearly depicted specific months that were drought prone and those that had enough rainfall. Furthermore, this analysis was used as a basis to select the driest month for further continuation of the study.

The spatial patterns of metrological drought using SPI-1 were mapped over the country for selected years in the study period. Spatial coverage of drought over the study domain was again obtained using the Kriging technique and is shown in Appendix C. In a similar manner, ranges of SPI values are mapped with 1 denoting extreme drought and 8 denoting extreme wet period.

Upon review of the entire months of the selected drought years, months January and February surpassed the threshold indicated (i.e showing dry characteristics) and were selected to proceed with further analysis.

1.1.1. Summary of Ethiopia’s prominent drought periods, 1979-2016

The analysis performed in this study revealed several important facts about dry and wet periods in Ethiopia:

1. For identified drought years, there was no lack of precipitation (as indicated by positive SPI),
2. Lag/lead of peaking months resulted in deviations from the ordinary that characterized the year a “drought year”,
3. The potential water resource need only supply for anomalous events (i.e. a maximum of one season)

Table 18 confirms that the recorded drought years exhibit the six lowest total precipitations in the country. The remaining years in the study period are also shown cross referenced with the corresponding years.

Table 18: Average precipitation amount - 1979-2016

Year	Spatial Average of	Year	Spatial Average of
------	--------------------	------	--------------------

	Annual Rainfall (mm)		Annual Rainfall (mm)
1979	884.38	1998	1188.39
1980	626.94	1999	827.28
1981	938.31	2000	840.75
1982	1016.07	2001	775.27
1983	1039.70	2002	661.60
1984	657.45	2003	799.94
1985	850.05	2004	768.63
1986	967.69	2005	876.21
1987	904.33	2006	949.66
1988	1052.78	2007	880.46
1989	1009.97	2008	833.02
1990	845.64	2009	729.89
1991	828.38	2010	1528.37
1992	848.42	2011	813.65
1993	852.03	2012	804.48
1994	921.14	2013	1002.17
1995	740.02	2014	969.55
1996	1024.93	2015	763.28
1997	1336.63	2016	900.75

848 mm/yr long term average precipitation amount (936.4 Bm³ volume wise) is available per year according to aquastat database which can be accessed through http://www.fao.org/nr/water/aquastat/countries_regions/ETH/index.stm.

Considering the total surface area of the country, the values shown in Table 18 confirm this figure and lay foundation for the hypothesis that follows identification of sources: *There is adequate rechargeable resource, what is required is a delivery system.* The total

capacity of the country goes up to a volume of 31.5Bm³ (FAO aquastat database 2014) which only covers 3.5% of what is available.

The problem of water shortage common for all drought years stems from the seasonality of rainfall and the lack of infrastructure for storage to capture excess runoff during flood seasons. It is based on this background that the rainwater harvesting holds significance. The remainder of this research presents an alternative to conventional water supply considering the fact that any land anywhere can be used to harvest rainwater.

A quantitatively based classification done by Berhanu et al., (2013) showed the high runoff generation area of the country has large coverage, indicating the availability of high surface water potential. If it were possible to devise a mechanism or further increase the storage capacity to capture, in the long run, this much available precipitation and surface runoff, it will be enough to sustain the country for the identified anomalous event (i.e. one season) and then some.

The next section of this research discusses the methods used to identify these patches of areas that are suitable for harvesting rain water and that will aid in sustaining the recurring drought.

4.3. Terrain Analysis

The D8 algorithm was used for computing flow accumulation and slope in ArcGIS's spatial analyst to be used as input for Terrain Analysis. The results for D8 flow accumulation is shown in Figure 20 with higher values indicating a greater area with large incoming accumulated water thereby influencing soil moisture. On the contrary, higher values from the slope computation indicate areas that are steep allowing water

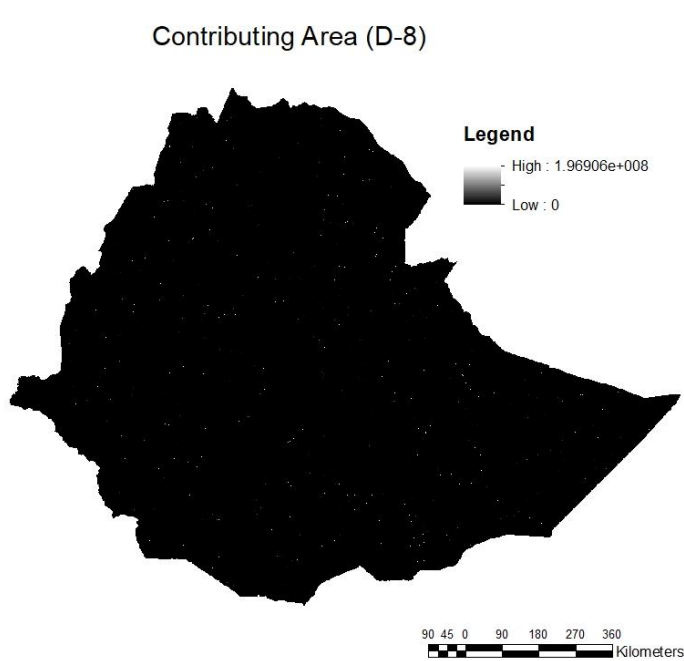


Figure 20: Spatial map of moisture contributing area of the country

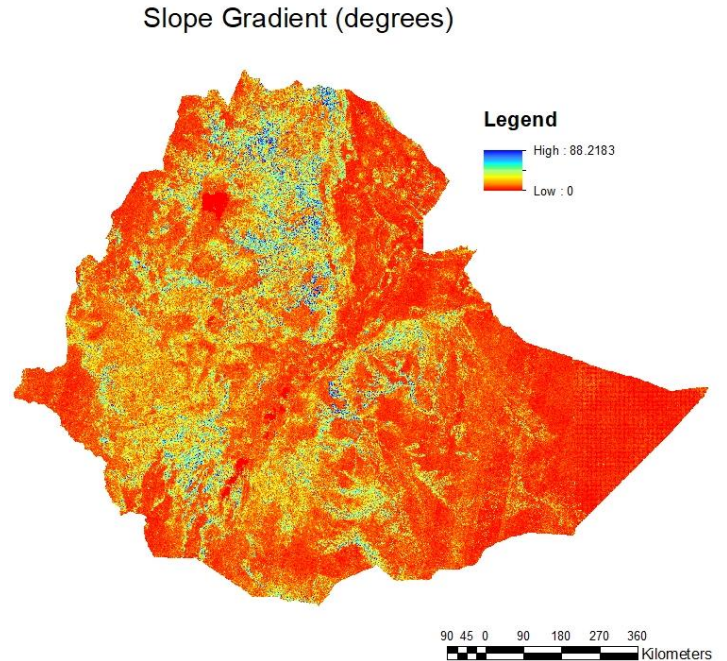


Figure 21: Slope distribution of the country

to flow readily (Figure 21).

As mentioned in the methods sections, an alternative FD-8 algorithm was applied but even though the effects on flow direction with the use of TauDEM seemed reliable, results from this were inconclusive and still did not significantly reduce the flow partitioning to result in a smoother flow. Therefore for overlaying, a different approach was improvised that involved the use of select features by location in ArcGIS which will be discussed later. Proceeding with the initial procedure of using the D-8 algorithm, results are depicted in the following section.

The combination of these inputs (contributing area and slope) which yielded the TWI has results that range from 3.39 to 31.08. The higher values indicate large contributing area coupled with low slope and hence a greater potential for water concentration, and the lower values indicate high slopes where water is free to drain.

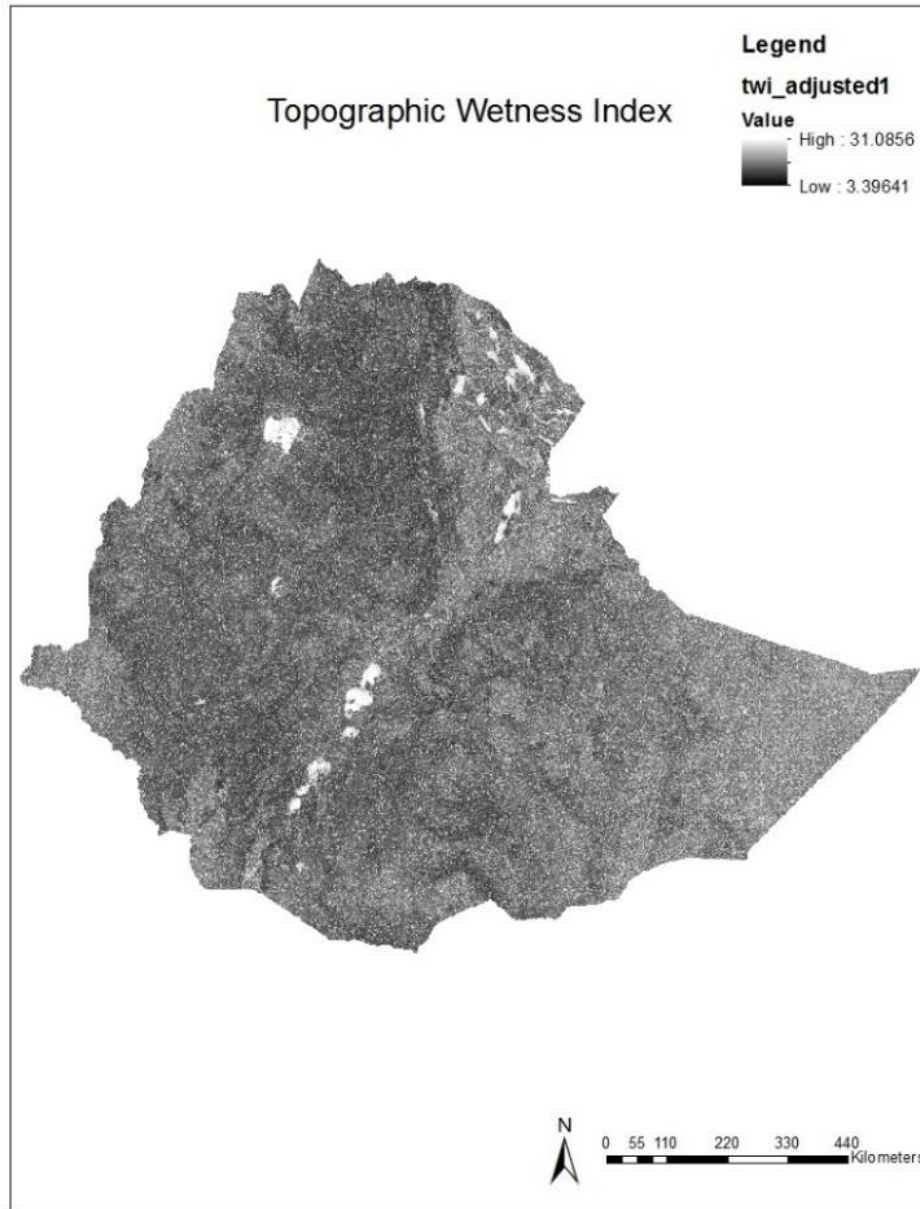


Figure 22: Spatial map of TWI of the country

The values obtained were reclassified and the TWI values were computed in ArcGIS spatial analyst based on literature and likely observation is mapped with six categories tabulated.

Reclassified - Topographic Wetness Index

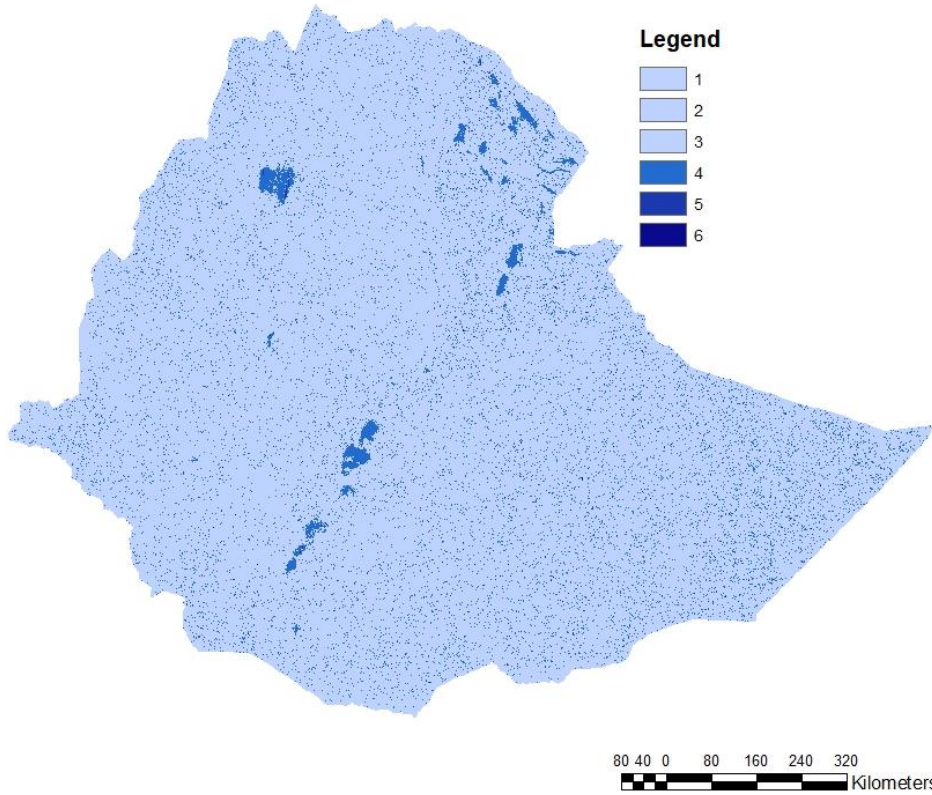


Table 19: TWI Category and Adopted range

Category	Range
1	0-5
2	5-10
3	10-15
4	15-20
5	25-30
6	>30

Figure 23: Reclassified TWI of the country

According to the map shown, a greater percentage falls within TWI ranges of 0-15 signifying suitability of water accumulation to be low. These locations were disregarded, as using them jointly would not necessarily result in water harvesting locations. On the contrary, ranges falling under 4, 5 and 6, i.e. TWIs greater than 15 exhibit high flow concentration capacities which make them the ideal choices for potential water harvesting. The map showing this filtered category is depicted in Figure 24.

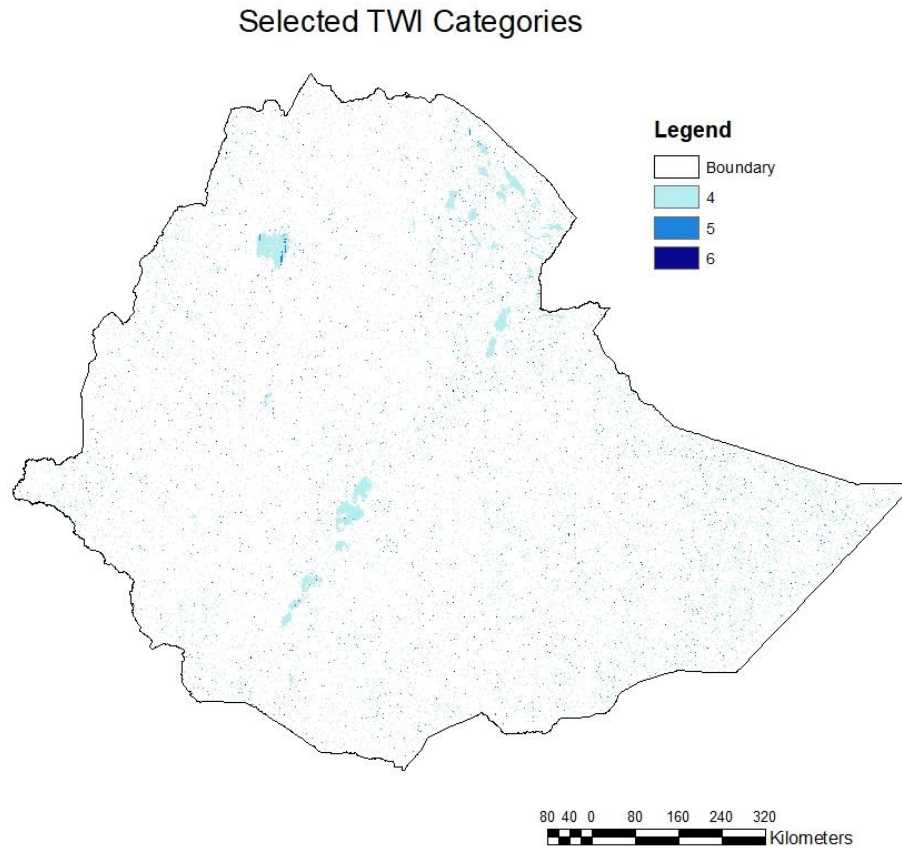


Figure 24: Desirable TWI category over threshold

Figure 24 depicts locations of TWI values that are 15 and higher to show the desirability levels. In this particular image, TWI ranges between 15 and 20 represent water bodies such as lakes found at a few locations over the study area. The other two categories, 25 and over are shown in what appear to be minute dots due to the scale factor but are actually stream lines that exhibit large TWIs.

4.4. Land use analysis

NDVI value for January 2015 was initially mapped into eight categories based on the classification shown in Table 3. The map in Figure 25 shows the partitioned classification to assess the contrasting features in further detail based on the reclassification made in Table 5.

The purpose of this preliminary mapping is to develop a desirable NDVI range where water harvesting can be categorized into.

Reclassified - Normalized Difference Vegetation Index

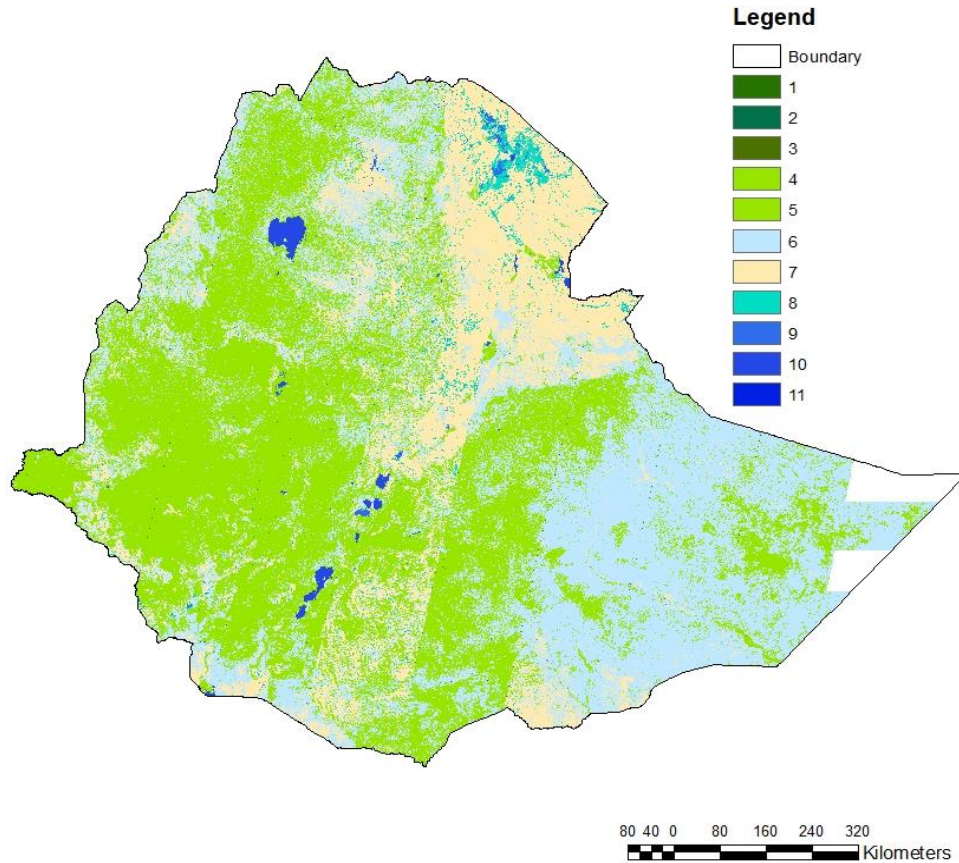


Figure 25: Spatial distribution of NDVI of the country

The land use analysis using NDVI showed that a greater percentage (36.3%) of the study area is covered by light green vegetation and 35.6% is covered by medium green vegetation. This result, for a month with dry characteristics, is quite large, implying that it is the outcome of perennial crops and their canopy effect.

The ranges shown in the legend of Figure 25 are further clarified in Table 20 along with percentage area classifications for each cover type.

Table 20: Summarized NDVI results and corresponding study area coverage

No.	Cover Type	NDVI - range	Percentage
-----	------------	--------------	------------

		value	area
1	Dense green leaf vegetation	0.85 – 1.0	0.04%
2		0.7 – 0.85	0.00%
3		0.5 – 0.7	0.01%
4	Medium green leaf vegetation	0.25 – 0.5	7.63%
5		0.09 – 0.25	35.61%
6	Light green leaf vegetation	0.09 – 0.14	36.28%
7	Bare soil	0.025 – 0.09	18.21%
8	Wet lands/swampy areas	0.002 – 0.025	1.36%
9	Light water bodies	-0.046 – -0.002	0.27%
10	Water bodies	-0.257 – -0.046	0.58%
11	Deep water bodies	-0.257 – -1	0.01%

Upon manual division of land-water threshold, the study was able to find that the NDVI had in fact the ability to discriminate water and dry land areas well. The map showing these desirable values, similar to that of the TWI is plotted in Figure 26 corresponding to the classification table shown in Table 21.

The resultant land use map is shown in Figure 26 and consists of three dominant land cover classes; namely light green vegetation, swampy/wetlands and water bodies.

The classification table shows the percentage of areal coverage of the three desirable features.

Table 21: Desirable NDVI Category of the study area with areal coverage

Category	Value	Areal coverage
3	Light green vegetation	36.28%
5	Swampy/wetland	1.35%
6	Water bodies	0.85%

A way of showing how indicative of water bodies this index is, is to see the mapped results from the NDVI values for known water bodies. The index has displayed known

lakes accurately when cross-checked to that of available hydro-sheds data. Although the percentage of areal coverage for swampy/wetlands is relatively small, the percentage by volume is quite large.

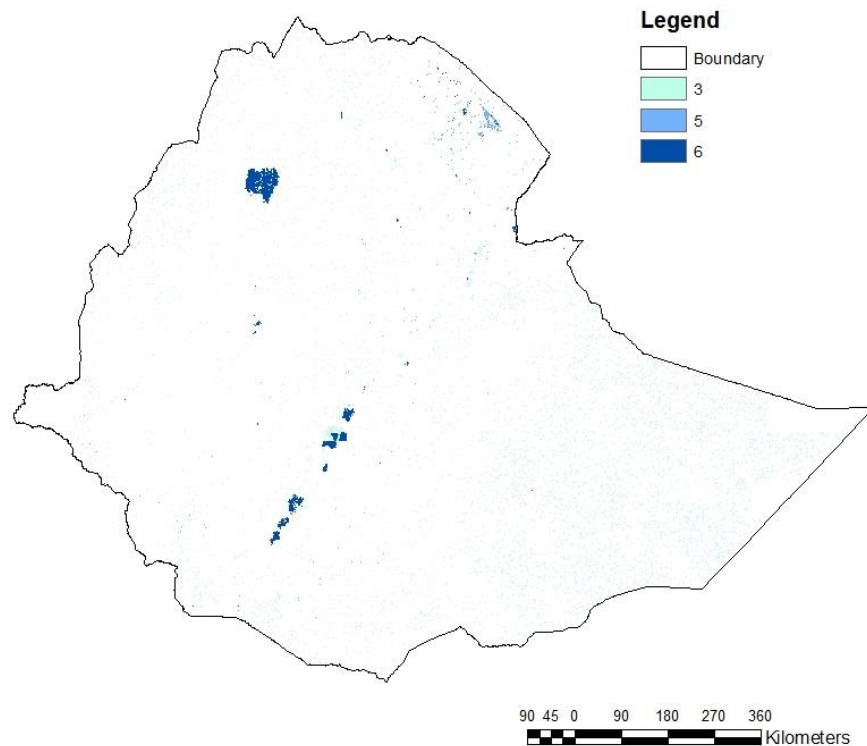


Figure 26: Spatial distribution of desirable NDVI for RWH for the country

Following Thenkabail's (2016) wetland delineation and mapping methods, it can be seen that other land cover types in the same/close category would be easily mistaken as wetlands (-0.25 - 0.1). This confusion was limited to some scale by only using the range (0.002 - 0.025) that was cross referenced with global earth images. These areas corresponded to shallow water formed around lake boundaries.

4.5. Water Harvesting Categories

Locating optimal sites for water harvesting was based on both maps (i.e. the physically derived TWI maps as well as land use that influenced water holding capacity of the zones). This connection was made a reality as both features met the requirement for harvesting rainwater and consist of three suitability values.

Locations ideal for rainwater harvesting under TWI properly signify sites that have the capacity for a greater water concentration. This was supplemented with NDVI values that again accurately indicated water bodies over land area. The joint use of these indices addressed soil characteristics, topography and vegetation condition. This joining is an advantage in the accuracy of the final results. As an illustration, certain scenarios were considered before joining these indices. A desirable NDVI alone would not be self-sufficient for identifying water harvesting sites, as it does not guarantee prolonged water concentration on that area which was made available with the presence of the TWI.

In a similar token, the TWI alone was not solely considered, as targets required to be environmentally sustainable with land use study. The presence of a large TWI guarantees higher soil moisture which are greener due to the presence of soil moisture. The use of NDVI avoids selecting large forest bodies to avoid environmental impact associated with constructing water harvesting structures by deforestation.

For this reason, the potential locations identified guarantee potential water existence, stagnation and are available with minimum amount of earth work and with minimal environmental impact.

Multiple overlay options were used to make sure both TWI and NDVI were addressed to identify water harvesting locations. From the initial analysis using raster calculator, nine possible combinations were obtained and are mapped in Figure 27. A script was written in ArcGIS' raster calculator where each grouping yielded the multi-class

combination of water harvesting zones. The script, guided by the “if-condition” classified the three distinct, yet separate classes into the nine classes as shown in the legend of the figure.

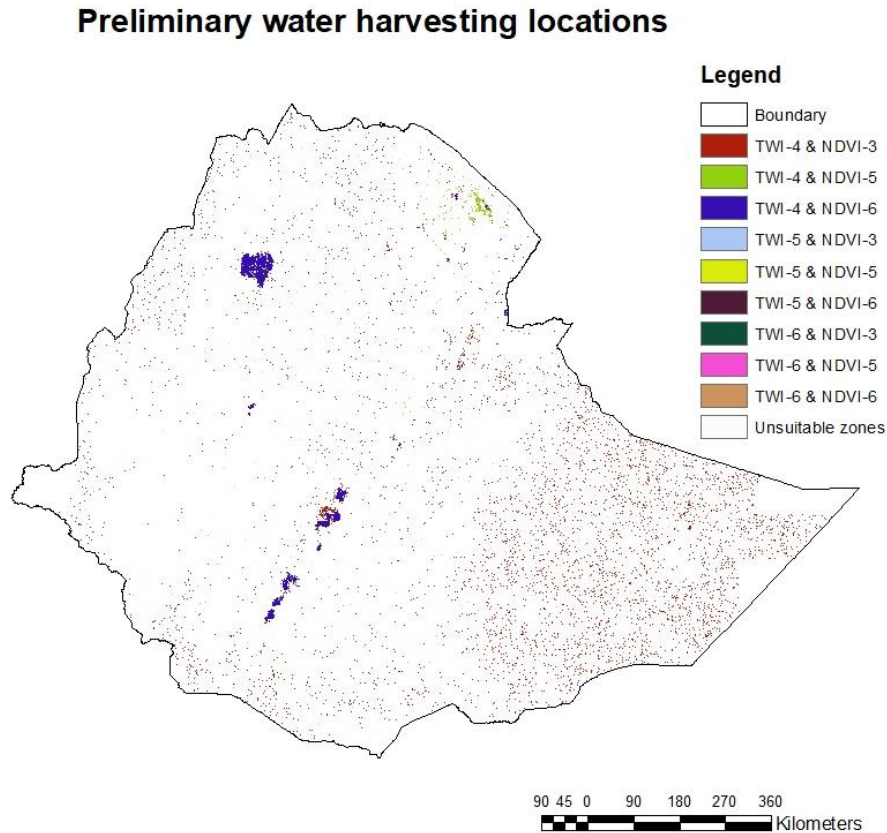


Figure 27: Preliminary identified water harvesting zones in the country

Based on this classification, both TWI and NDVI values in Category 6 have the highest potential for locating water bodies as both are high-flow concentration and are deep water bodies respectively. Guaranteeing the highest rank in the classification. A relatively lower concentration is seen with the combination of TWI-4 and NDVI-3 which has a lower rank.

As can be seen in Figure 27, the result is highly governed by the TWI value obtained which suffers from high streaking effects and did not indicate the spatial extent of the identified locations well enough. For this reason, a better approach that uses the

'identify features by location' tool in ArcGIS was used. The tool identifies areas that the TWI range over 15 overlaps with. Before interpreting the obtained spatial result, further analysis was conducted that filters these areas.

With these criteria and methodologies, the surface water harvesting potential areas were identified and classified in three categories according to their desirability levels. The mapped results capture the spatial area of each zone in a much better way, providing a wider water harvesting area.

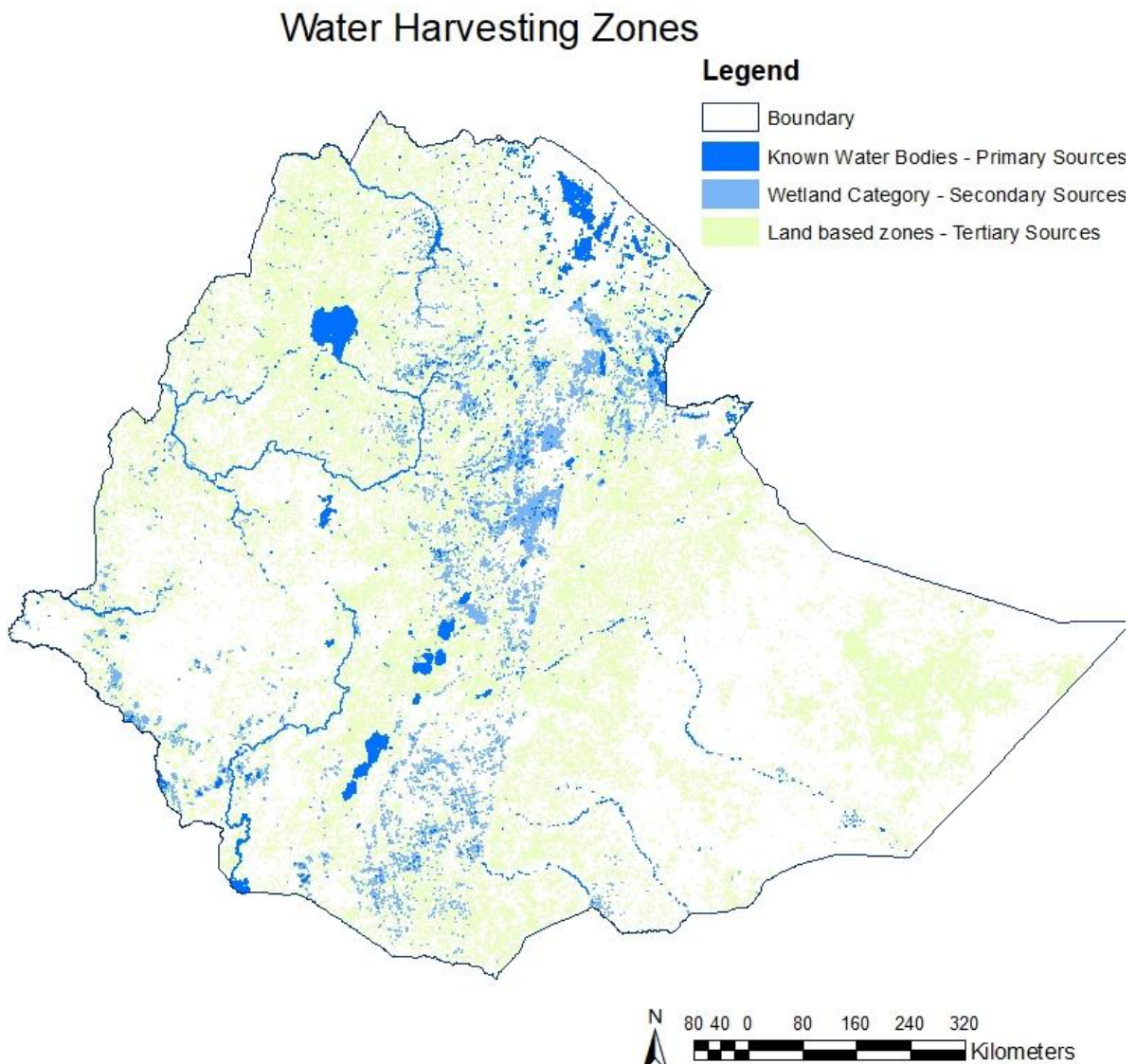


Figure 28: Water Harvesting Categories

These classifications indicate a greater percentage coverage area wise in the Primary sources, a lesser percentage coverage in the Secondary sources and an even lesser landmass coverage in the land based sources.

The first category (Primary water sources) identifies the most desirable class which is water bodies themselves where the maximum surface water harvesting zones cover 0.79% of the country's landmass and is distributed in the locations shown in Figure 29. Up to 30,000 zones were located under this category with areas ranging 576 m² (for the smallest pixel zone) to 3,059 km².

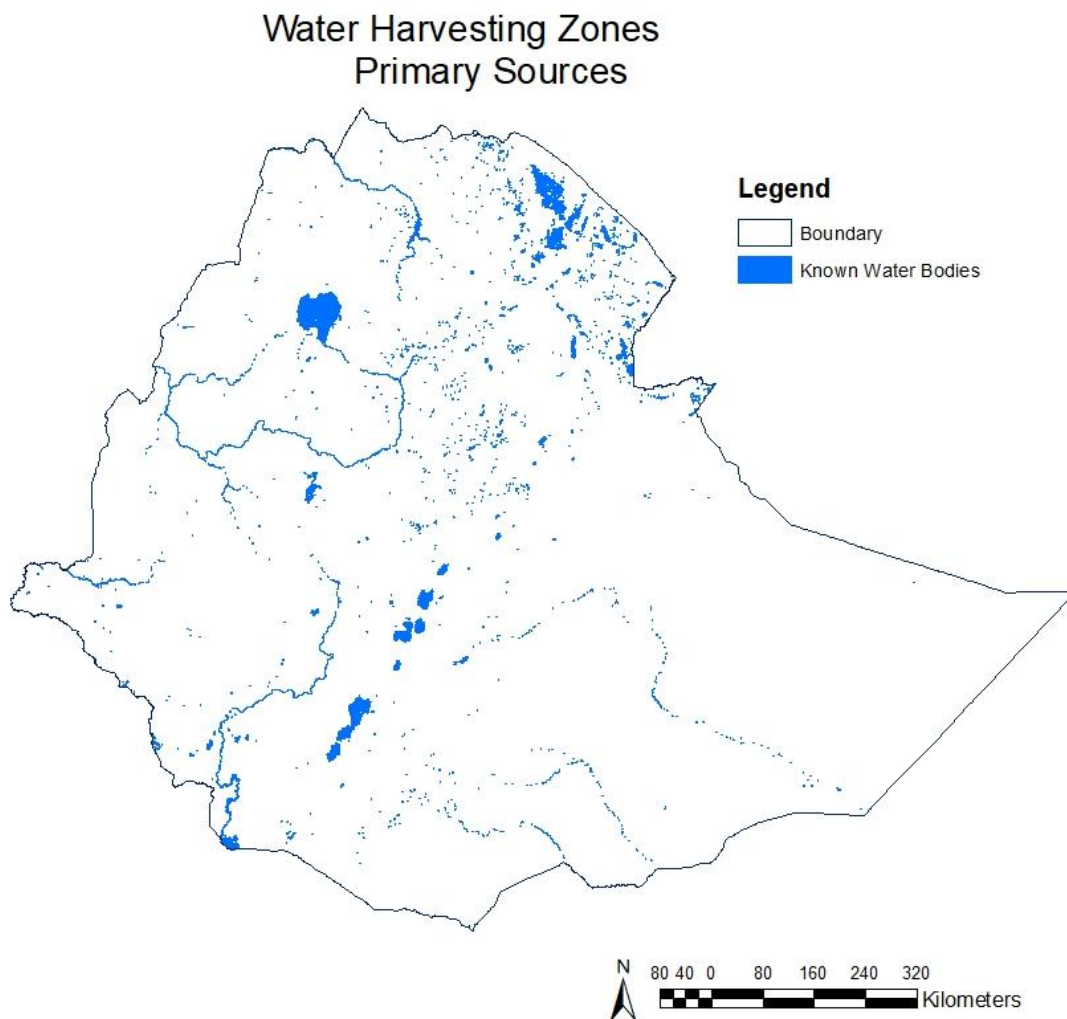


Figure 29: Primary source locations

Since these locations are already known lakes, the accurate identification of these areas guarantees that the mechanism used is reliable. For evaluation purpose, the locations were cross checked with an available water volume analysis report shown in Table 22. The Volume analysis typically identifies the locations shown in Figure 29.

Table 22: Ethiopia’s water volume analysis - Natural Lakes and Artificial Reservoirs

	Primary Sources	Approximate Volume (BCM)
1	Lake Tana	28.4
2	Lake Abaya	9.82
3	Lake ChewBar	4.5
4	Lake Abe	2
5	Lake Ziway	1.1
6	Lake Shala	36.7
7	Lake Chamo	3.3
8	Lake Langano	3.8
9	Lake Abiyata	1
10	Lake Ashenge	0.25
11	Lake Awassa	1.3
12	Lake Besseka	0.28
13	Lake Hayk	1.01
	Total	93.46

	Primary Sources	Watershed	Capacity (BCM)
1	Geferssa	Awash	0.007
2	Koka	Awash	1.08
3	Fincha	Abay	0.65
4	Legedadi	Awash	0.042
5	Melkawakena	Wabi shebele	0.75
6	Angereb	Tekeze	0.005
7	Alwero	Baro akobo	0.075
8	Midimar	Tekeze	0.01
9	Dire	Awash	0.019
10	Tekeze	Tekeze	9.00
11	Gilgel Gibe	Omo-gibe	0.083
12	Koga	Abay	1.01
13	Kessem	Awash	0.50
14	Tendaho	Awash	1.80
15	Gibe-3	Omo-gibe	14.70
16	Ribb	Abay	0.243
17	Megech	Abay	1.80
18	Arjo-dedesa	Abay	1.40
19	Hidase	Abay	79.00
	Total		112.174

The second category (Secondary sources) identifies locations which are swampy areas (wet lands) found in between categories “water bodies” and “bare-land” (in terms of spectra identification) that are intersected by the desirable values of the TWI.

This is the original finding of this research. These locations are expected to be moderate surface water harvesting potential zones, covering 0.47% of the total landmass of Ethiopia. The identified areas range from 576m² to over 70 km² and amount to over 118,000 locations on a national scale.

Secondary Rainwater Harvesting sites

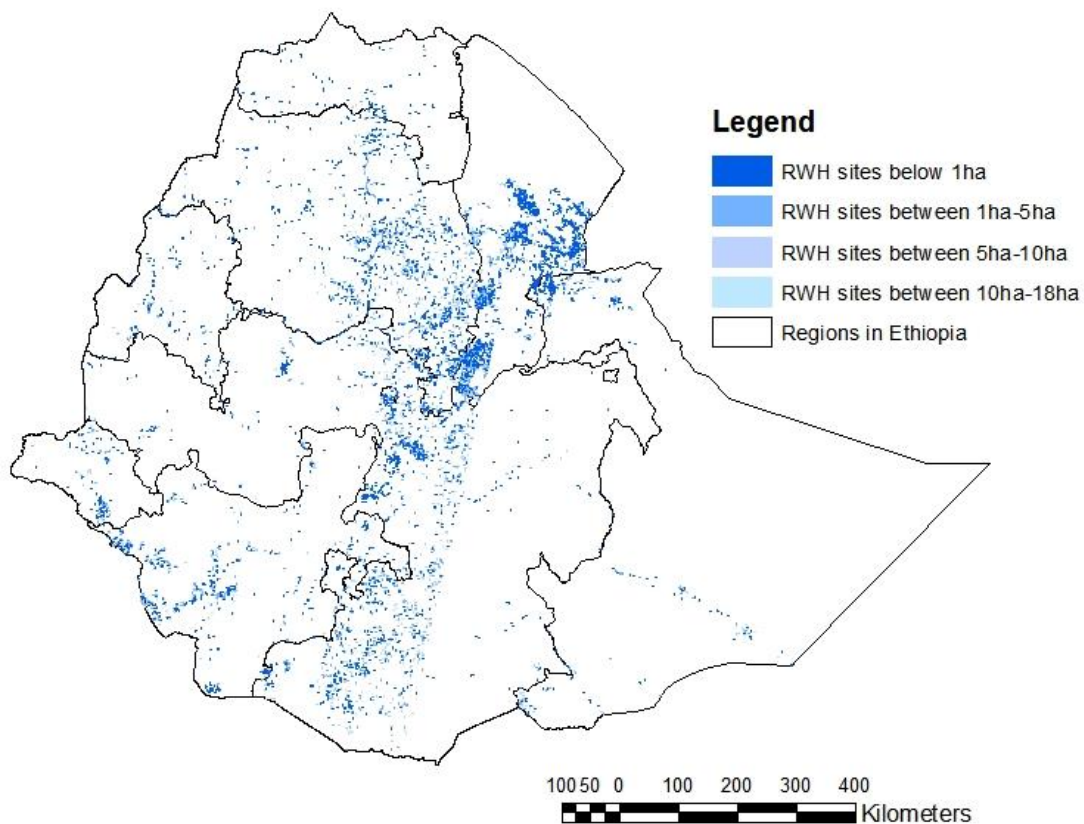


Figure 30: RWH map of the country

Water harvesting locations depicted in this category are the result of the TWI desirable category (over 15) combined with the wetlands identified in the NDVI classification. This category was given more attention in this study as it consist of locations that have not been located or exploited thus far. It is thus, the final output taken from the overall

joint analysis. The map shown in Figure 2830 depicts potential water harvesting areas that are more or less distributed throughout the country.

Highly arid regions in the country have been flagged as locations that are not suitable for rainwater harvesting, according to the drought analysis, even though potential zones were located according to the method used, the rate of evaporation around these areas would be high.

Similarly, even though the drought analysis showed frequent drought pummeling of certain areas located in the eastern and south eastern portions of the country, the final output in Figure 30 for the secondary sources did not find many suitable areas for water harvesting corresponding to those locations implying that surface water source would not be feasible.

To tend to these locations, reports from the results of simulation studies in Wabi Shebele Basin master-plan (2005) suggest that, at the end of the second phase (year 2020), a total area of 94,492 ha can be covered and that 3.4 m³/s water supply demands can be met. This suggested amount in the master plan study is expected to maintain the demand of that area.

In a similar manner, upon comparison with the reality, potential water harvesting locations identified in the eastern regions, specifically in the Danakil depression, are actually scattered saline lakes. As huge deep beds of natural salt are found in the area, these identified zones were filtered out and ground water resource, which is currently under usage, is recommended for continued use in these areas as well.

According to the identified locations in Figure 30 and using Figure 31 as a supplementary image, some locations that are not frequently affected by drought and that get regular amount of annual precipitation have been identified with potential water harvesting zones. For locations with close proximity to these zones, inter-basin water transfer, though expensive, is also a permanent solution to the desertification of

water-scarce regions east and southeast of the domain. Additional requirements can be supplemented through ground water resources.

The analyses up to now concluded by the suitability analysis showed that there are sites uniformly distributed across the country that have the potential to be water harvesting points. As an illustration, capacity determination was carried out for small scale zones identified under this category. The next section deals with quantifying these locations which can be converted to actual use on average demand.

The Secondary sources were given more attention as it has not been exploited so far. This capacity determination targeted small locations with characteristics of small reservoirs or ponds for water harvesting with an embankment volume of less than 0.75 million cubic meters (ICOLD 1998). Such locations tend to reduce the area of shallow water which is very conducive to reduce the evaporation loss.

Considering a 4m average height that is common for ponding structures, the areal coverage of a single location can go up to 18ha. As such, the results from the capacity analysis were summarized in ranges in Table 23.

Table 23: Number and volume of identified locations

Areal range	Number of sites identified	Area (m²)	Average Volume (BCM)
Below 1ha	93,189	168,199,560.3	0.61
From 1 ha to 5 ha	14,168	330,731,510.1	1.32
From 5 ha to 10 ha	4,137	293,752,399.7	1.17
From 10 ha to 18 ha	2,704	364,078,909.7	1.46

Depending on the specific use and duration of supply, Table 23 has been arranged to clearly show the potential sites and their corresponding average volume.

Areas that were considered small reservoirs summed up to a total of 4.56BCM by volume partially distributed throughout the country. The addition of the identified water harvesting locations will bring the total sum to about 210 BCM by volume.

Joining the drought analysis results and the water harvesting hotspots gives a wider and highly vivid image of what to expect when these sources are developed. A preliminary view is shown in Figure 31 which locates areas affected by extreme, severe and mild drought conditions in the year 1984. The monthly SPI results for the months May and August are selected to show how these identified locations would supplement below average precipitation areas in August by storing water in May.

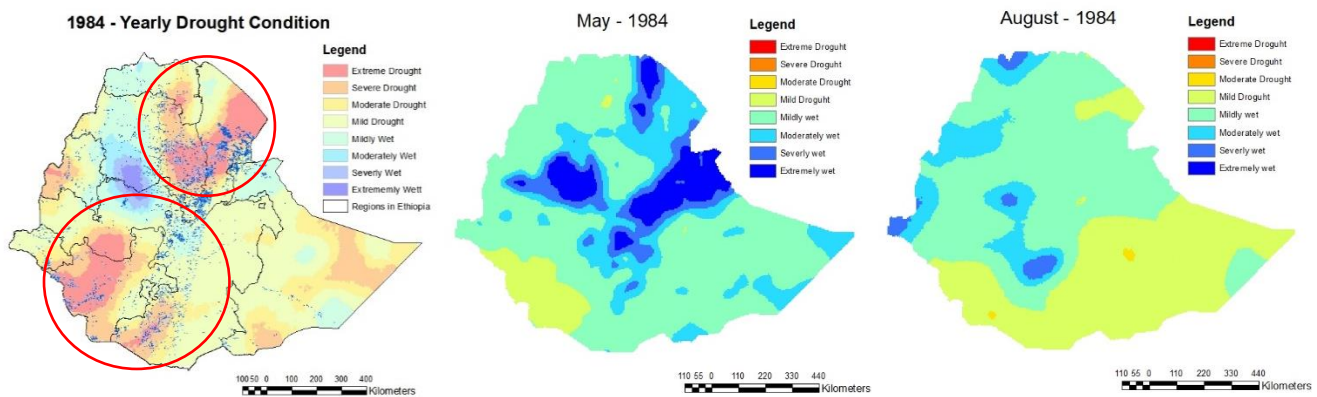


Figure 31: Drought year 1984 illustration with secondary rainwater harvesting sites

Depicted in Figure 31, developing water harvesting hotspots shown in blue can be used to serve below average precipitation zones indicated in August of the same year. The need for small scale water harvesting is of most importance as the seasonality of rainfall is addressed and due to the fact that expected periods in the “Kiremt” season are lacking during all identified drought years. Tending to the scarce “Kiremt” season by conserving rainwater in these identified locations during abnormally wet periods in May and June with the average harvesting depth is expected to sustain the drought prone areas that are commonly under stress.

The third category, tertiary sources, was identified as land based water harvesting locations which is composed of light green vegetation that was selected considering the moisture collected on that location and as an outcome had resulted with a relatively good NDVI value. These locations were considered as minimum suitability for water harvesting until actual land based survey is conducted. For this reason volume was not computed for the third water harvesting category.

5. Conclusions and Recommendations

5.1. Conclusion

In summary, climatological variability, compounded with the effect of climate change, will have direct and indirect impacts on a wide range of social, economic and environmental aspects. Although the quantification of the impact is lacking, the water management of the system is likely to be more challenging in the future. Increasing demand for water and shortfalls in surface water resources due to drought could potentially lead to excessive ground water exploration making it difficult to meet possible future requirements.

Drought analysis in this study identified six prominent drought years using the Standardized Precipitation Index. Monthly SPI of these years showed that it was not the lack of precipitation throughout the drought years that caused the drastic effects, but the seasonal effect of the observed precipitation. Months May and June showed greater extremes of wet events as compared to the expected peaking periods of July and August which made the need of water harvesting even more appropriate and essential. This result also confirmed the hypothesis that the rechargeable resource exists but the delivery system is lacking.

Water harvesting zones using a combination of soil characteristics, topography, vegetation and weather were identified and presented consisting of three suitability values. According to the obtained results, over the existing storage, preliminary capacity analysis for small scale zones showed that this method offers the possibility of harvesting and conserving 4.56 BCM of rainwater by developing suitable rainwater harvesting structures.

This research has identified locations that would otherwise have required the need of separate surveys on site. These sites are also cost effective as they require very little to no earth work.

According to volume analysis of the secondary sources, the computed amount that can be made available can suffice to meet a considerable amount of the drinking water requirement of the corresponding area. This conserved water can also be used for irrigation. As acknowledged by most, in situ water conservation on various arable lands in the study domain for recharging soil profile and for runoff harvesting are vital for drought mitigation.

Since assessment of water harvesting potential of an area is essential before construction of any RWH structures and methods are built or implemented, the findings of this research are believed to be significant.

5.2. Recommendations

Drought is a phenomenon with a range of impacts, and water is the most crucial factor in its mitigation. Drought relief funds can be applied towards developing rainwater harvesting structures that could provide supply to drought-vulnerable regions in Ethiopia.

A major benefit of this research is that it can be used as a stepping stone for various downstream analyses. With the availability of these water harvesting locations, major water demands in the country can be estimated and provided a solution associated with precipitation falling in that area.

Not only can the harvested rainwater be of use for surface water supplies by storing water in the locality itself, but in the long run can be recharged into the ground through simple and effective methods which accounts for rejuvenation of water bodies. Check dams are one of the few water harvesting structures which control the runoff and increase the infiltration by hindering water flow, which in turn opens new streams and raises the water table. Modern technologies of rainwater harvesting and groundwater recharge such as anicut, percolation tank, subsurface barrier and pond with infiltration wells have been developed to rejuvenate the depleted freshwater aquifers (Narain,

2005). It is thus recommended that the country could adopt such mechanisms to fully and efficiently use the capacity of the identified locations.

For basin level studies, spatial and temporal strategies for RWH development are advised. The findings from this research allow a strategy for RWH development both spatially and temporally in order to increase the runoff capturing efficiency. The spatial rainwater concentration involves the rainwater collection efficiency which is addressed by the joined use of TWI and NDVI, by enlarging the catchment when deemed necessary and the drought analysis portion supplements the temporal concentration by storing the rain fall in the rainy season for use in the dry season. Effective use of these attributes in RWH is advised.

Additional studies along with site verification need to be conducted regarding the identified locations under water harvesting Category-2 and 3 (i.e. Secondary and Tertiary sources), as this research only covers capacity analysis of a smaller portion of the identified locations for water harvesting. It is safe to assume that with the study of the remaining locations, one would be able to find large volumes with the aim of maintaining sustainability.

It is strongly recommended that evapotranspiration be considered when computing storage for analysis at basin scale. Since the impact is quite large when considering large scale ponding structures, and due to the fact that the drought analysis was based only on a precipitation driven index.

Regarding the accuracy of the obtained volumes, detailed studies on downstream specific basins shall be addressed via the surface volume tool in ArcGIS since it has the ability to measure the amount of three-dimensional space occupied by a feature. Hence, volume measurements can be calculated using the 3D surface analysis software. This can be supplemented with onsite topographical and bathymetric surveys.

Remote sensing technologies, including landsat images with clarified bands or other comparable options should be further reviewed and used to conduct a more refined

analysis on this same study. As wetlands are among the most difficult ecosystems to classify using remote sensing data due to their high spatial heterogeneity and temporal variability, site verification for located RWH sites should be conducted. It is also recommended that scientific knowledge of the current status and future trends of wetlands in the identified regions be grasped as it is important for formulating planning measures and effective management policies.

For further resource management, land use systems should match water availability. Land use master plan studies should be based on the located water harvesting zones as great amount of rainwater can be stored and used during a potential drought event.

6. References

- Abebe, A., Lasage, R., Alemu, E., John, G., & Woldearegary, K. (2012). Opportunities for building on tradition - time for action. In W. Critchely, & J. Gowing, *Water Harvesting in Sub-Saharan Africa* (pp. 70-84). USA and Canada: Routledge.
- Abramowitz, M. a. (1965). Handbook of mathematical functions.
- Agarwal, A. (n.d.). DROUGHT? Try capturing the rain. New Delhi.
- Ali, G., Birkel, C., Tetzlaff, D., Soulsby, C., McDonnell, J. J., & Tarolli, P. (2013). A comparison of wetness indices for the prediction of observed connected saturated areas under contrasting conditions. *John Wiley & Sons, Ltd.*
- Alley, W. M. (1984). The Palmer Drought Severity Index: Limitations and Assumptions. *Journal of Climate and Applied Meteorology*, 1100-1109.
- Ammar, A., Riksen, M., Ouessar, M., & Ritsema, C. (2016). Identification of suitable sites for rainwater harvesting structures in arid and semi-arid regions: A review. *Science Direct*, 108-120.
- ANDREU, J., PÉREZ, M. A., FERRER, J., & VILLALOBOS, A. (2007). DROUGHT MANAGEMENT DECISION SUPPORT SYSTEM BY MEANS OF RISK ANALYSIS MODELS. In T. V. GIUSEPPE ROSSI, *METHODS AND TOOLS FOR DROUGHT ANALYSIS AND MANAGEMENT* (pp. 195-216). Springer.
- Awulachew, S. B., Yilma, A. D., Loulseged, M., Loiskandl, W., Ayana, M., & Alamirew, T. (2007). Water Resources and Irrigation Development in Ethiopia. *International Water Management Institute*.
- Bachewe, F., Yimer, F., & Minten, B. (2017). *Agricultural price evolution in droguht versus non-droguht affected areas in Ethiopia*. ESSP Working paper 106.
- Bakir, M., & Xingnan, Z. (2008). GIS and remote sensing applications for rainwater harvesting in the Syrian Desert (Al-Badia). *International Water Technology conference*, 73-82.
- Barua, S. N. (2011). Comparative evaluation of drought indexes: case study on the Yarra River catchment in Australia. *Journal of Water Resources Planning and*, 215-226.
- Bayissa, Y. A., Moges, S. A., Xuan, Y., Andel, S. J., Maskey, S., Solomatine, D. P., . . . Tadesse, T. (2015). Spatio-temporal assessment of meteorological drought under the influence of varying record length: the case of Upper Blue Nile Basin, Ethiopia. *Hydrological Sciences Journal*.

- Bayissa, Y., Tadesse, T., Demisse, G., & Shiferaw, A. (2017). Evaluation of Satellite-Based Rainfall Estimates and Application to Monitor Meteorological Drought for the Upper Blue Nile Basin, Ethiopia. *Remote sensing*.
- Berhanu, B., Melesse, A. M., & Seleshi, Y. (2013). GIS-based hydrological zones and soil geo-database of Ethiopia. *Elsevier*, 21-31.
- Berhanu, B., Seleshi, Y., & Melesse, A. M. (2014). Surface Water and Groundwater Resources of Ethiopia: Potentials and Challenges of Water Resources Development. Switzerland: Springer International Publishing.
- Berhanu, B., Seleshi, Y., Demisse, S. S., & Melesse, A. M. (2016). Bias correction and characterization of climate forecast system re-analysis daily precipitation in Ethiopia using fuzzy overlay. *Royal Meteorological Society*.
- Berhanu, B., Silesh, Y., & Melesse, A. M. (2014). Surface Water and Groundwater Resources of Ethiopia: Potentials and Challenges of Water Resources Development. In A. M. Melesse, W. Abtew, & S. G. Setegn, *Nile River Basin: Ecohydrological Challenges, Climate Change and Hydropolitics* (pp. 97-117). Springer.
- Beven, K. J., & Kirkby, M. J. (1979). A physically based, variable contributing area model of basin hydrology. *Hydrological Sciences - Bulletin*.
- Bhattacharya, k., Azizi, P. M., Shobair, S. S., & Mohsini, M. Y. (2004). Drought impacts and potential for their mitigation in southern and western Afganistan. *Drought Series*.
- Bhatti, H. A., Rientjes, T., Haile, A. T., Habib, E., & Verhoef, W. (2016). Evaluation of Bias Correction Method for Satellite-Based Rainfall Data. *Sensors*.
- Ceglar, A. (n.d.). DROUGHT INDICES.
- Critchley, W., & Gowing, J. (2012). *Water Harvesting in Sub-Saharan Africa*. Routledge Taylor & Francis Group.
- Degefu, W. (1987). Some aspects of Metrological Drought in Ethiopia. In M. H. Glantz, *Drought and Hunger in Africa: Denying famine a future* (pp. 23-36). UK: Cambridge University Press.
- Degefu, W. (1988). Some Aspects of Meteorological Drought in Ethiopia. In M. J. Glantz, *Drought and Hunger in Africa*. Cambrige University Press.
- Dracup, J. K. (2002). The Quantificaton of Drought: An Evaluation of Drought Indices. *American Meteorological Society* .
- Dracup, J., Lee, K., & Paulson Jr, E. (1980). On the definition of Drought. *Water Resources Research*, 297-302.

- Fang, G. H., Yang, J., & Y. N. Chen, C. Z. (2015). Comparing bias correction methods in downscaling meteorological variables for a hydrologic impact study in an arid area in China. *Hydrology and Earth System Sciences*, 2547-2559.
- Fazzini, M., Bisci, C., & Billi, P. (2015). The Climate of Ethiopia. *Springer*, 65-87.
- G, L., A, B., & W., v. D. (2007). Estimates of future discharges of the river Rhine using two scenario methodologies: direct versus delta approach. *Hydrol. Earth Syst. Sci.*, 1145-1159.
- Gadiso, B. E. (2007). *Drought assessment for the Nile Basin using meteostat Second Generation data with special emphasis on the upper Blue Nile Region*. Netherlands: International Institute of Geo-information science and Earth observation.
- Grabs, T., Seibert, J., Bishop, K., & Laudon, H. (2009). Modeling spatial patterns of saturated areas: A comparison of the topographic wetness index and a dynamic distributed model. *Elsevier*.
- Guntner, A., Seibert, J., & Uhlenbrook, S. (2004). Modeling spatial patterns of saturated areas: An evaluation of different terrain indices. *WATER RESOURCES RESEARCH*.
- Guttman, N. B. (1999). ACCEPTING THE STANDARDIZED PRECIPITATION INDEX: A CALCULATION ALGORITHM. *JOURNAL OF THE AMERICAN WATER RESOURCES ASSOCIATION*, 311-322.
- HC., T. (1966). A note on the gamma distribution.
- Karavitis, C. A., Alexandris, S., Tsesmelis, D. E., & Athanasopoulos, G. (2011). Application of the Standardized Precipitation Index (SPI) in Greece. *Water*, 787-805.
- Keller, A., Sakthivadivel, R., & Seckler, D. (2000). *Water Scarcity and the Role of Storage in Development*. Colombo: IWMI.
- Khadr, M., & Schlenkhoff, A. (2014). Mapping of Meteorological Drought Patterns using SPI and Different Interpolation Methods. *Lehfeldt & Kopmann*, 81-91.
- Kindkade-Levario, H. (2007). *Design for Water: Rainwater Harvesting, Stormwater Catchment, and Alternative Water Reuse*. New Society Publishers.
- Mackey, B. (2002). *Wildlife, Fire & Future Climate: A Forest Ecosystem Analysis*.
- Mays, L. W. (2009). *Integrated Urban Water Management: Arid and Semi-Arid Regions: UNESCO-IHP*. Taylor and Francis.
- McKee, T. B., Doesken, N. J., & Kleist, J. (1993). The Relationship of Drought Frequency and Duration to time Scales. *Eight Conference on Applied Climatology*, 17-22.
- Michael Hayes, M. S. (2000). *Monitoring Drought Using the Standardized Precipitation Index. Drought Mitigation Center Faculty Publications*.

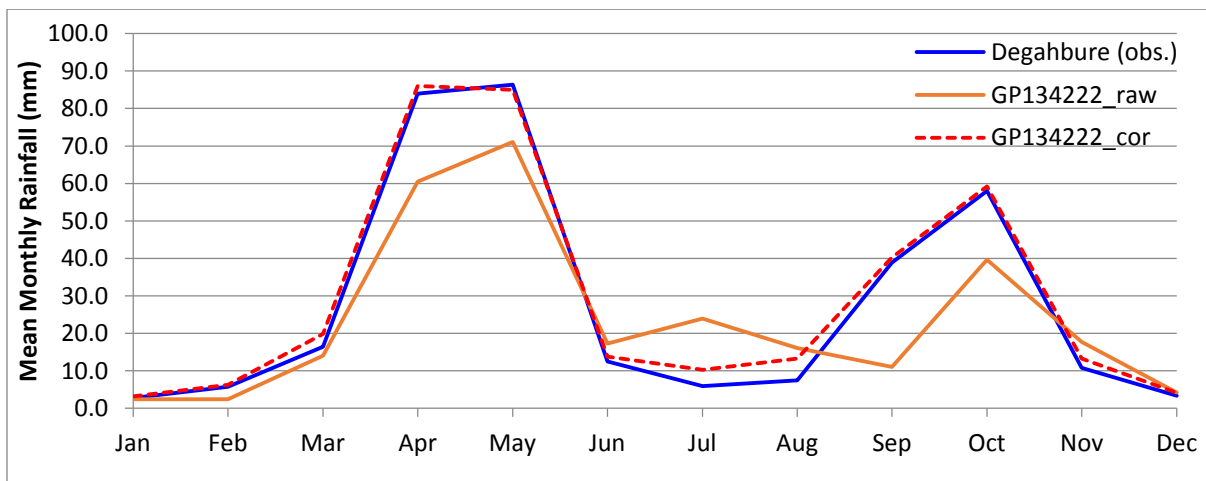
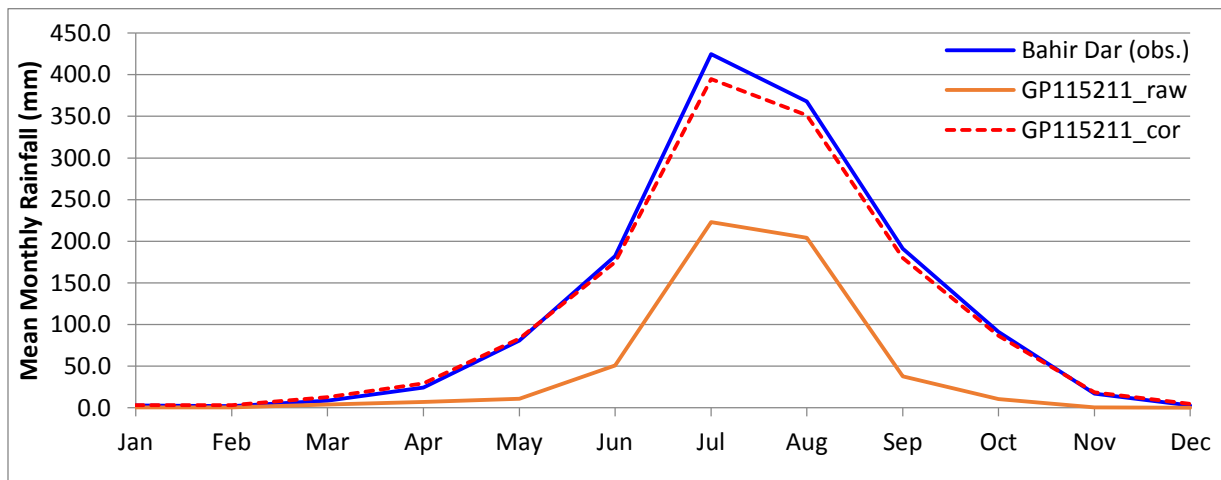
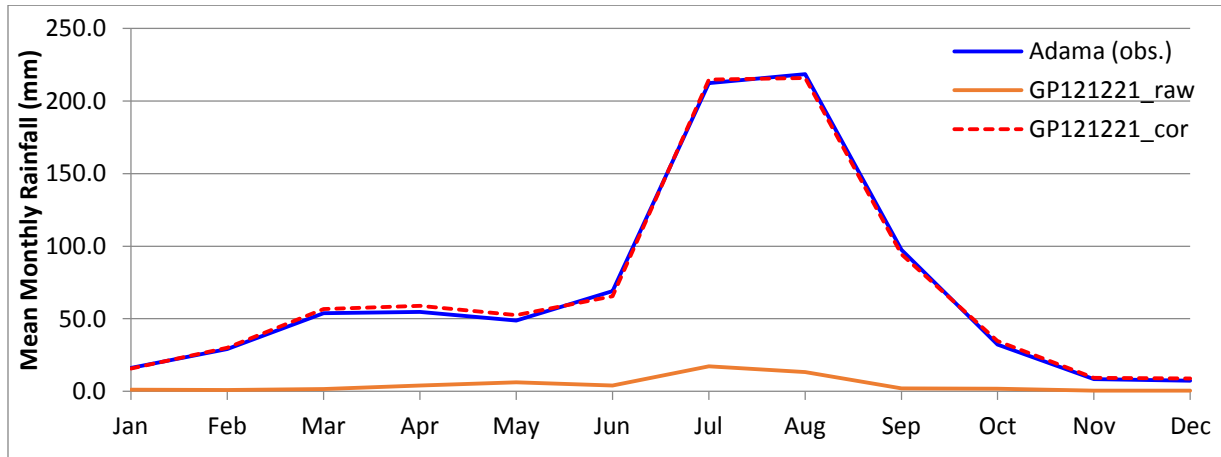
- Milena Różycka, P. M. (2016). Topographic Wetness Index and Terrain Ruggedness Index in geomorphic characterisation of landslide terrains, on examples from the Sudetes, SW Poland. *Zeitschrift für Geomorphologie, Supplementary Issue*.
- Missimer, R. M. (2012). *Aridity and Drought*. Springer.
- Moore, I. D., Gessler, P. E., Nielsen, G. A., & Peterson, G. A. (1993). Soil Attribute Prediction Using Terrain Analysis. *Soil Sci, Am.*, 443-452.
- Mortada, H. 2005. Confronting the Challenges of Urban Water Management in Arid Regions: Geographic, Technological, Sociocultural, and Psychological Issues, *Journal of Architectural and Planning Research*, Vol. 22, No. 1, Spring. (n.d.).
- Negash Wagesho, N. G. (2013). Temporal and spatial variability of annual and seasonal rainfall over Ethiopia. *Taylor & Francis*.
- Palchaudhuri, M., & Biswas, S. (2013). Analysis of Meteorological Drought Using Standardized Precipitation Index - A Case Study of Puruliya District, West Bengal, India. *International Journal of Environmental, Chemical, Ecological, Geophysical Engineering*, 167-174.
- Palmer, W. C. (1965). Meteorological Drought. *Office of Climatology Weather Bureau*.
- Panda, S. A., Bagga, J., Beineke, L. W., & B.S. (2016). *Theoretical Computer Sciences and Discrete Mathematics*. Springer.
- Panigrahi, B., & Goyal, M. R. (2016). *SOIL AND WATER ENGINEERING: Principles and Applications of Modeling*. Taylor & Francis Group.
- Payen, J., Faures, J.-M., & Vallee, D. (2012). *Small reservoirs and water storage for smallholder farming: The case of a new approach*. AGWATER Solutions.
- Pereira, L. S., & Gowing, J. (2005). *Water and the Environment: Innovation issues in irrigation and drainage*. London: E & FN Spon.
- Prinz, D., Oweis, T., & Oberle, A. (1998). Rainwater Harvesting for Dry Land Agriculture - Developing a Methodology Based on Remote Sensing and GIS. *Proceedings, XIII*. Rabat: International Congress Agricultural Engineering .
- Qin, C.-Z., Zhu, A.-X., Pei, T., Li, B.-L., Scholten, T., Behrens, T., & Zhou, C.-H. (2009). An approach to computing topographic wetness. *Springer Science+Business Media*.
- Resources, M. o. (n.d.). WABI SHEBELE RIVER BASIN INTEGRATED DEVELOPMENT MASTER PLAN STUDY PROJECT. 2005.
- Rokni, K., Ahmad, A., Selamat, A., & Hazini, S. (2014). Water Feature Extraction and Change Detection Using Multitemporal Landsat Imagery. *Remote Sensing*, 4174-4189.

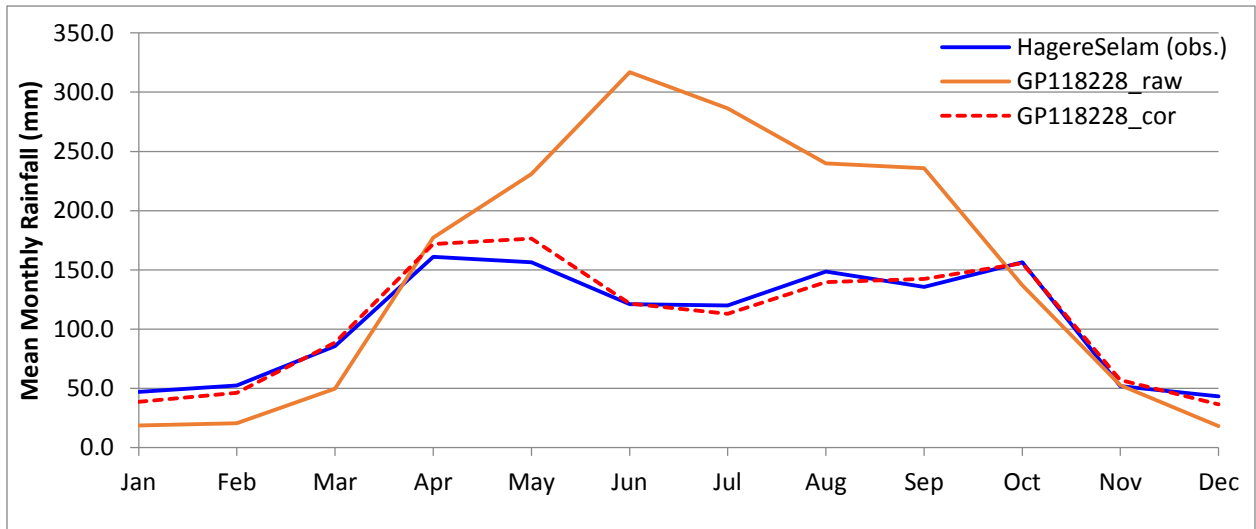
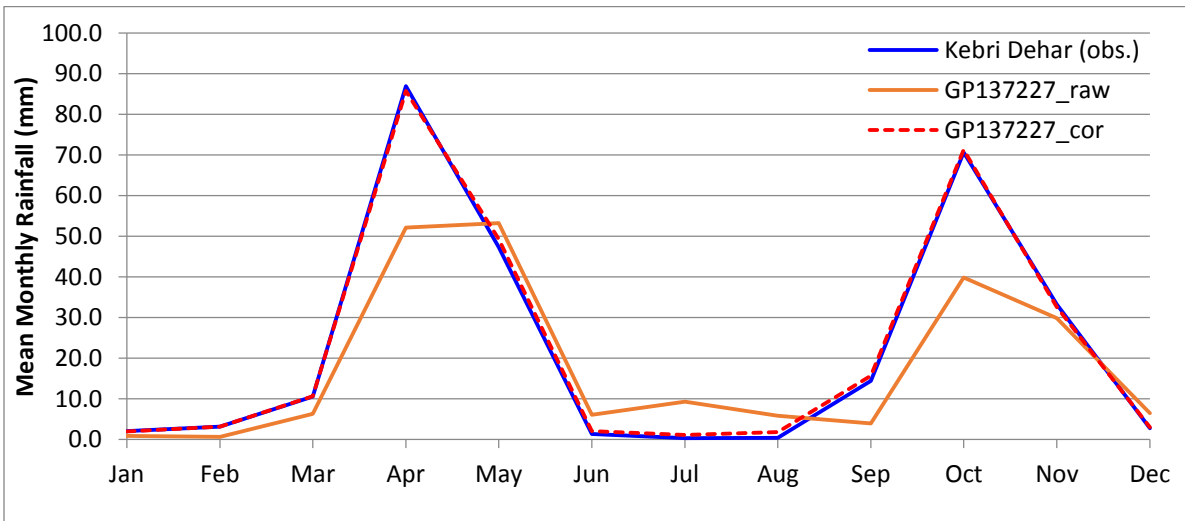
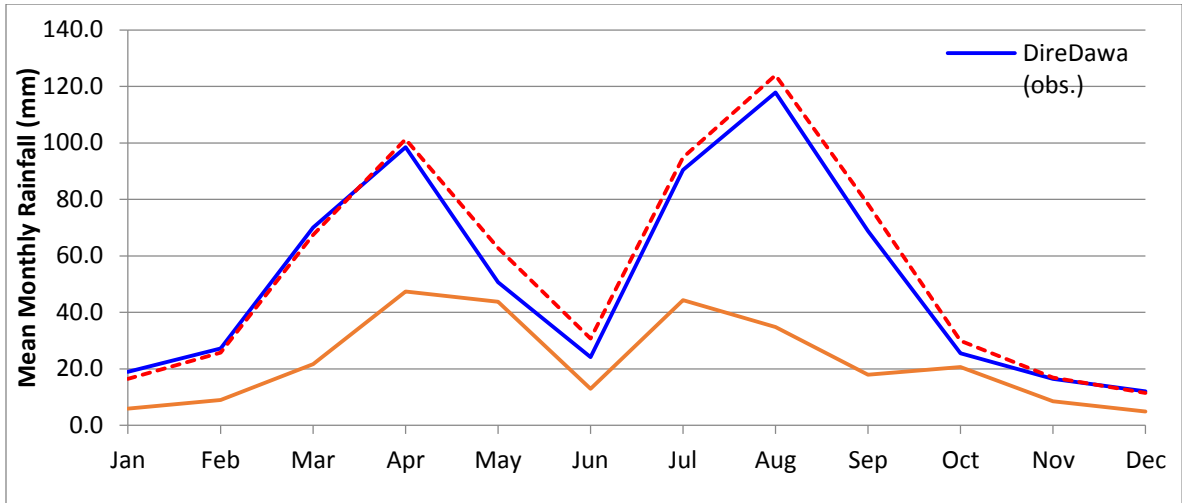
- Rokni, K., Ahmad, A., Selamat, A., & Hazini, S. (2014). Water Feature Extraction and Change Detection Using Multitemporal Landsat Imagery. *Remote Sensing*, 4173-4189.
- Ruhoff, A. L., Castro, N. M., & Risso, A. (2011). Numerical Modelling of the Topographic Wetness Index: An Analysis at Different Scales. *International Journal of Geosciences*, 476-483.
- Saha, S., Moorthi, S., & Pan, H.-L. (2010). The NCEP Climate Forecast System Reanalysis. *AMERICAN METEOROLOGICAL SOCIETY*, 1015-1057.
- Samuel, M. P., & Mathew, A. (2008). Rejuvenation of Water Bodies by Adopting Rainwater Harvesting and Groundwater Recharging Practices in Catchment Area- A Case Study. *The 12th World Lake Conference*, 766-776.
- Sintayehu, R. (2007). *Agricultural Drought Assessment for Upper Blue Nile Basin, Ethiopia using SWAT*. Netherlands: Delft.
- Sørensen, R., Zinko, U., & Seibert, J. (2006). On the calculation of the topographic wetness index: evaluation of different methods based on field observations. *Hydrology and Earth System Sciences*.
- Tarboton, D. G. (2011). A tutorial for using TauDEM to delineate a single watershed. Utah.
- Temimi, M., Leconte, R., Chaouch, N., Sukumal, P., Khanbilvardi, R., & Brissette, F. (2010). A combination of remote sensing data and topographic attributes for the spatial and temporal monitoring of soil wetness. *Elsevier*, 28-40.
- The Standardized Precipitation Index. (2000). *SADC Regional Remote Sensing Unit*.
- UNESCO. (2010). *Application of satellite remote sensing to support water resources management in Africa: Results from the TIGER Initiative*. Paris: International Hydrological Programme.
- USAID. (1987). *Ethiopia Drought/Famine fy 1985-1986*. Addis Ababa.
- Viste, E., Korecha, D., & Sorteberg, A. (2012). Recent Drought and Precipitation Tendencies in Ethiopia. *Theoretical and Applied Climatology*.
- Wang, W., Xie, P., Yoo, S.-H., Xue, Y., Kumar, A., & Wu, X. (2010). An assessment of the surface climate in the NCEP climate forecast system reanalysis. *Springer*, 1601-1620.
- Wardlow, B. D., Anderson, M. C., & Verdin, J. P. (2012). *Remote Sensing of Drought: Innovative Monitoring Approaches*. Taylor and Francis Group.
- (2011). *Water Scarcity*.
- Wilson, J. P., & Gallant, J. C. (2000). *Terrain Analysis: Principles and Applications*. John Wiley & Sons.

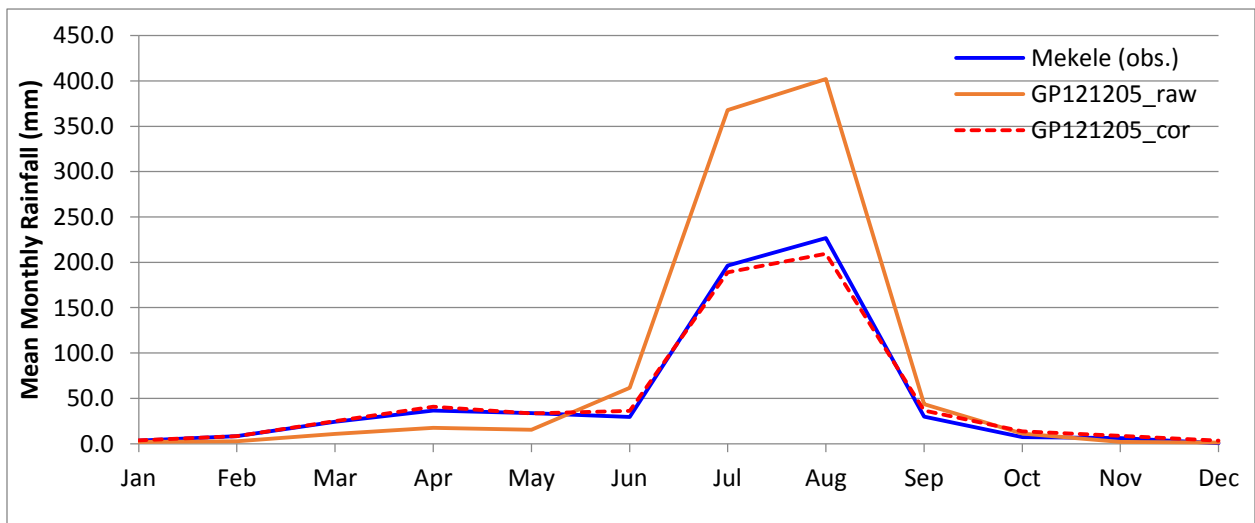
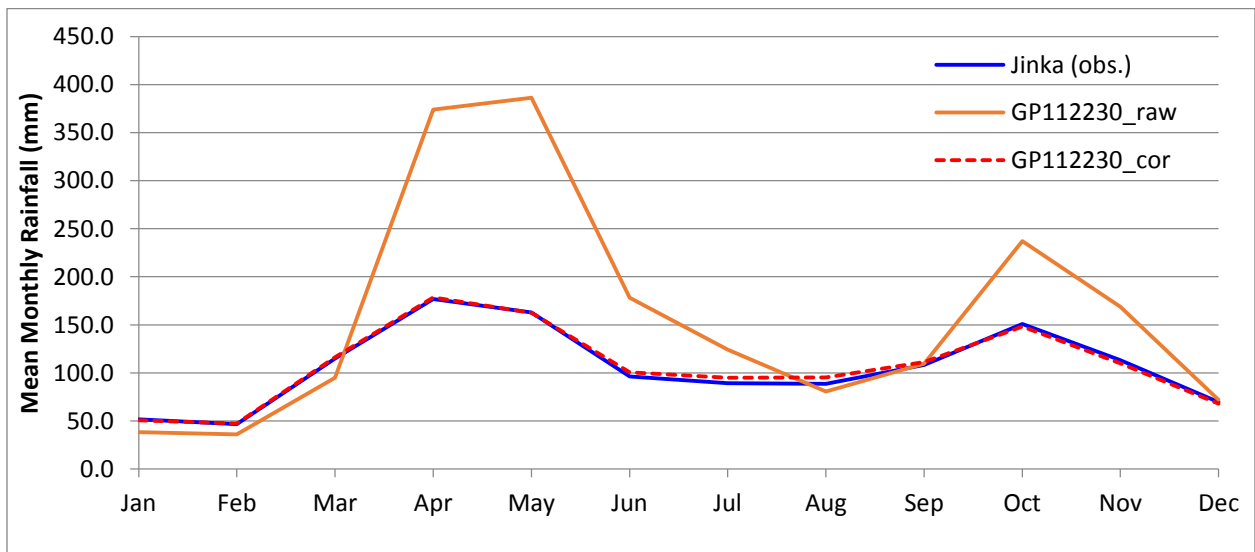
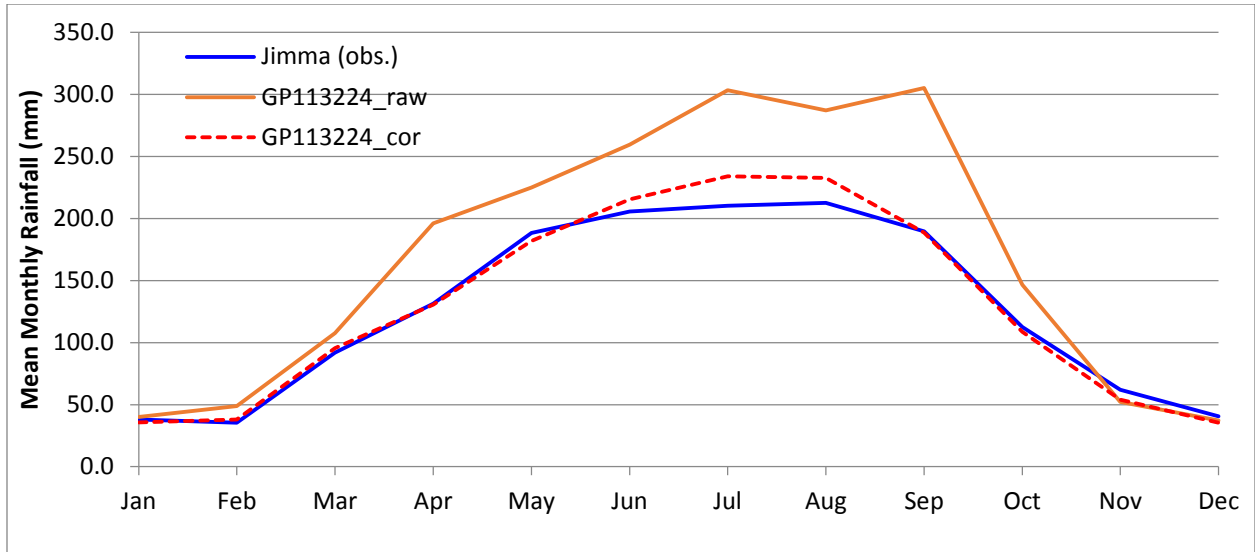
- Winnaar, G. d., Jewitt, G., & Horan, M. (2007). A GIS-based approach for identifying potential runoff harvesting sites in the Thukela River Basin, South Africa. *Science Direct*, 1058-1067.
- Worqlul, A. W., Maathuis, B., Adem, A. A., Demissie, S. S., Langan, S., & Steenhuis, a. T. (2014). Comparison of rainfall estimations by TRMM 3B42, MPEG and CFSR with ground-observed data for the Lake Tana basin in Ethiopia. *Hydrology and Earth System Sciences*.
- Wu, H., Svoboda, M. D., Hayes, M. J., Wilhite, D. A., & Wen, F. (2007). Appropriate application of the Standardized Precipitation Index in arid locations and dry seasons. *Royal Meteorological Society*, 65-79.
- Yengoh, G. T., Dent, D., Olsson, L., Tengberg, A. E., & III, C. J. (2015). *Use of the Normalized Difference Vegetation Index (NDVI) to Assess Land Degradation at Multiple Scales*. SpringerBriefs in Environmental Science.
- Zargar, A., Sadiq, R., Naser, B., & Khan, a. F. (2011). A review of drought indices. *NRC Research Press*, 333-349.
- Zhu, Q., Li, Y., & Tang, X. (2015). *Rainwater Harvesting for Agriculture and Water Supply*. Springer.

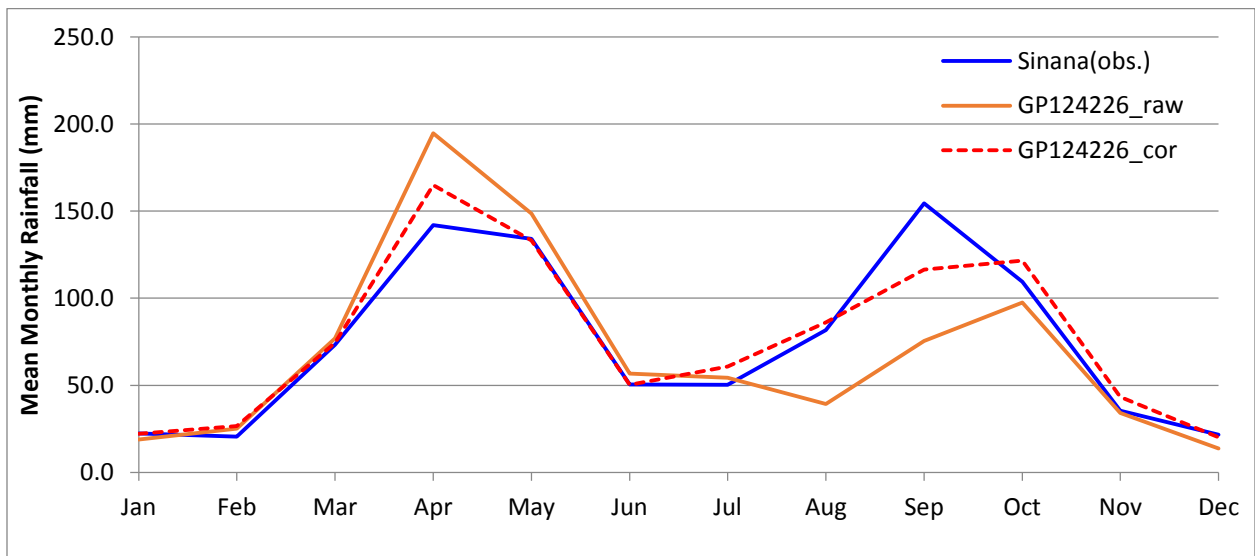
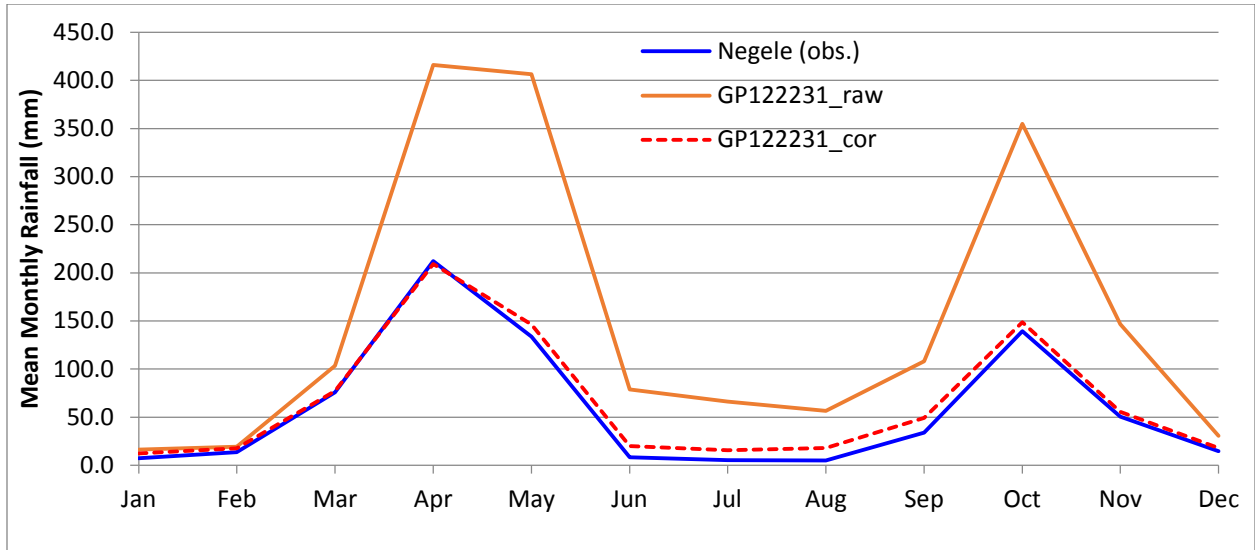
7. Appendices

Appendix A: Statistical measures of mean monthly raw and corrected CFSR and observed datasets

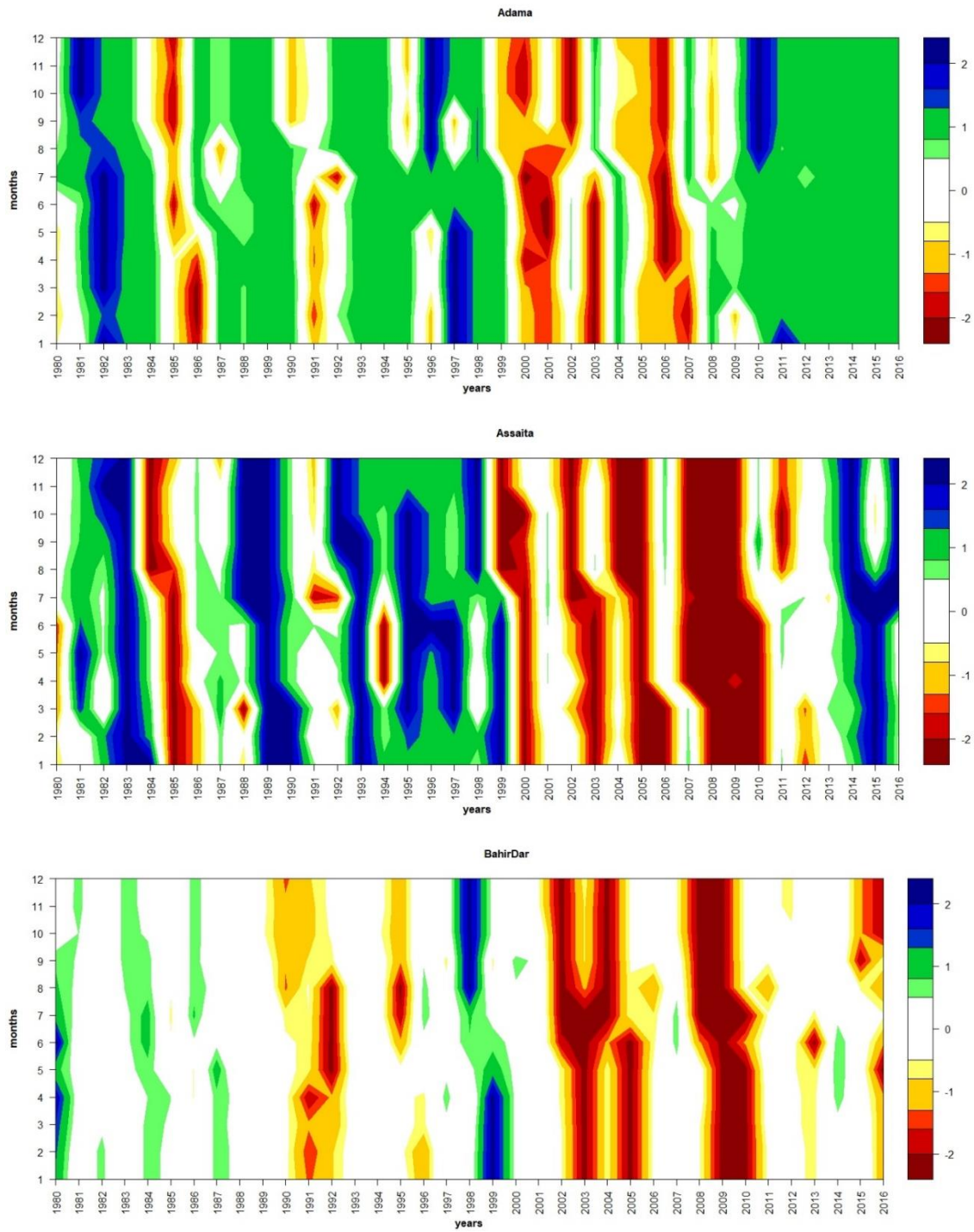


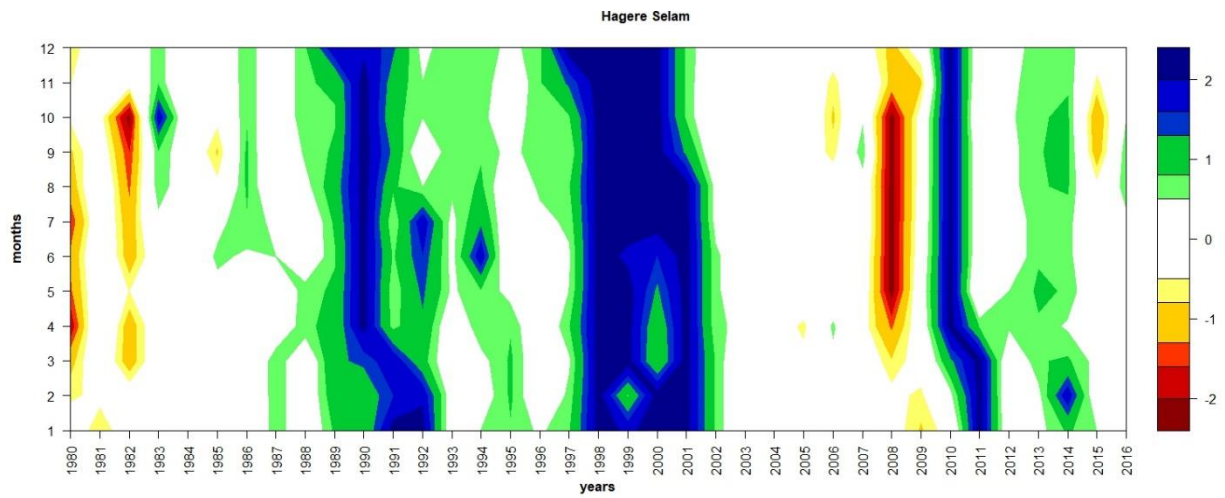
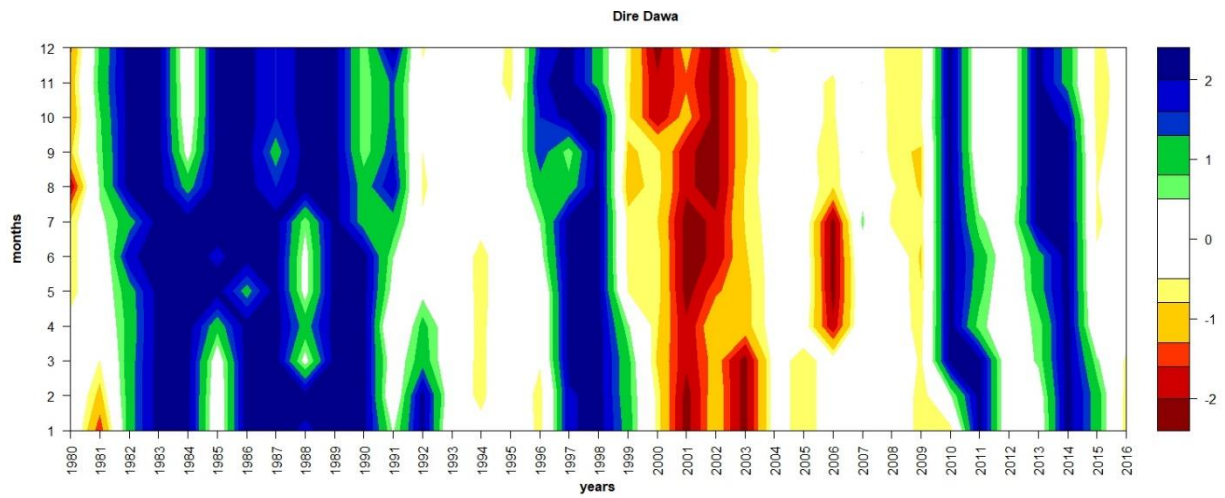
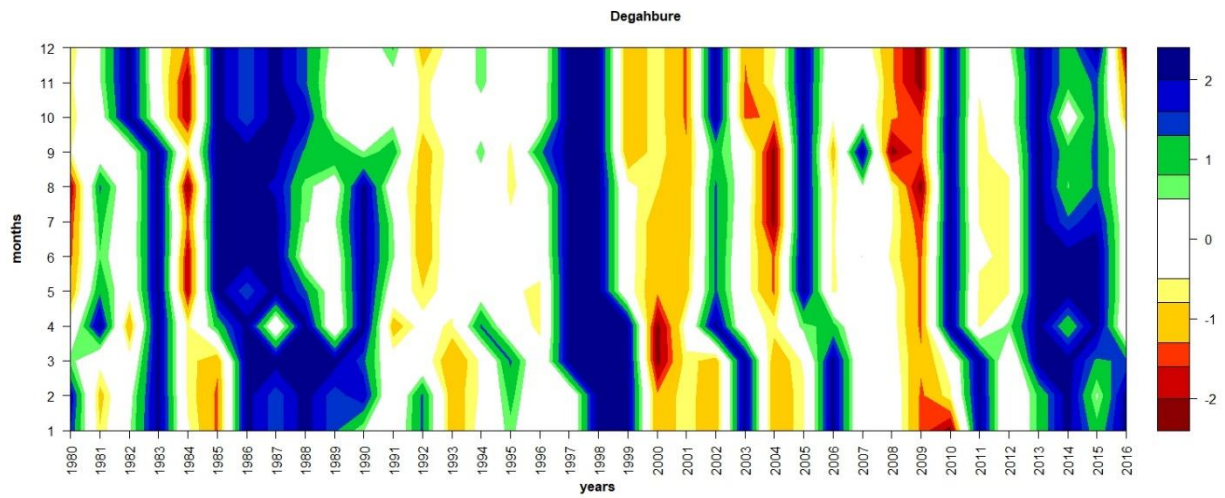




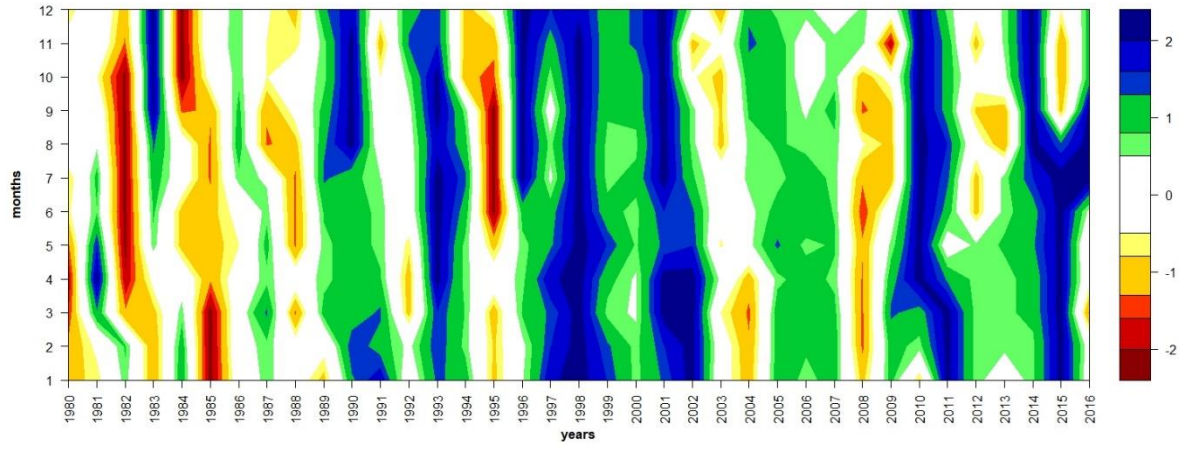


Appendix B: 12-month SPI graphs for 12 representative grids points corresponding with each rainfall regime

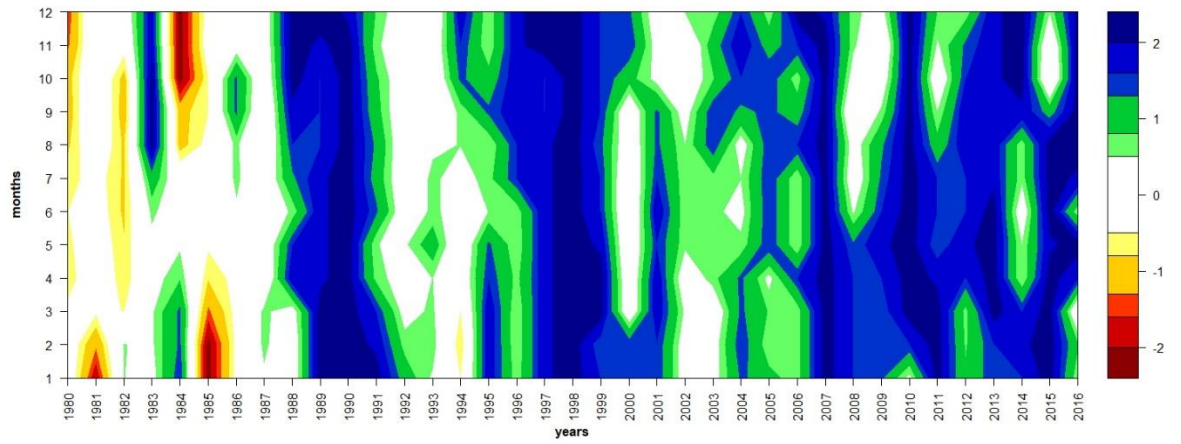




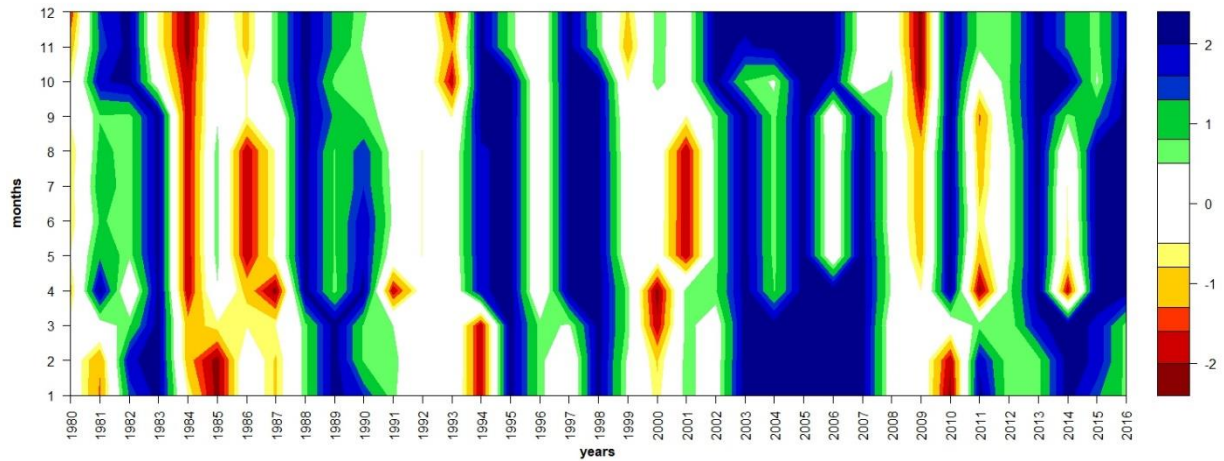
Jimma

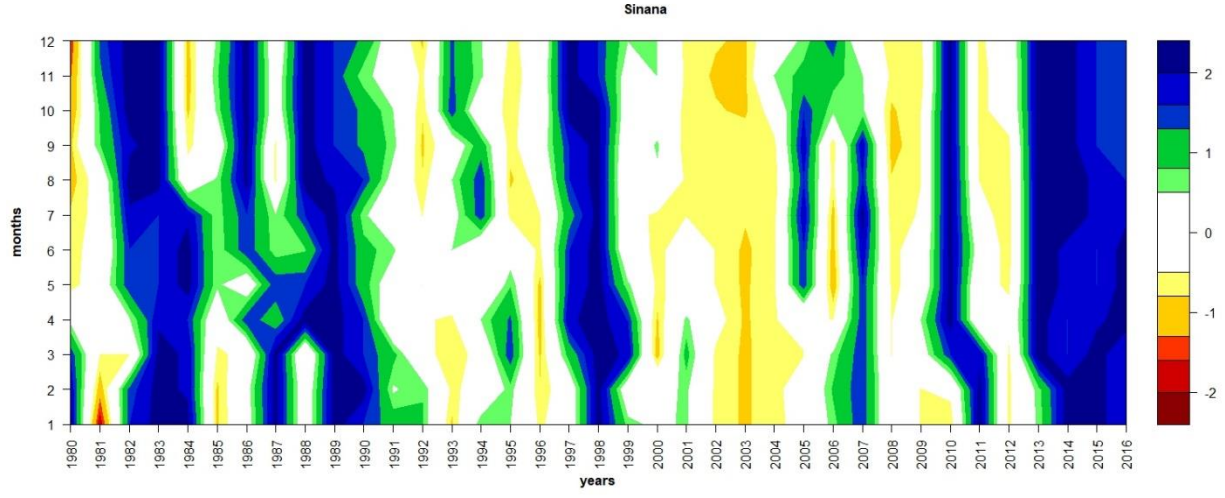
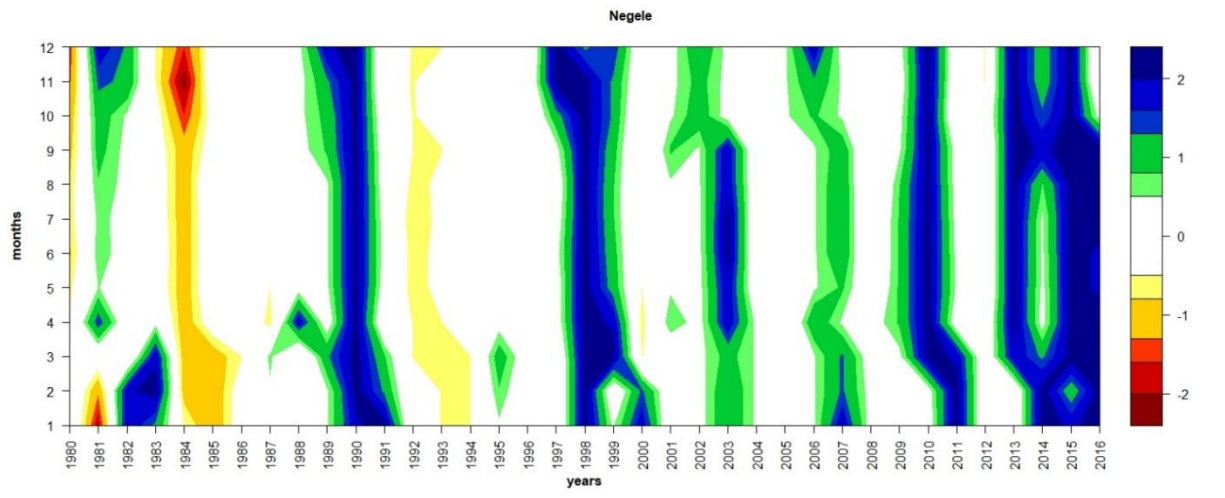
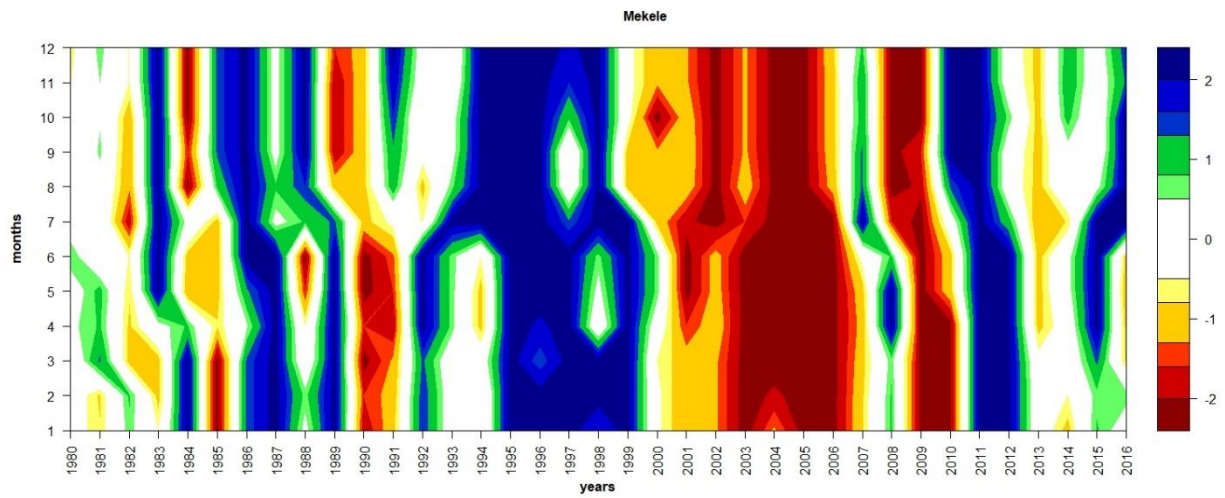


Jinka

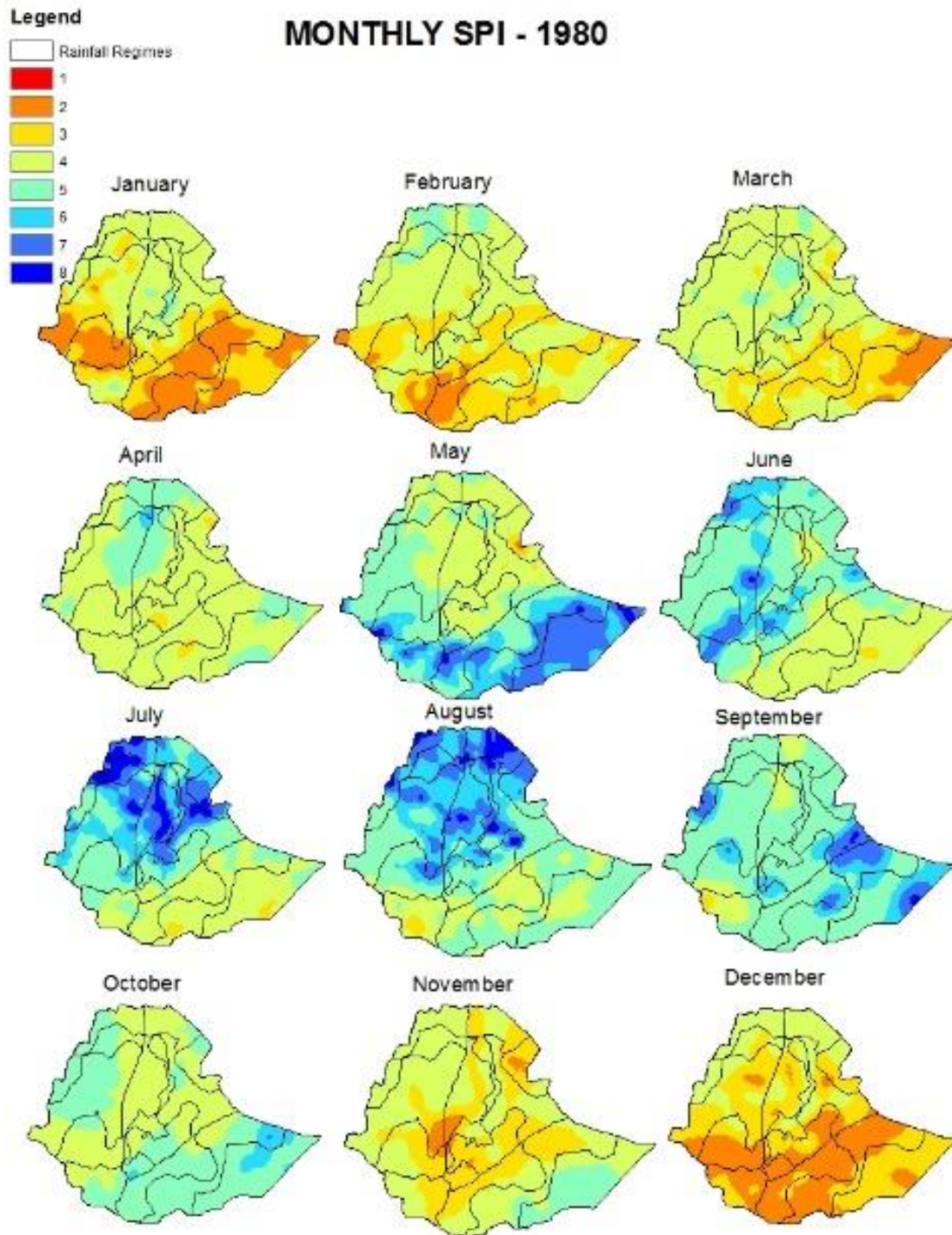


Kebri Dahar



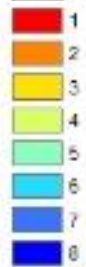


Appendix C: Spatial patterns of 1-month SPI values interpolated across the study area for all drought years

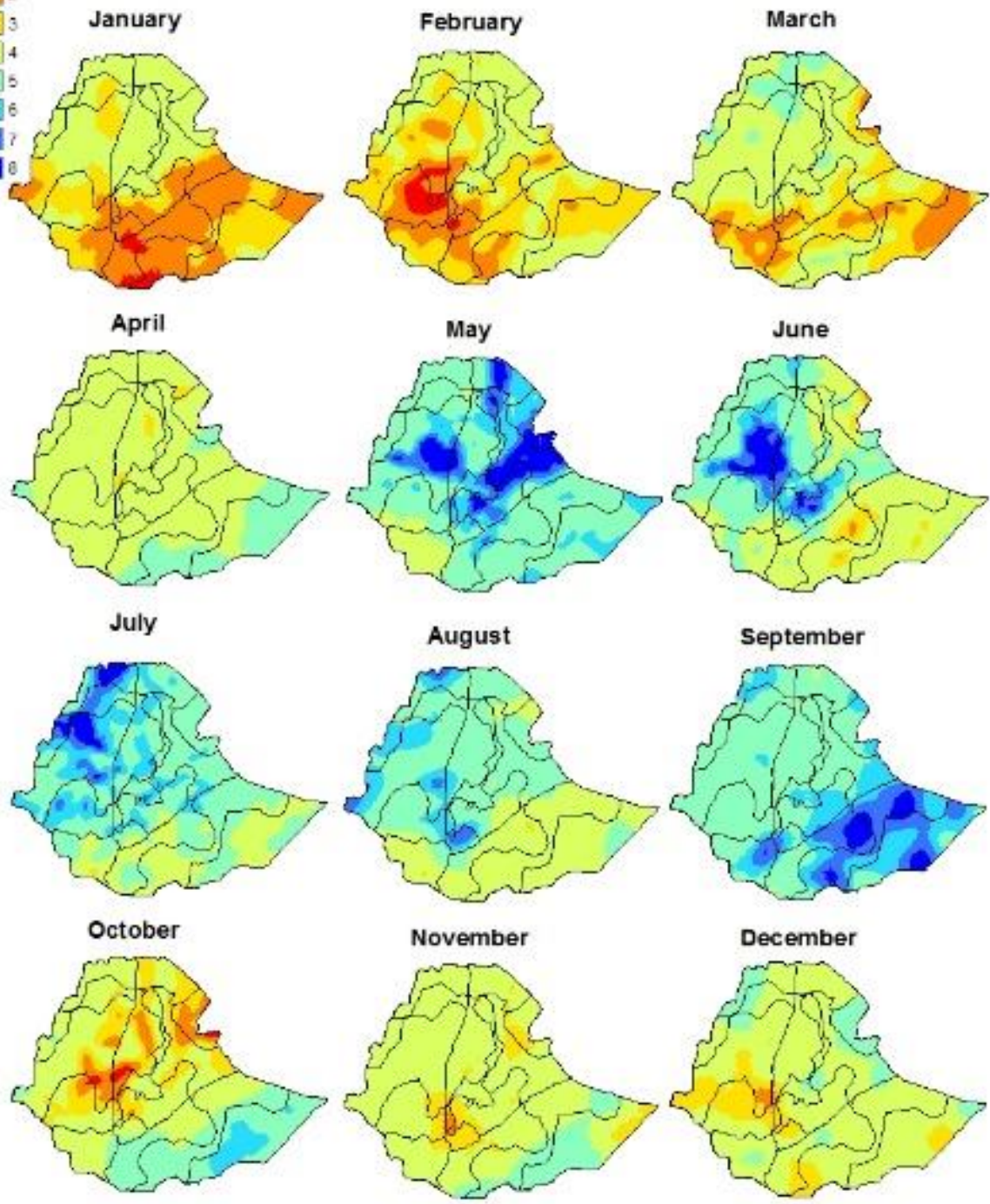


Legend

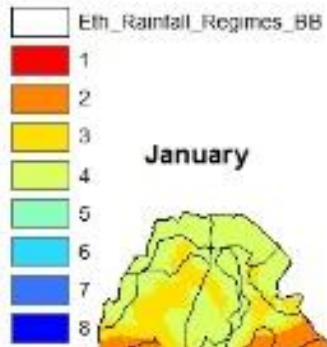
☐ Rainfall Regimes



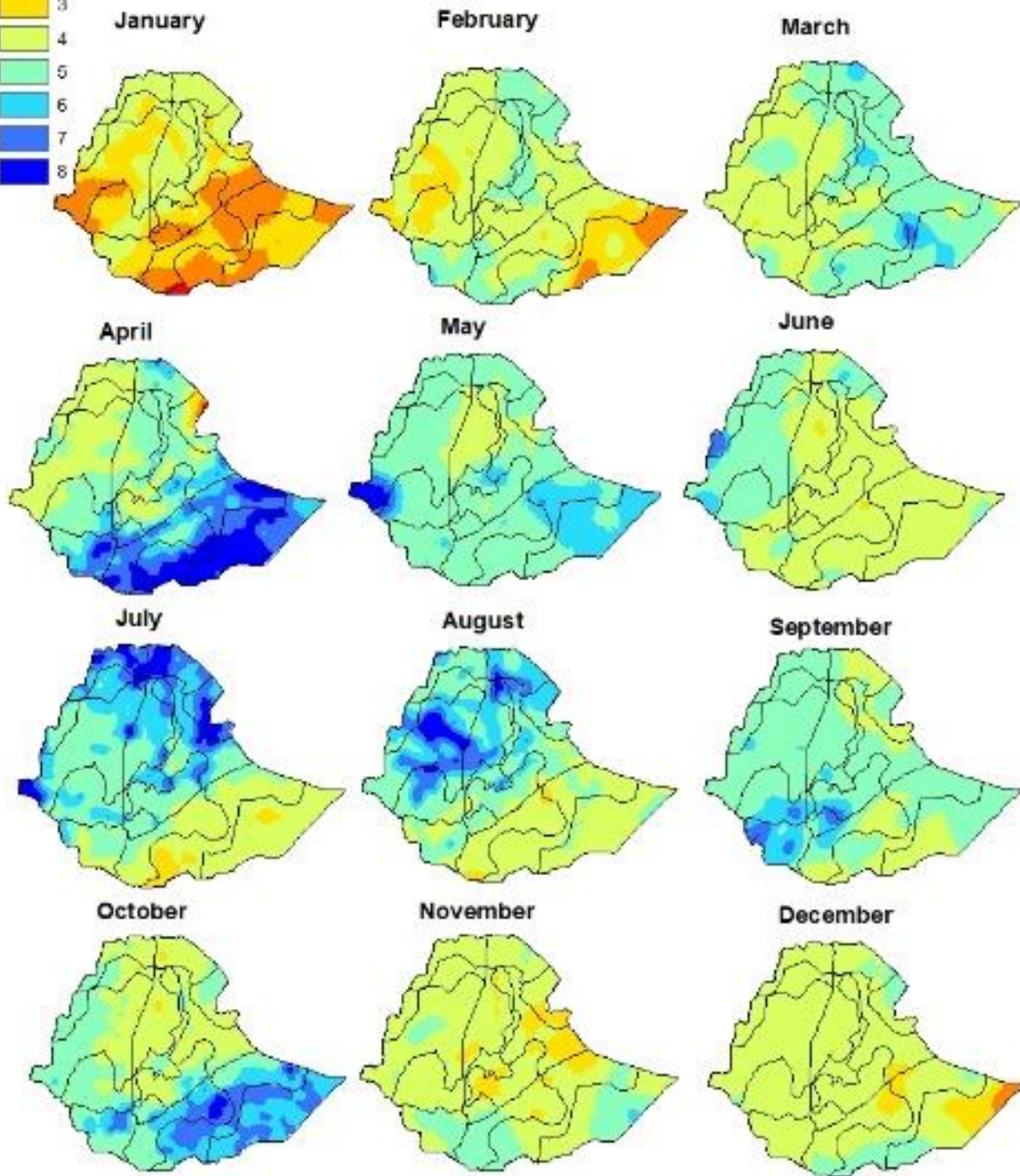
MONTHLY SPI - 1984



Legend



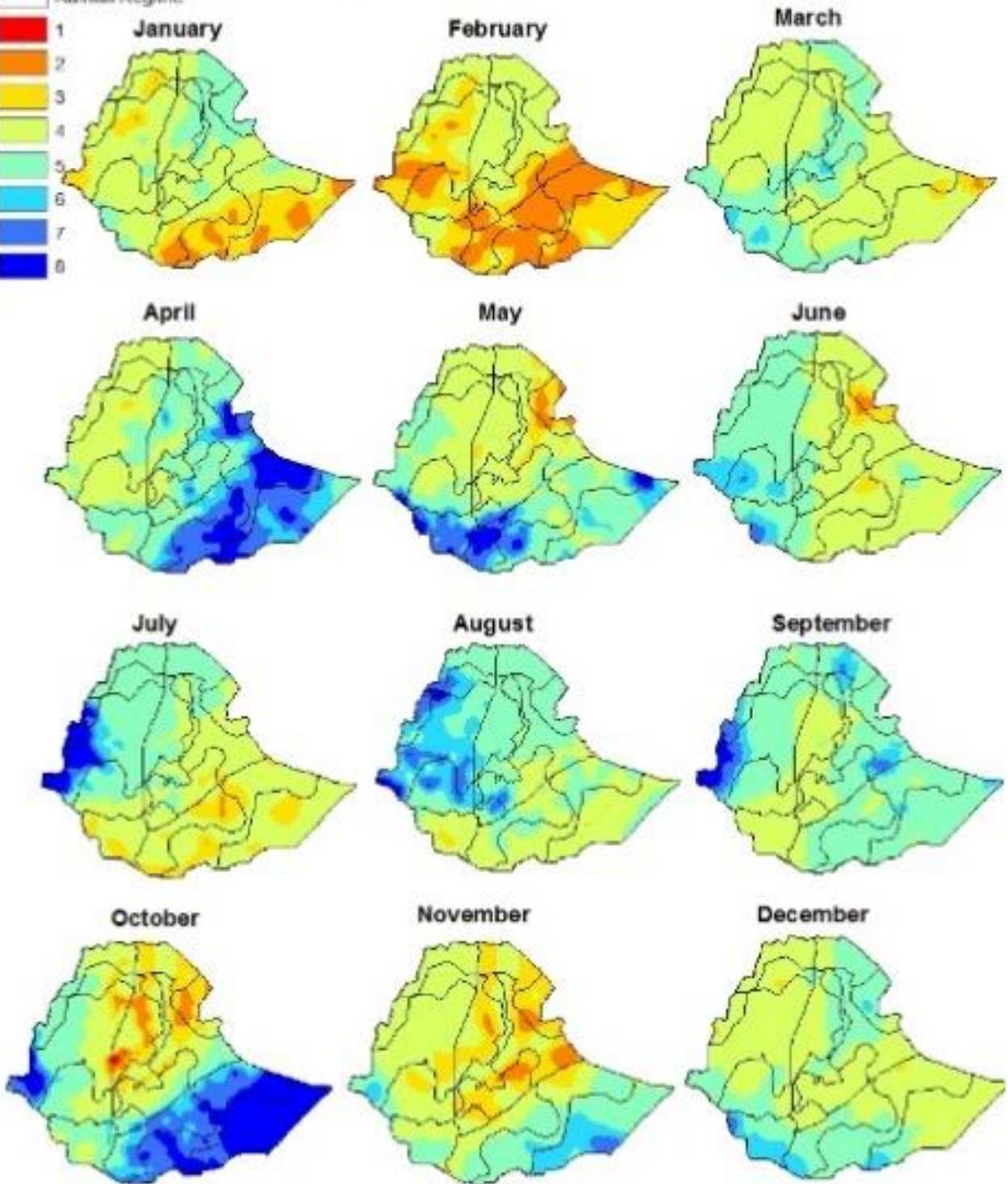
MONTHLY SPI - 1995



Legend



MONTHLY SPI - 2002

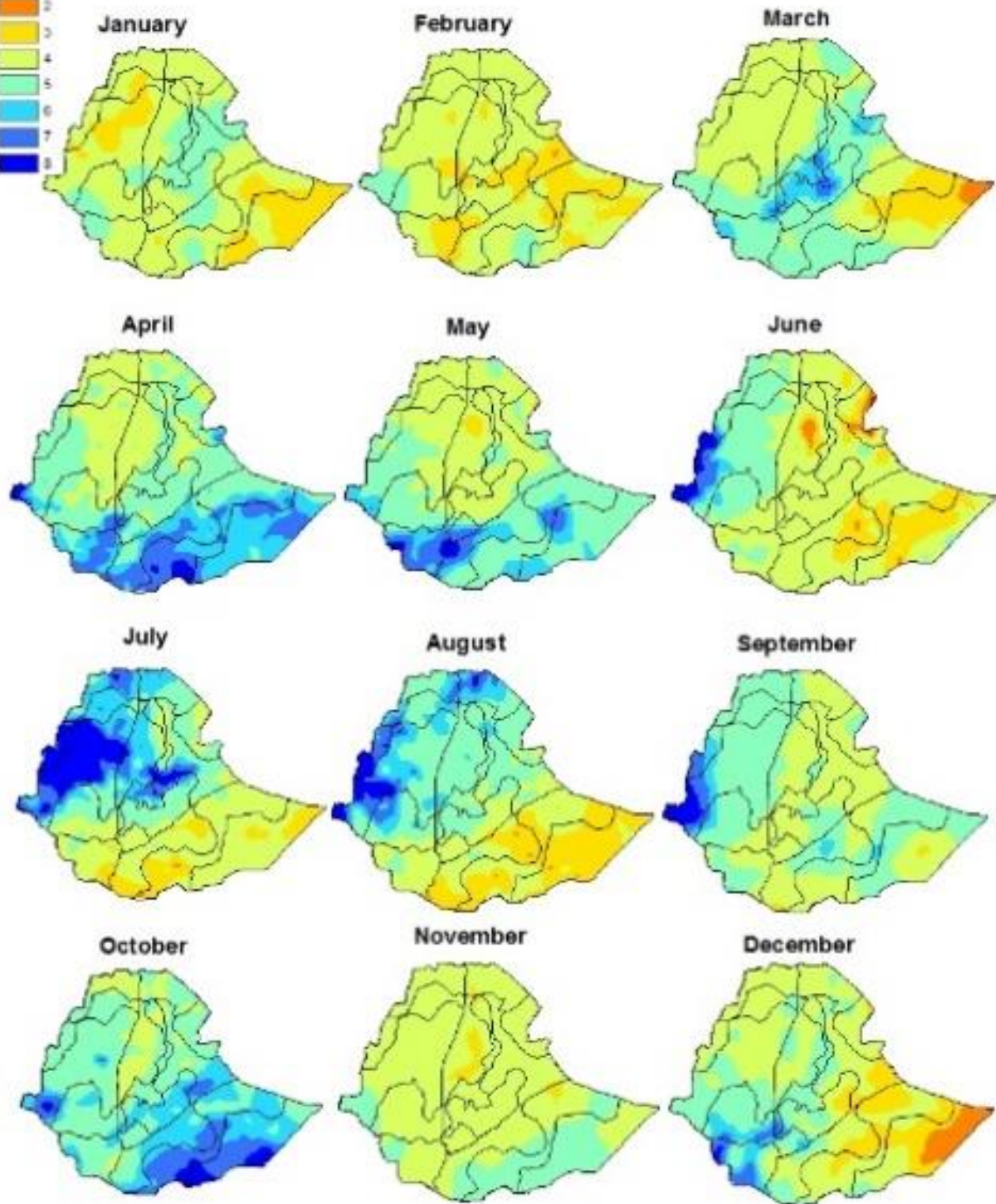


Legend

▭ Rainfall Regimes



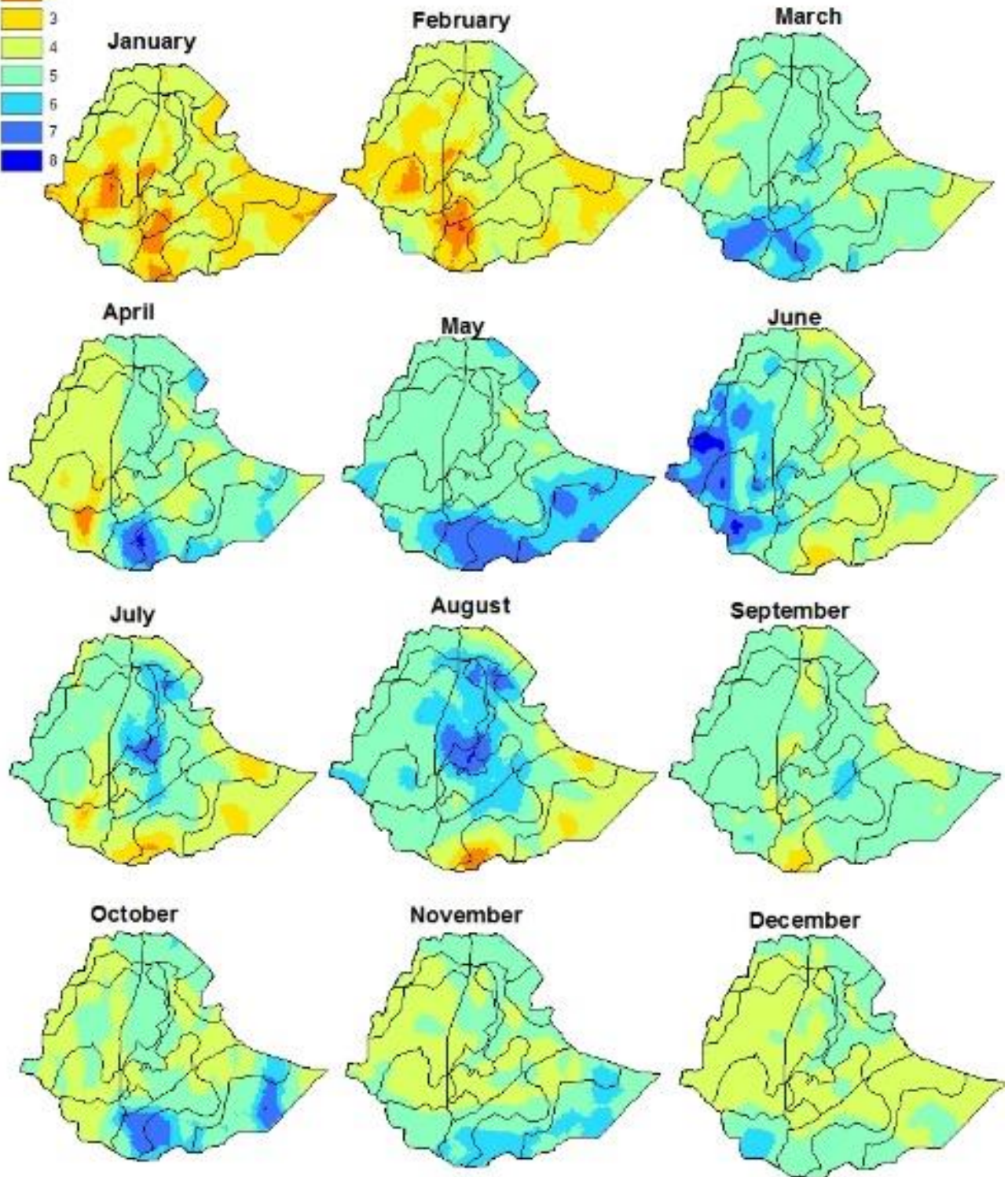
MONTHLY SPI - 2009



Legend

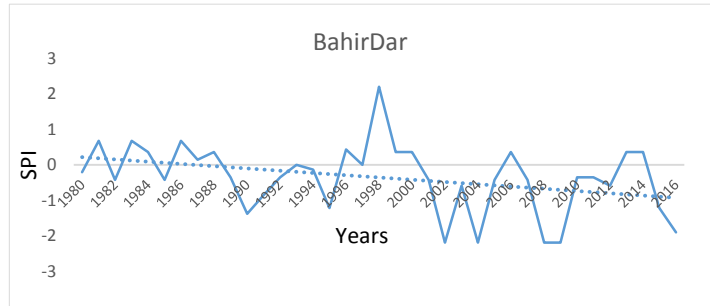


MONTHLY SPI - 2015

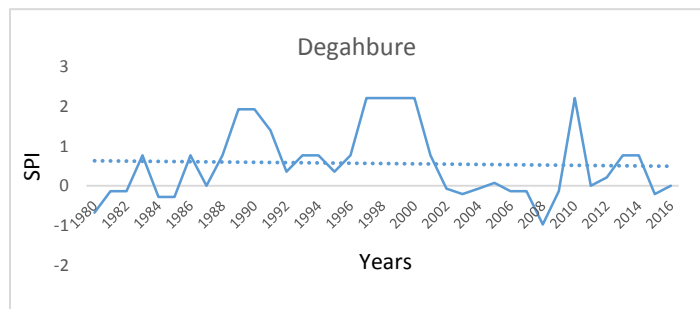


Appendix D: Time series plots of 12-monthl SPI for representative grid points with Man-Kendall trend test.

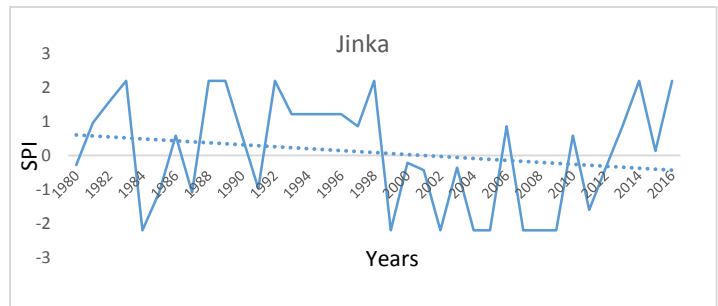
BahirDar	
S=	-165.00
V(S)=	5839.33
Zmk=	-2.146
/Zmk/=	2.146
$Z_{(1-\alpha/2)}$ =	1.96
Comment:	There is a trend with 95% confidence



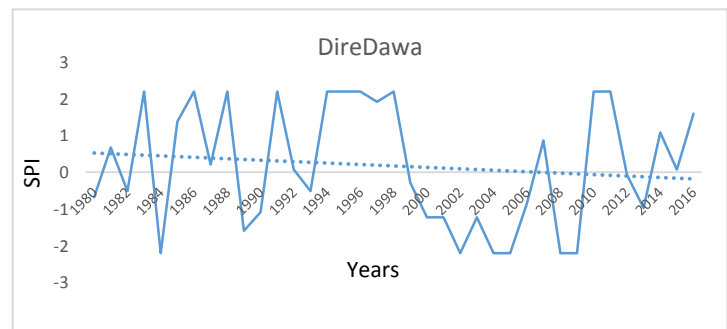
Degahbure	
S=	-44.00
V(S)=	5825.333
Zmk=	-0.563
/Zmk/=	0.563
$Z_{(1-\alpha/2)}$ =	1.96
Comment:	There is no trend



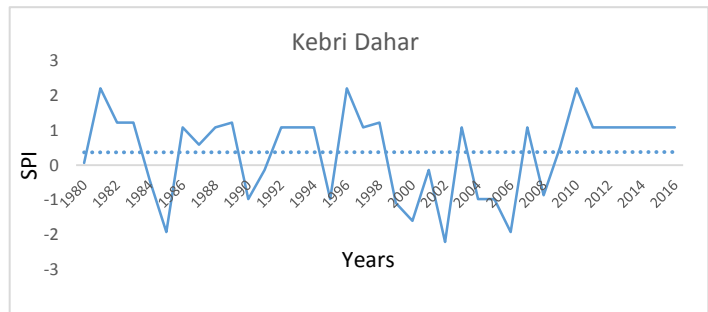
Jinka	
S=	175.00
V(S)=	5832.33
Zmk=	2.28
/Zmk/=	2.28
$Z_{(1-\alpha/2)}$ =	1.96
Comment:	There is a trend with 95% confidence



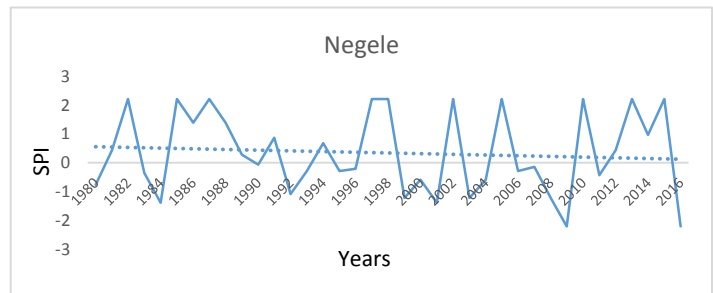
DireDawa	
S=	-143.00
V(S)=	5790.33
Zmk=	-1.87
/Zmk/=	1.87
$Z_{(1-\alpha/2)}$ =	1.96
Comment:	There is no trend



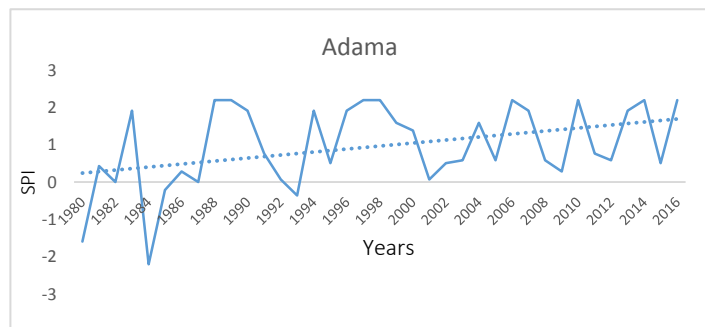
Kebri Dahar	
S=	195.00
V(S)=	5812
Zmk=	2.545
/Zmk/=	2.545
$Z_{(1-\alpha/2)}$ =	1.96
Comment:	There is a trend with 95% confidence



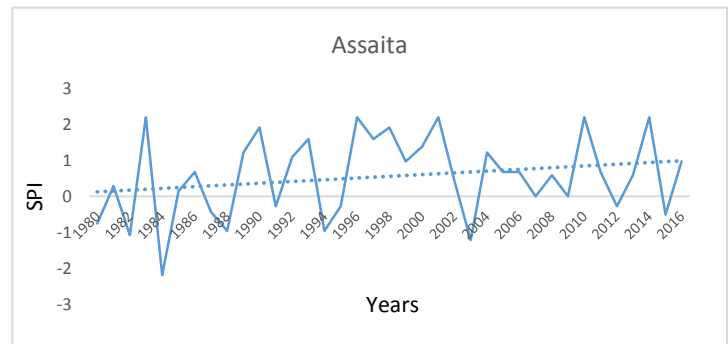
Negele	
S=	102.00
V(S)=	5843.67
Zmk=	1.32
/Zmk/=	1.32
$Z_{(1-\alpha/2)}$ =	1.96
Comment:	There is no trend



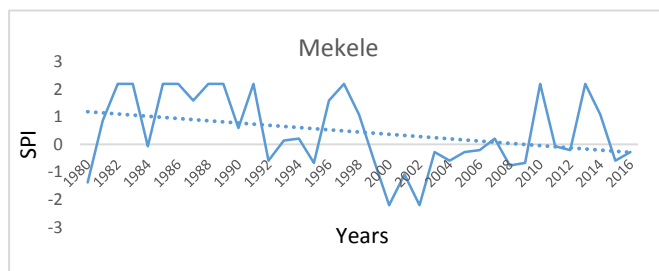
Adama	
S=	-26.00
V(S)=	5781.33
Zmk=	-0.33
/Zmk/=	0.33
$Z_{(1-\alpha/2)}$ =	1.96
Comment:	There is no trend



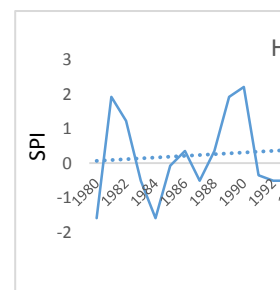
Assaita	
S=	-87.00
V(S)=	5819
Zmk=	-1.127
/Zmk/=	1.127
$Z_{(1-\alpha/2)}$ =	1.96
Comment:	There is no trend



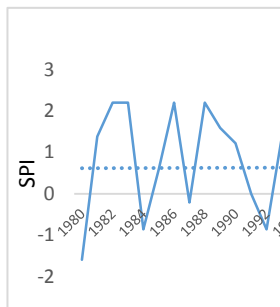
Mekelle	
S=	-63.00
V(S)=	5785
Zmk=	-0.815
/Zmk/=	0.815
Z _(1-a/2) =	1.96
Comment:	There is no trend



HagereSelam	
S=	-63.00
V(S)=	5785.67
Zmk=	-0.82
/Zmk/=	0.82
Z _{1-a/2} =	1.96
Comment:	There is no trend



Jimma	
S=	74.00
V(S)=	5845.33
Zmk=	0.95
/Zmk/=	0.95
Z _{1-a/2} =	1.96
Comment:	There is no trend



Sinana	
S=	-3.00
V(S)=	5838.333
Zmk=	-0.026
/Zmk/=	0.026
Z _{1-a/2} =	1.96
Comment:	There is no trend

